August 1970
Report 1341-26F

APPLICATIONS OF CUMULATIVE DAMAGE IN THE PREPARATION OF PARAMETRIC GRAIN DESIGN CURVES AND THE PREDICTION OF GRAIN FAILURES ON PRESSURIZATION

FINAL REPORT

1 April 1969 through 28 February 1970

VOLUME I - TEXT

By

K. W. Bills, Jr., D. M. Campbell, R. D. Steele and
J. D. McConnell

Aerojet Solid Propulsion Company
Sacramento, California

and

Consultants: L. R. Herrmann, University of California and
R. J. Farris, University of Utah

Prepared for

Department of the Navy
Naval Ordnance Systems Command (ORD-0331)
Contract No. N00017-69-C-4423

Report 1341-26F

APPLICATIONS OF CUMULATIVE DAMAGE IN THE PREPARATION OF PARAMETRIC GRAIN DESIGN CURVES AND THE PREDICTION OF GRAIN FAILURES ON PRESSURIZATION

VOLUME I - TEXT

PREPARED FOR

DEPARTMENT OF THE NAVY
NAVAL ORDNANCE SYSTEMS COMMAND (ORD-0331)
CONTRACT NO. N00017-69-C-4423

Prepared by:

K. W. Bills, Jr.
Associate Scientist
Propellant Physics

Approved by:

G. J. Svob, Manager
Integrated Grain Design
and Weights, Department 4320

FOREWORD

The program covered by this report covers specific experiments, analyses, and theoretical studies conducted at the Sacramento facility of Aerojet-General Corporation. Program management and technical guidance was under the direction of Mr. K. W. Bills, Jr. The viscoelastic stress analyses and computer programming were performed by Mr. D. M. Campbell and Mr. J. D. McConnell. Improvements in linear and non-linear viscoelastic stress analyses were accomplished by Dr. L. R. Herrmann, Assistant Professor of Civil Engineering, University of California at Davis. Mr. R. D. Steele was responsible for the testing of propellant grains and laboratory measurements of propellant properties with the able assistance of Mr. A. B. Curtis and Mr. L. A. Waddle.

Technical discussions with Dr. J. H. Wiegand, Mr. R. J. Farris and Mr. G. J. Svob have materially aided the development of new concepts. Mr. Farris acted as a Consultant for the last quarter of the program.

Aerojet Solid Propulsion Company

Report 1341-26F

VOLUME I

TABLE OF CONTENTS

TABLE OF CONTENTS (Cont'd)

TABLE OF CONTENTS (Cont'd)

Aerojet Solid Propulsion Company

Report 1341-26F

VOLUME II

TABLE OF CONTENTS

I. INTRODUCTION AND SUMMARY

This program was designed to accomplish realistically obtainable objectives with the aim that the resulting technology would be immediately useful. The goal was to advance the state-of-the-art in viscoelastic stress analyses and to extend the range of application of the linear cumulative damage relation for solid propellants. When indicated, the research and development efforts were directed to the development of practical tools for engineering, propellant development and mechanical property characterizations.

The results of these and previous[1-4] efforts have been to develop the most advanced, axisymmetric, thermoviscoelastic stress analysis capability. Copies of some of the resulting computer programs have been requested and delivered to nine propulsion contractors, government laboratories, and universities.

The linear cumulative damage analyses appear to apply to all of the propellants we have evaluated. The only apparent exception noted to date was reported by J. McKay Anderson for a double base propellant.[5] However, on examining his data we found that he may have ignored the fact that the critical stress (the stress below which no failures would be produced) was about 50 psi. Our evaluation of the data, using σ_{cr} = 50 psi, seemed to resolve the results with the linear cumulative damage rule.

The specific objectives of the program are discussed next followed by a summary of the major accomplishments of the program.

A. OBJECTIVES

The specific objectives of the program were: (1) to provide practical engineering design curves for rocket grains, in terms of their stress, strain and damage behaviors; (2) to make basic improvements in stress analysis methods; and (3) to verify the linear cumulative damage predictions for grain failures on motor pressurizations. The program was planned to include theoretical, analytical and experimental studies.

The first of these objectives was met by a parametric study of cylindrical grains subjected to different thermal loadings. This study was designed to isolate the principal variables contributing to thermal stress failures in solid rocket motor systems. A practical product of this effort was the generation of some parametric design curves for rocket grains, in terms of their stress, strain and damage behaviors. These simplified, parametric design curves should be suitable for early grain design and propellant selection.

The second effort was devoted to adding additional capability to the current two-dimensional viscoelastic, stress analysis; namely, a procedure to account for strain-dependent dilatation was added to the axisymmetric solid analysis and the present analysis was modified to handle arbitrary planar geometries in the conditions of generalized plane stress and plane strain.

The third objective was to be met through studies of the effects of pressurization on propellant behavior. The general plan was to test hypotheses concerning the time-pressure shift factor. The developed relations would be used to predict failures in grains subjected to rapid internal pressurization.

The program was notably successful in meeting its objectives and, in particular, in advancing the practical state-of-the-art. The major accomplishments of the past year are described in the next section.

B. SUMMARY

The newly developed, thermoviscoelastic, stress analysis capability was put to effective use in a simple parametric study. The effects of grain design parameters upon the stresses, strains and cumulative damage produced by thermal loading histories were evaluated for two propellant systems (one had a carboxyl-terminated polybutadiene binder and the other a hydroxyl -terminated polybutadiene binder). Two different thermal histories were considered. The results of the analyses are presented graphically in appendices, but the key results important to preliminary grain design evaluations are presented in the text.

Unique methods were developed for normalizing the relaxation moduli and the calculated stress and strain values. The application of these methods should provide significant cost savings in engineering analyses; in addition to being a major guide to improved methods for selecting and formulating propellants to meet a given grain structural problem.

Any prediction of grain failures, regardless of the failure criterion used, is limited by the accuracy of the predicted stresses, strains, or strain energies employed in making the prediction. Therefore, in the development of the linear cumulative damage analyses it was necessary to make basic improvements in the stress and thermal analyses of propellant grains. Although the existing analytical methods gave us advanced capabilities, they were, nevertheless, limited. The two-dimensional analyses gave numerical difficulties after 500 calculation-time points, and they were limited to circular bore grains. In addition, the non-linear viscoelastic effects of strain-dilatation in propellants were ignored. The current program was designed to extend the present analytical methods in these areas. The numerical difficulties were associated with the short word length of the IBM 360/65 computer, which lead to truncation errors. Dr. Herrmann reformulated the method of solution in an attempt to alleviate this difficulty, and was partially successful.

The previously generated, analytical capability was designed to analyze case-bonded cylindrical grains. For arbitrary solids of revolution, a complete analysis would entail a three-dimensional capability, which is a remote possibility. Therefore, the existing thermoviscoelastic analysis capability was extended to include evaluations of planar sections. This will permit us to evaluate real grain cross-sections, but without considering the influence of the end conditions. Also, the capability should permit the experimental evaluation of propellant specimens, which have been made in thin slabs, and relate their behavior to available analyses. Thus, we could better assess new grain designs and propellants before making them in full-scale grains.

The fact that the viscoelastic response of solid propellants is highly non-linear has been well established by numerous investigators. An attempt was made to determine whether or not these non-linearities negate stress analysis predictions based upon linear theory. It was found that the response of grains to various loading conditions is mainly determined by the dilatational behavior of the propellant. Although insufficient experimental data are available to permit a comprehensive characterization of the non-linear dilatational effects, an analytical evaluation appeared to be very straightforward and useful. The non-linear behavior was approximated by an equation which could be incorporated into the existing analysis with a minimum of effort. This was done and the analysis programmed for the computer at University of California, Davis, and simple problems evaluated. The procedure was verified on a sample problem and found to be qualitatively in accord with observations on real grains.

The linear cumulative damage and maximum principal stress failure relations for solid propellants have been thoroughly developed and verified in application to the thermal cycling of motors. The next application of these relations was to the prediction of grain failures on motor pressurization. However, analytical and theoretical difficulties existed for the case of a three-dimensional test with superimposed hydrostatic pressure. To put this problem in perspective a brief review was made of the applicable relations. These relations and a new evaluation of propellant failure mechanisms provided the technical basis for defining and using the time-pressure shift factor, a_p, in a three-dimensional grain problem; the value of a_p was found to be dependent upon the critical stress σ_{cr}.

The effect on propellant failure properties of the damage accumulated from some past history was considered next. This is an important problem when considering firings of motors after they have seen severe handling or prolonged thermal cycling histories. It was found that propellant ultimate properties are significantly affected only when the grain is nearing a failure. We have considered this to be an unlikely event for the well designed grain. But, for grains designed with high bore and bend stresses the previous damage would be high and a large number of them would fail from the loads imposed by the previous history. These latter motors

could show marked effects on ultimate properties, some of which would produce ballistic failures on motor firing.

An especially successful effort was the development of a grain pressurization analog test. This test permits the direct evaluation of a propellant in determining its ability to function as a grain during motor pressurization and we feel that the analog test offers a great potential for evaluating propellants in general. Like the analog tests for grain thermal storage and cycling, this test provides rapid, easily obtained data, either in some standard test mode, or in a test condition simulating a given motor application.

A total of ten grains were tested using the pressurization analog test. Five were tested after some special stress relieving notches were devised and put into use. For these tests a PBAN propellant was used, with all the grains being tested to failure. The stresses, strains and damage fractions were calculated using a planar analysis option of the two-dimensional viscoelastic computer program. The observed failure conditions were compared with those calculated by the LCD analysis and by a simple strain failure criterion. In this test we used a camera with a very shallow depth of focus (about 1/2 inch) which caused us to miss the actual times for the appearance of grain cracks. Obviously, better optical procedures will have to be used before this test can be used routinely; the equipment for this being commercially available.

The linear cumulative damage criterion did not accurately predict failures on pressurization. This is because the analysis does not account for finite deformations of the grain, whereas strains greater than 40% were calculated for all cases, nor does it account for strain dilatation. Also, since the actual failure times were not accurately known we do not know the extent of the error.

The most important point to be made is that the linear cumulative damage predictions were consistently conservative. Strain failure criteria were even more conservative, predicting failures at much lower strain levels and shorter times.

Considerable technical data were generated in the course of this program. To handle the data conveniently we have made liberal use of appendices. These were so extensive that they are presented in a separate volume. Volume I is the technical text of the report and gives the key results of our research. Volume II contains Appendices A through M.

II. PARAMETRIC DESIGN CURVES

A. APPROACH

The fully automated, thermoviscoelastic, stress analysis provides the means for studying the effects of various design and material parameters in order to define the principal parameters contributing to grain failures under given loading conditions. From a limited number of analyses for temperatures, stresses, strains, and cumulative damage, parametric design curves may be generated which can be used for the preliminary evaluation of new grain designs or for the initial selection of propellant compositions.

A one-dimensional analysis method[4] was used to accomplish this task. It had been planned to include finite-length grains in this study, but the recently developed two-dimensional thermoviscoelastic analysis[3] developed numerical errors on repeated thermal cycling calculations, although these were partially corrected later, as noted in Section III.

The materials, designs, and thermal histories used in this study are discussed next followed by a presentation of the key results. Then, a unique method for normalizing the moduli and the analytical values for the stress and strain is presented. The applications of this approach are discussed with respect to both engineering and propellant development.

B. MATERIALS, DESIGNS AND THERMAL HISTORIES

The geometries, cycling histories and propellants being used are as follows:

Geometries

B/A = 1.25, 2.00, 5.00
B = 4 in., 8 in.

Histories

(1) Thermal cycling in steps: cooling from 160 to -65°F in nine discreet steps with recovery back to 160°F.

(2) Direct thermal cycling between 160 and -65°F.

Propellants

(1) Carboxyl-terminated polybutadiene propellants (CTPB) - cure temperature: 135°F.

(2) Hydroxyl-terminated polybutadiene propellants (HTPB) - cure temperature: 135°F.

The properties and parameters employed in the stress and temperature distribution analyses are given below.

STEEL CASE

Case Thickness:	0.060 in.
Coefficient of linear thermal expansion:	5.90×10^{-6} in./in./°F
Density:	0.283 lbs/in.^{3}
Specific Heat:	0.116 BTU $lb^{-1}{}^\circ F^{-1}$
Thermal Conductivity:	2.50 BTU $in.^{-2}$ hr^{-1} $(°F/in.)^{-1}$
Heat Transfer Coefficient:	0.0125 BTU hr^{-1} $in.^{-2}{}^\circ F^{-1}$
Poisson's Ratio:	0.30
Young's Modulus:	3.0×10^7 psi

SOLID PROPELLANTS

Coefficient of linear thermal expansion:	5.67×10^{-5} in./in./°F
Density:	0.0633 lb/in.^{3}
Specific Heat:	0.315 BTU lb^{-1} $°F^{-1}$
Thermal Conductivity:	0.02333 BTU $in.^{-2}$ hr^{-1} $(°F/in.)^{-1}$
Bulk Modulus:	5×10^5 psi

The relaxation moduli for the two propellants are given in Figure 1 and their a_T curves in Figure 2.

The relaxation data specifically input to the computer analyses were Prony series constants and discreet values of $\log_{10} a_T$. These values are given in Appendix A of this report. *

The cumulative damage parameters[1-4] used in these analyses are listed here.

	CTPB PROPELLANT	HTPB PROPELLANT
σ_{to}, psi	130	120
σ_{cr}, psi	0	0
B, dimensionless	8.43	8.30
t_o, min.	1	1

The CTPB propellant is of a type currently in extensive use. The HTPB propellant represents the best of the newly developed, next generation propellants. The latter propellant has successfully endured 15 cycles between 160 and -75°F at 38% inner-bore strains followed by 4 weeks aging at 160°F, then thermally cycled again. The first failures were observed on the ninth cycle following aging.

C. COMPUTER ANALYSES

The analyses performed on the program are shown in Table I. They include both elastic and viscoelastic stress analyses for each of the conditions indicated. The elastic analyses employ the equilibrium modulus for each of the given propellants. They were obtained as part of an effort to normalize the grain stresses.

Three variations (1, 2 and 3) of the CTPB propellant were included in the analysis plan, also. This was done to provide an evaluation of the normalization schemes generated in this study. Variation 1 of the CTPB propellant has the same relaxation behavior as does the CTPB propellant, except that the equilibrium modulus was doubled. The properties of variation 2 have all the pre-exponential terms in the Prony series (which describes mathematically the relaxation behavior) double those obtained for the CTPB propellant, whereas the same terms for variation 3 are triple those for the base propellant.

* Appendices contained in Volume II.

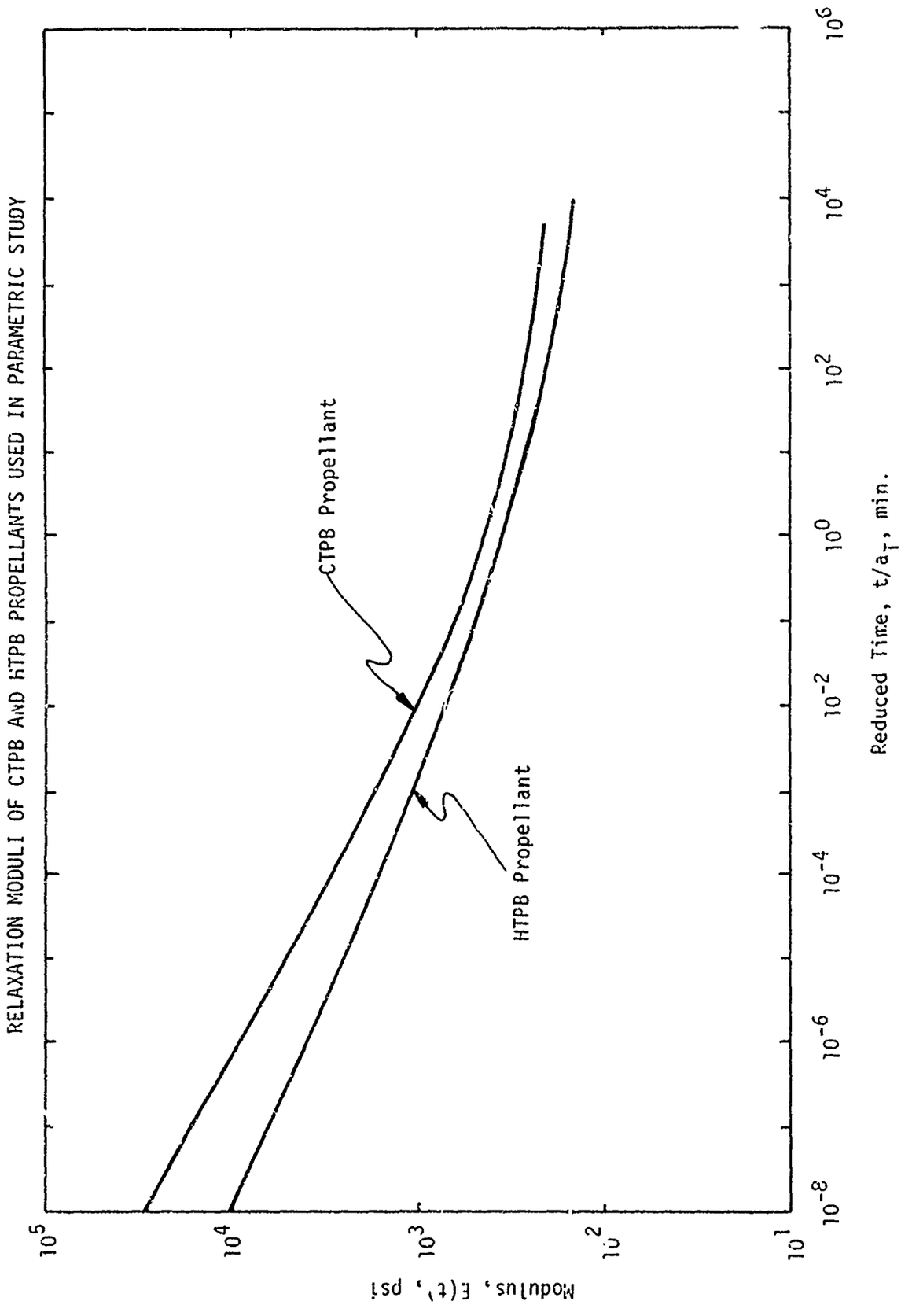
RELAXATION MODULI OF CTPB AND HTPB PROPELLANTS USED IN PARAMETRIC STUDY
CTPB Propellant
HTPB Propellant
Modulus, E(t), psi
Reduced Time, t/a_T, min.
10^5
10^4
10^3
10^2
10^1
10^-8
10^-6
10^-4
10^-2
10^0
10^2
10^4
10^6

Figure 1

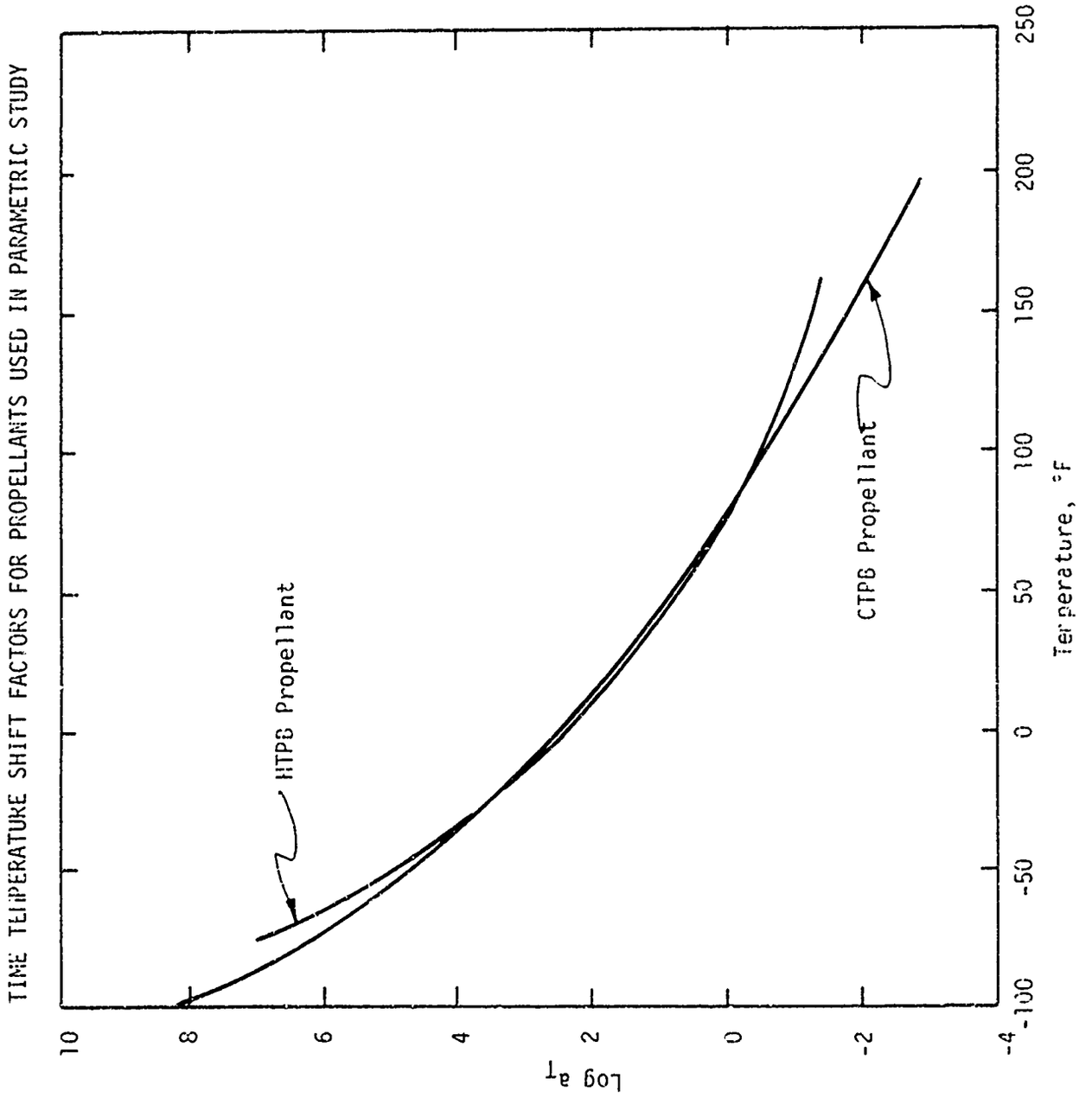
TIME TEMPERATURE SHIFT FACTORS FOR PROPELLANTS USED IN PARAMETRIC STUDY
HTPB Propellant
CTPB Propellant
Log a_T
Temperature, °F
10
8
6
4
2
0
-2
-4
250
200
150
100
50
0
-50
-100

Figure 2

PLANE STRAIN ANALYSES PERFORMED
- Elastic and Visccelastic -

History	Radius Ratio, B/A	Outer Radius, B = 4 in.		Outer Radius, B = 8 in.				
		CTPB Prop.	HTPB Prop.	CTPB Prop.	Variation 1 of CTPB Prop.*	Variation 2 of CTPB Prop.*	Variation 3 of CTPB Prop.*	HTPB Prop.
1	1.25	X	X	X				X
	2.0	X	X	X	X			X
	5.0	X	X	X	X			X
2	1.25	X	X	X	X	X		X
	2.0	X	X	X	X	X		X
	5.0	X	X	X	X	X	X	X

X - Indicates analysis completed

* This is a variation of the properties of the CTPB propellant.

History 1: Thermal cycling in steps: 9 steps between 160° and -65°F.
History 2: Direct thermal cycling between 160° and -65°F.

Table 1

For the analyses made here the propellant-liner bond strength was assumed to be equal to that of the propellant. Frequently, in real bond systems this is not the case.

Six grain designs were employed here, all of them simple cylinders of infinite length. The outer radius, B, of the grains covered a range of typical small motors 4 and 8 inches. The inner radius, A, was varied over a wide range as shown by the radius ratios, B/A, which had the values of 1.25, 2 and 5.

The completed analyses provided extensive data which must be evaluated in a number of ways. The next two sections describe these evaluations.

D. PARAMETRIC EVALUATION

The stress, strain and damage values versus time from the computer solutions are presented graphically in Appendices B and C for Histories 1 and 2, respectively. Selected points on these curves were used to make simplified crossplots which may be used to guide engineering design. These we have termed "parametric design curves". They are presented below.

Before considering the parametric design curves some general observations on the viscoelastic analyses themselves are required. These are made in the following paragraphs.

1. Observations on the Viscoelastic Analyses

The time interval employed in each temperature change was arbitrarily set at 24 hrs. Depending on one's point of view this may, or may not, be a fortunate choice. The smallest diameter grains quickly reach thermal equilibrium so that extensive relaxation of the stresses are calculated. On the other hand, the largest grains do not reach thermal equilibrium in the time allotted, so their grain strains are not fully developed.

Figure 3 provides a comparison, for selected designs, of the temperatures at the inner-bore during the initial heating from 135° to 160°F. The largest grain, with B/A = 5 and B = 8 in. falls short of the oven temperature (160°F) by nearly 5.8°F. A similar result, Figure 4, is obtained for temperatures at the propellant-to-liner bond, except the final temperature, 158.2°F, for the largest grain is closer to the oven temperature, 160°F. Figure 5 shows the inner-bore temperature for this grain over a little more than one thermal cycle. On the heating step from -65° to 160°F the thermal lag is considerable.

COMPARISON OF TEMPERATURES AT THE INNER-BORE FOR THE CTPB PROPELLANT ON INITIAL HEATING FROM 135° TO 160°F

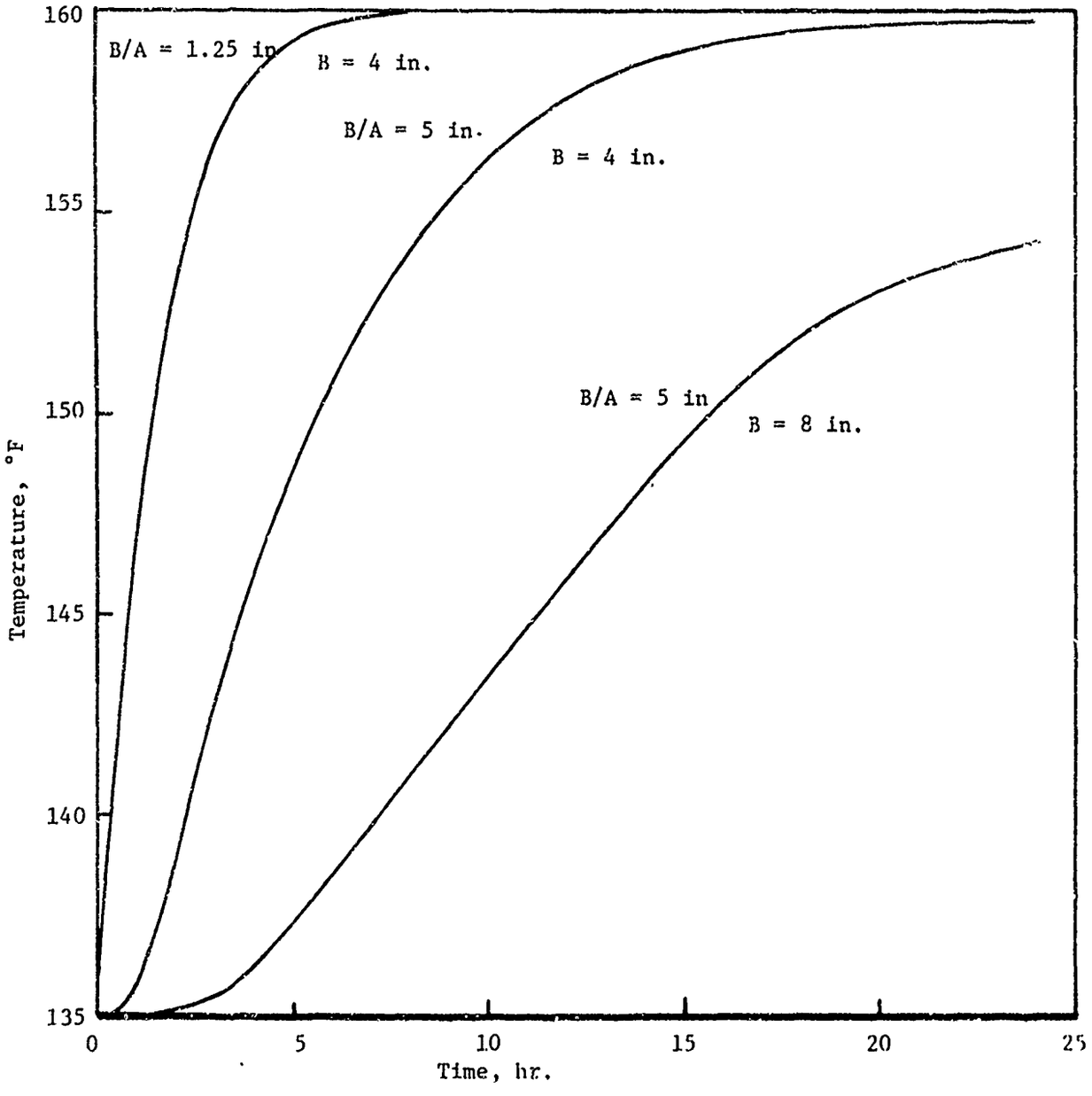

Figure 3

PARAMETER STUDY OF THERMAL SOLUTIONS: CTPB PROPELLANT - HISTORY 1 -
STEP 1: ENVIRONMENTAL TEMPERATURE CHANGE: 135° TO 160°F
-TEMPERATURES AT THE BOND -

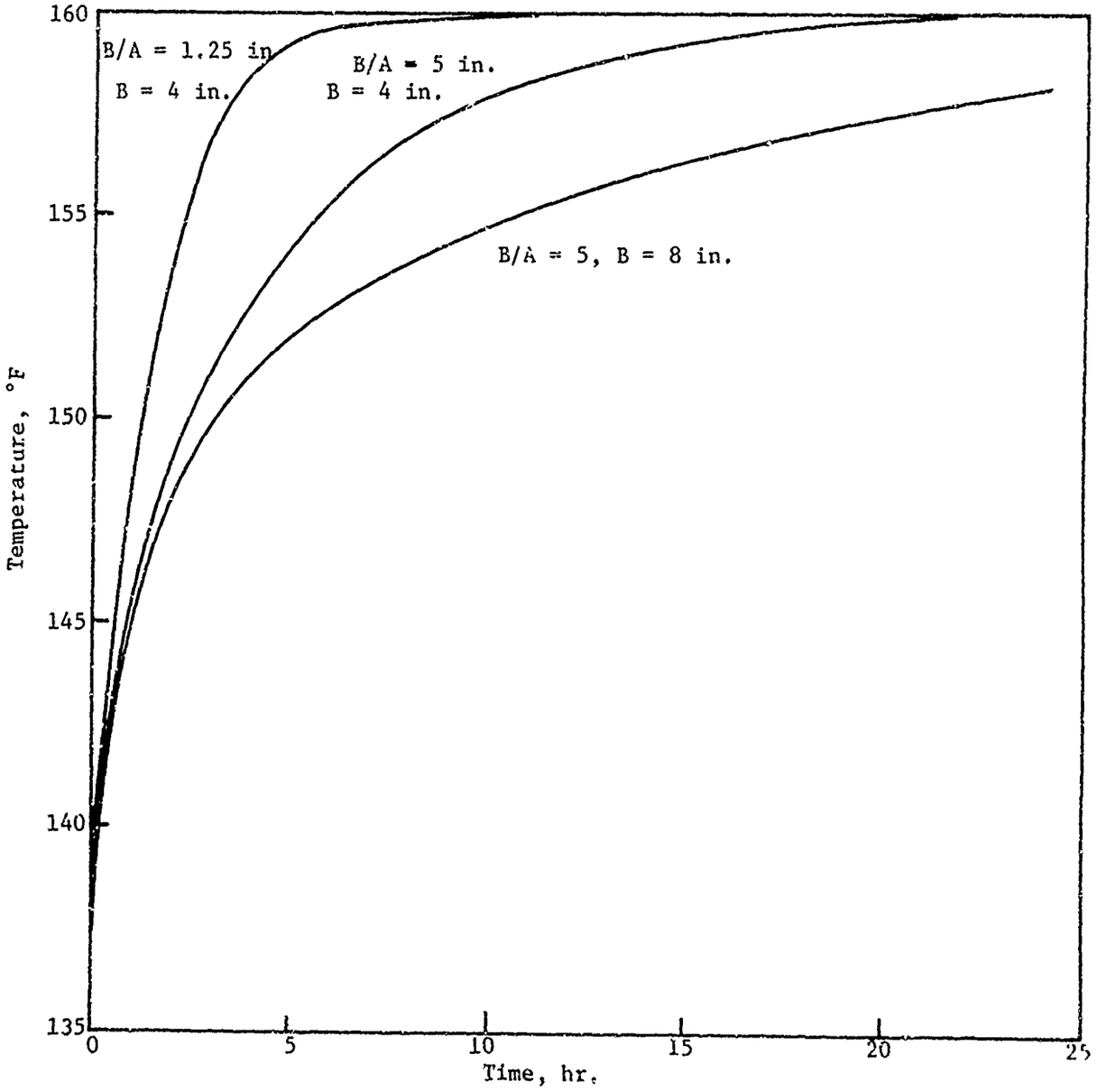

Figure 4

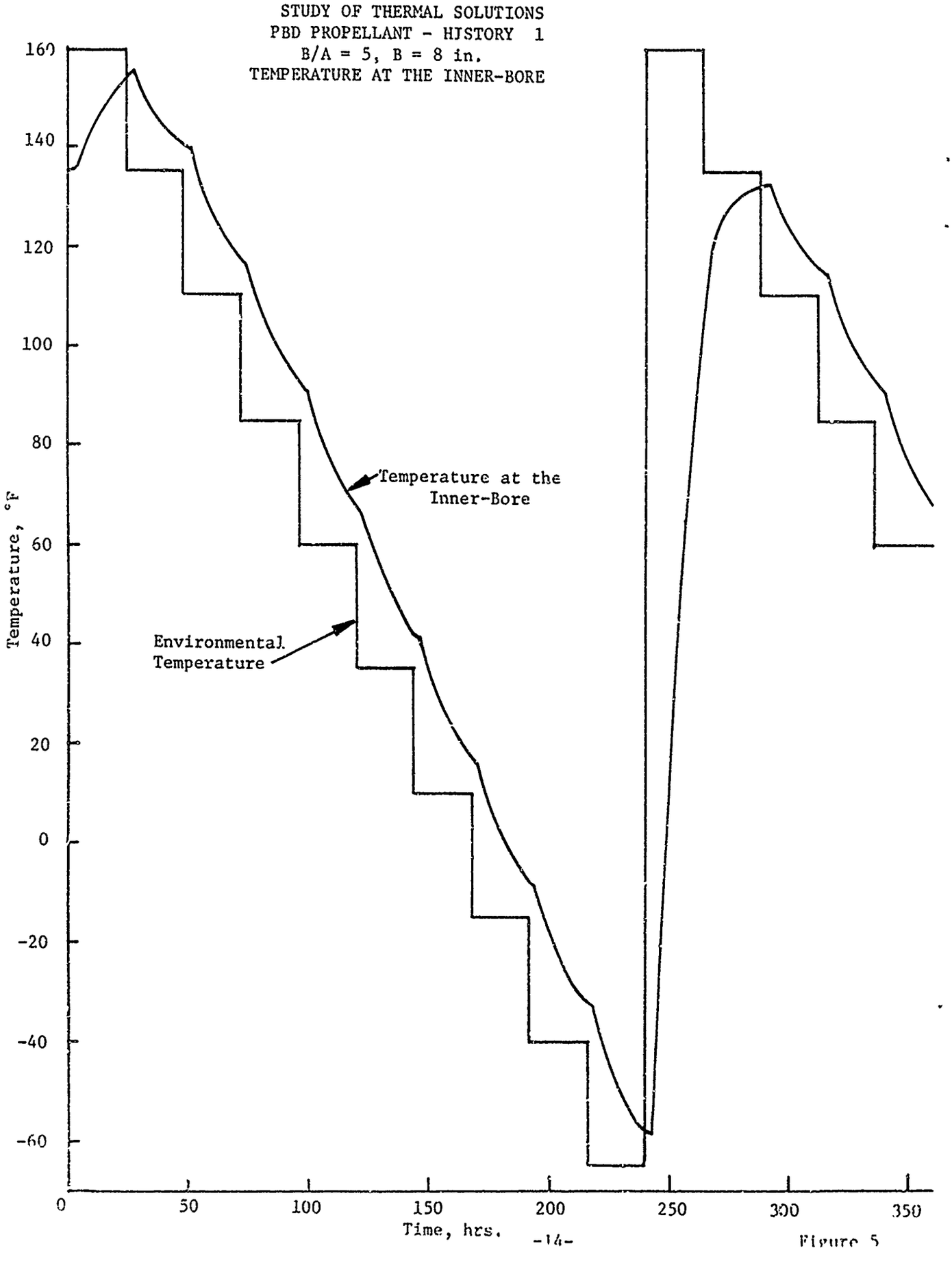
STUDY OF THERMAL SOLUTIONS
PBD PROPELLANT - HISTORY 1
B/A = 5, B = 8 in.
TEMPERATURE AT THE INNER-BORE
Temperature at the Inner-Bore
Environmental Temperature
Temperature, °F
160
140
120
100
80
60
40
20
0
-20
-40
-60
0
50
100
150
200
250
300
350
Time, hrs.

Figure 5

From the point of view of the thermo-viscoelastic stress analysis the thermal lag produces no problems. Also, no real problems exist for the parametric design curves. But, an unexpected result does occur. This is best shown in Figure 6 where the inner-bore hoop stresses are compared for two grains of 4 in. and 8 in. outer radii, with both grains having the radius ratio, B/A, equal to 5. Here the smaller grain reaches higher stress levels than are obtained for the larger diameter grain, which is the opposite of what was expected. This does not make the parametric analysis invalid. Instead, it shows the strong time-dependence of thermoviscoelastic analyses. The effect is attributed to the longer times required to cool the large diameter grains. This longer time permits more stress relaxation to occur while the bulk of the grain is still warm.

After an initial transient condition, during the first two steps, the thermal lag becomes repeatable. The stresses reflect this repeatability also as shown in Figure 7, where the inner-bore hoop stresses are given for the rather complicated thermal History 1. The first two thermal steps give stresses which differ from those seen in the second cycle, for the same environmental temperatures. But, after this, the inner-bore stresses are practically identical from one cycle to the next.

An interesting result of the combined effects of thermal expansion gradients, viscoelasticity and thermal transients is shown in Figure 8. Here, the environmental temperature is increased suddenly from -65° to 160°F. Initially, the inner-bore hoop stress increases from 153.3 to 160.4 psi. This is attributed to the initial expansion of the steel case before the propellant experiences any warming. Then, as the bulk of the outer propellant is heated, it expands putting the bore into compression and the stresses fall to the highly compressive value of -67 psi. Further heating causes the grain to approach more uniform thermal expansions and the bore stresses go into tension, followed by stress relaxation effects.

These comments have shown some of the characteristics of the analyses. The following sections discuss the details of the analytical solutions and the related parametric design curves. Their use is limited to propellants whose a_T properties are similar to those of the CTPB and HTPB propellants described here, and whose moduli can be normalized as described in Section II.E.

2. History 1

This thermal history involves cooling in 25°F steps from 160° to -65°F followed by a single heating step back to 160°F. The analytical solutions for this thermal history are given in Appendix B where the calculated values of stress, strain and damage are plotted versus the time for each of the designs considered. To guide engineering design, abstractions of these data were made and prepared as simple parametric design curves. These are described below for the two reference propellants.

COMPARISON OF INNER-BORE HOOP STRESSES FOR THE CTPB PROPELLANT - HISTORY 1
(B/A = 5.0 in.)

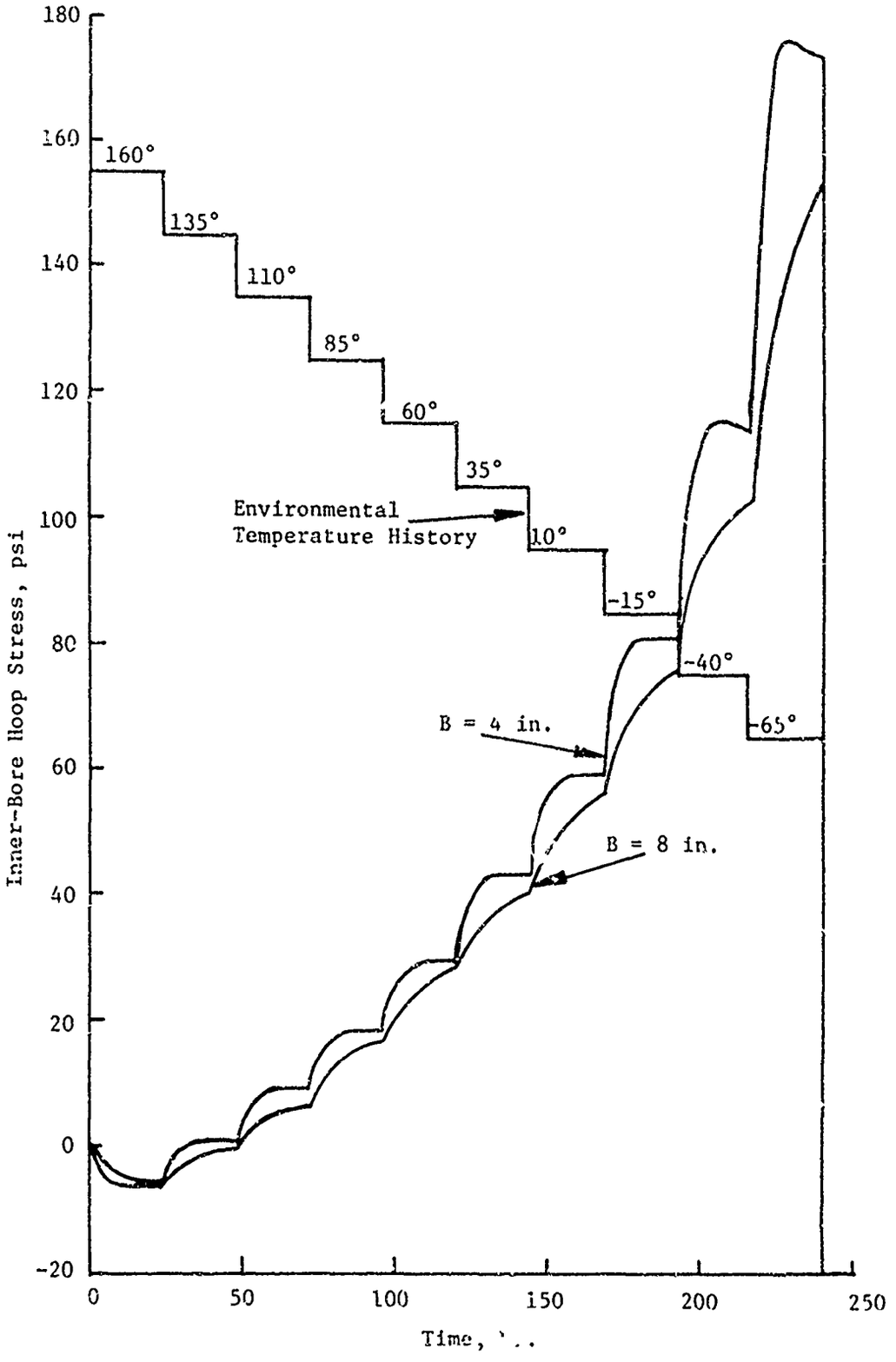

Figure 6

INNER-BORE HOOP STRESSES FOR THE FIRST TWO THERMAL CYCLES OF HISTORY 1
- CTPB PROPELLANT -
(B/A = 5, B = 8 in.)

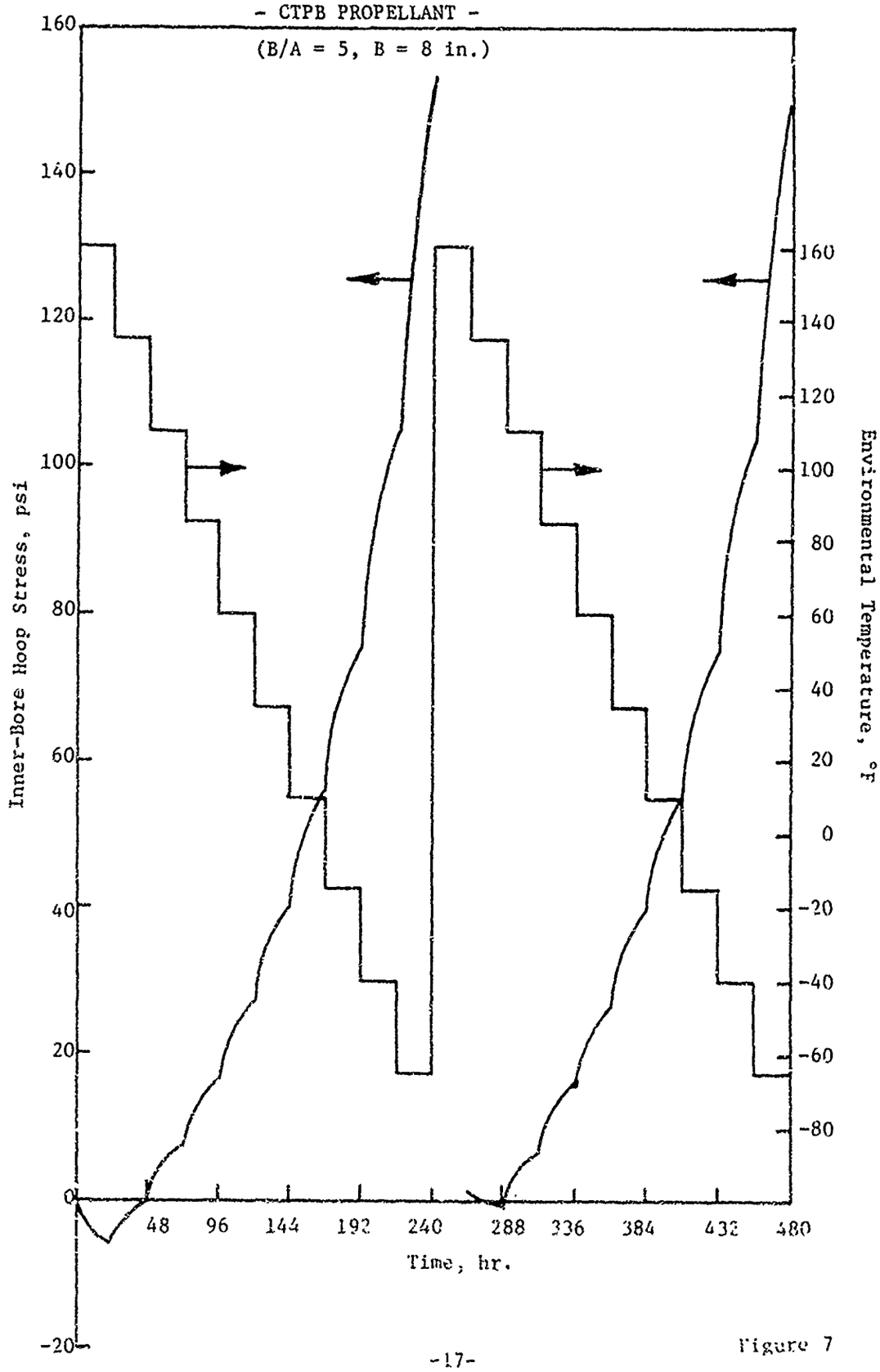

Figure 7

TRANSIENT BORE STRESSES DURING HEATING STEP FROM -65° TO 160°F
-CTPB PROPELLANT-

(B/A = 5, B = 4 in.)

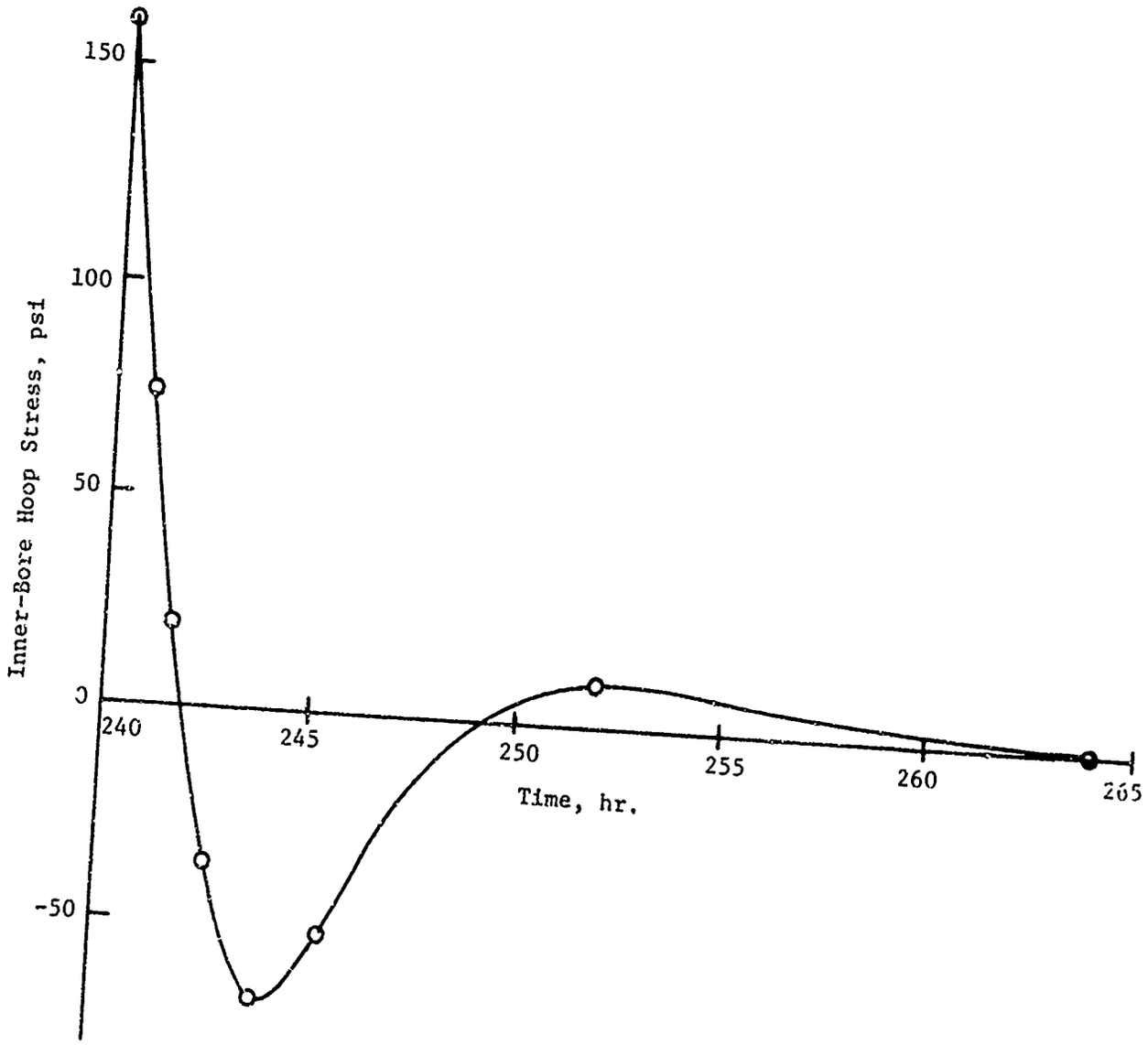

Figure 8

a. Parametric Design Curves for the CTPB Propellant - History 1

These curves are contained in three graphs, Figures 9 and 11. The solutions for the bore hoop strains and radial bond stresses were taken at 240 hours where these values are at their maxima. The cumulative damage values were those for 288 hours, the time to complete one cycle of thermal History 1.

The inner-bore hoop strains are plotted versus $(B/A)^2$ in Figure 9, since this gives nearly linear curves. The curves for the two outer radii of 4 and 8 inches were surprisingly close to each other.

The radial bond stresses, Figure 10, gave nearly linear curves when plotted against $(B/A)^2$. As indicated earlier, the stresses were greater for the grains with a 4 in. outer radius than for those with an 8 in. outer radius.

Figure 11 presents a collection of design data for the cumulative damage. First, the total damage fraction, ΣD, for one complete thermal cycle (240 hours) following History 1 is plotted versus B/A (when $(B/A)^2$ is used the curves show much greater curvature). The logarithm of the total damage values for the inner-bore and for the bond are given. The two different size grains, 4 and 8 in. outer radii, give surprisingly similar results.

Also given in Figure 11 is the average number of cycles to failure, N, for grains following thermal History 1. The right hand coordinate scale gives the logarithm of N with the log increasing toward the bottom of the page. The same curves apply to both the total damage and to the average number of cycles to failure since N is the reciprocal of the total damage for one cycle.

The results given in Figure 11 show that at B/A = 5 the 4 in. radius grain would fail at the bore after an average of 5.4 cycles while the 8 in. radius grain would survive an average 6.5 cycles.

To use Figures 9 to 11 effectively for real grains, statistical considerations must also be made. They are required to take account of inherent manufacturing and material imperfections plus all those problems arising from the machinations of insidious gremlins whose sole pleasure comes from urinating on the pillar of science. The data given in Figures 9 to 11 represent the average values of the stresses, strains and cumulative damage fractions. But we are seldom interested in the averages when it comes to grain failures, instead we emphasize that it is the first grain failures that are important. These first failures not only give the earliest test of the properties but can be used with the analysis of Freudenthal[8] to estimate the mean performance of the group under test.

PARAMETRIC DESIGN CURVES FOR INNER-BORE HOOP STRAIN AT 240 HR.

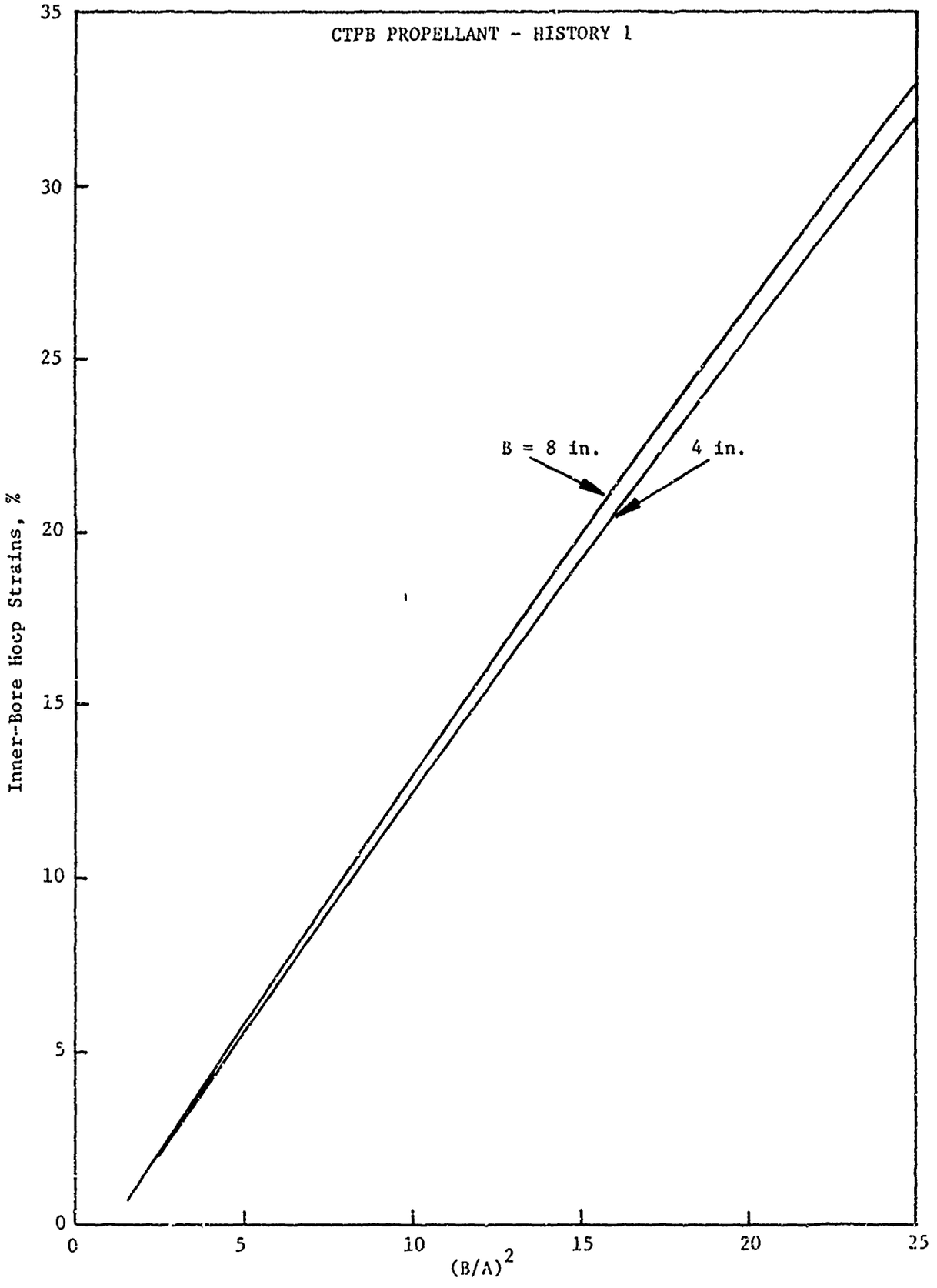

Figure 9

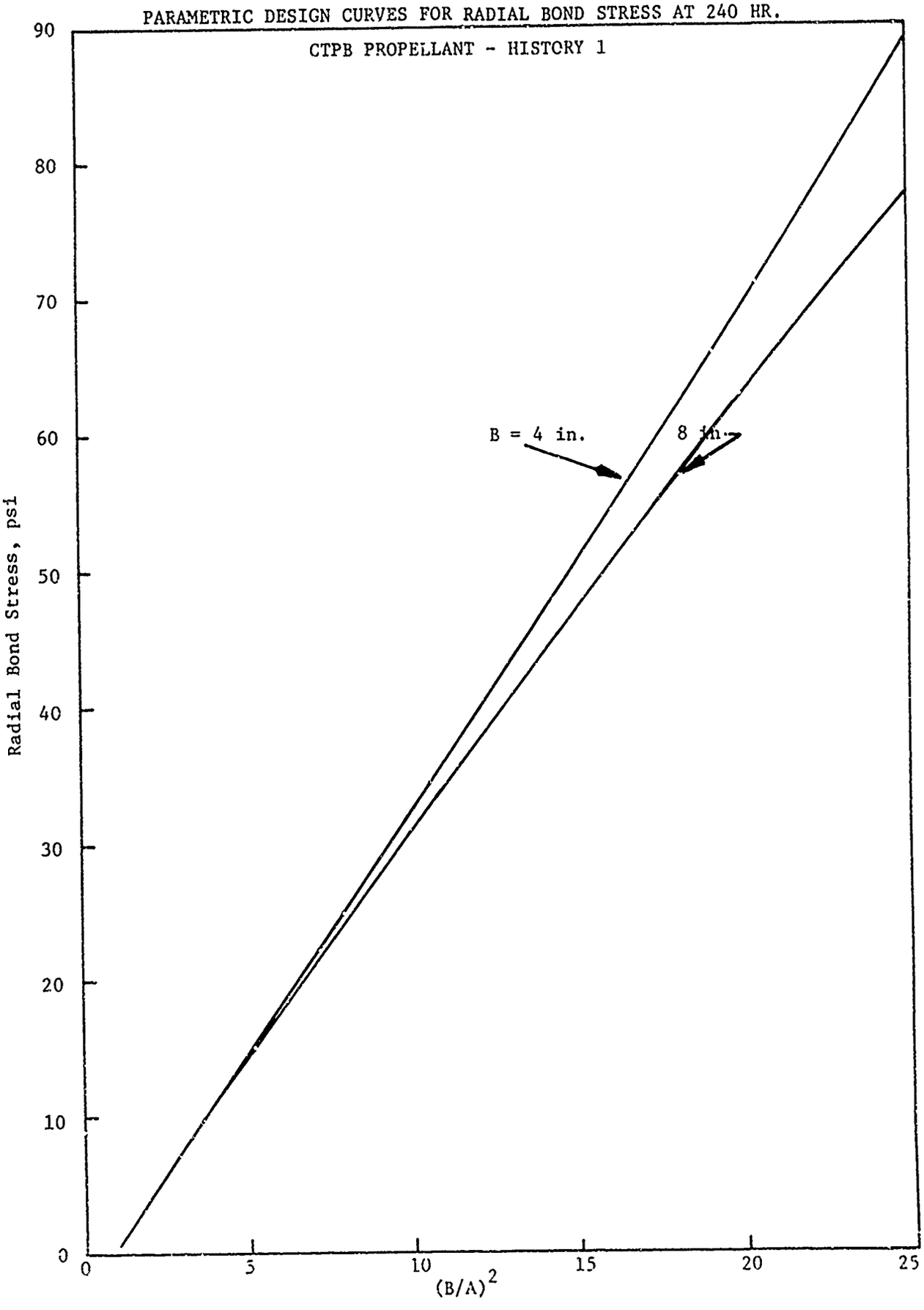
PARAMETRIC DESIGN CURVES FOR RADIAL BOND STRESS AT 240 HR.
CTPB PROPELLANT - HISTORY 1
Radial Bond Stress, psi
90
80
70
60
50
40
30
20
10
0
B = 4 in.
8 in.
0
5
10
15
20
25
(B/A)2

Figure 10

PARAMETRIC DESIGN CURVES GIVING CUMULATIVE DAMAGE PER 240 HOUR CYCLE BETWEEN 160° AND -65°F AND NUMBER OF CYCLES TO FAILURE FOR CTPB PROPELLANT

HISTORY 1

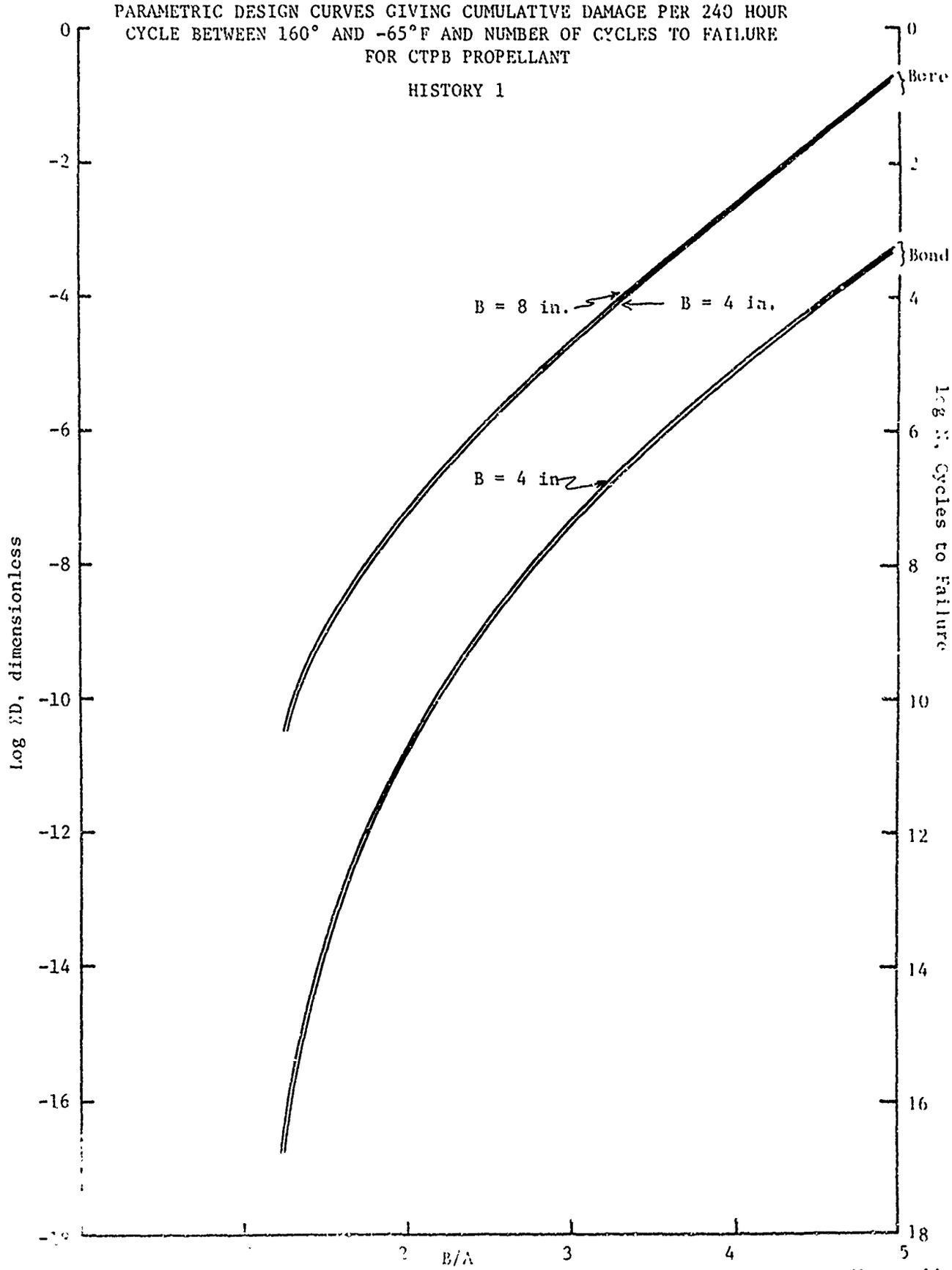

Figure 11

We have discussed the statistical approach in the past[3]. In general, we find that the first grain failure depends upon the number of grains being observed and upon the parameters which describe the statistical distributions of propellant and propellant-liner bond failures.[8] Since we do not know these latter values accurately we must put bounds on any estimates where they are used. These bounds are called "confidence limits". They are set according to a selected degree of statistical assurance that the real behavior falls within the limits set. Nearly identical values were obtained for the inner-bore hoop strains of the two propellants (Figures 9 and 12), while the bond stresses for the HTPB propellant (Figure 13) are less than those for the CTPB propellant, Figure 10 (80.2 psi versus 88.2 psi at a $(B/A)^2$ of 25). The design curves for the CTPB propellant, following History 1, are simply presented above. Now, we shall consider those for the HTPB propellant.

b. Parametric Design Curves for the HTPB Propellant - History 1

These curves are given in Figures 12 to 14. They were prepared as described above for the CTPB propellant. Essentially the same cumulative damage results are obtained for the two propellants (Figures 11 and 14), although markedly different values were expected based upon motor thermal cycling tests; dashed lines on Figure 14 show this.

It is believed that dilatation in the HTPB propellant provides the basic reason for the observed, superior, thermal cycling capability. As shown in References 1 and 2, strain dilatation causes marked decreases in the inner-bore stresses, strains and the associated damage fractions. This effect is described analytically in Section III.B of this report. There are no dilatation data available for the HTPB propellant. But, it is anticipated that the propellant must dilate more "readily" than the CTPB propellants. It is possible that the greater ease of strain dilatation may evince itself only in two- and three-dimensional test modes.

Although the dilatation and other effects may be real, they are not available to us. Therefore, in designing grain structures with HTPB propellant, we should use the curves shown in Figures 12 to 14 as conservative guides.

As described above, statistical methods must be employed to define appropriate boundaries on the stresses and strains and to predict the "expected" first-failures for any set of motors under consideration.

This completes the evaluation of thermal History 1 and the presentation of its parametric design curves. The next two sub-sections provide the same results for thermal History 2.

Aerojet Solid Propulsion Company
Report 1341-26F

PARAMETRIC DESIGN CURVES FOR INNER-BORE HOOP STRAIN AT 240 HR, HTPB PROPELLANT - HISTORY 1

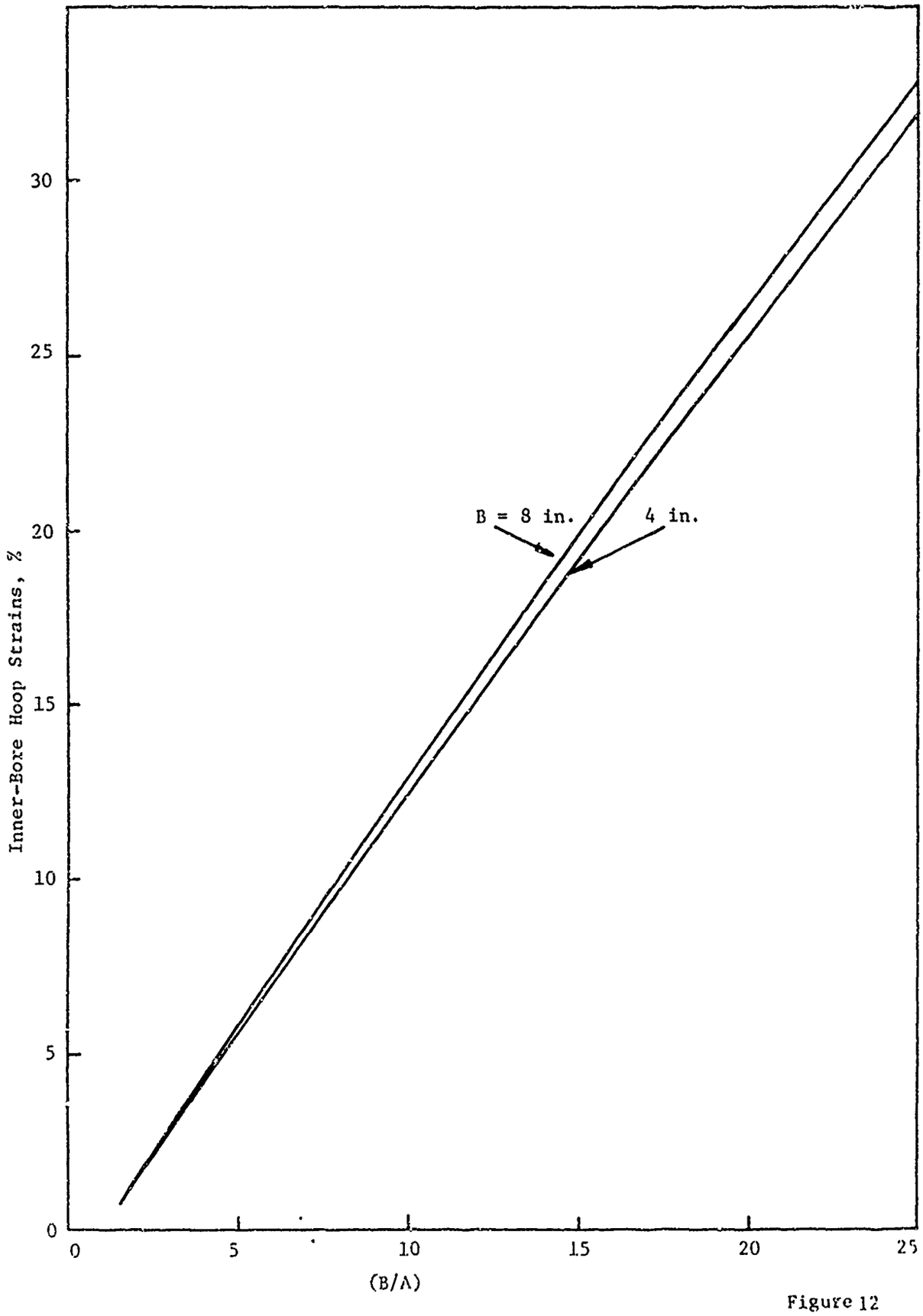

Figure 12

PARAMETRIC DESIGN CURVES FOR RADIAL BOND STRESS AT 240 HR.
HTPB PROPELLANT - HISTORY 1

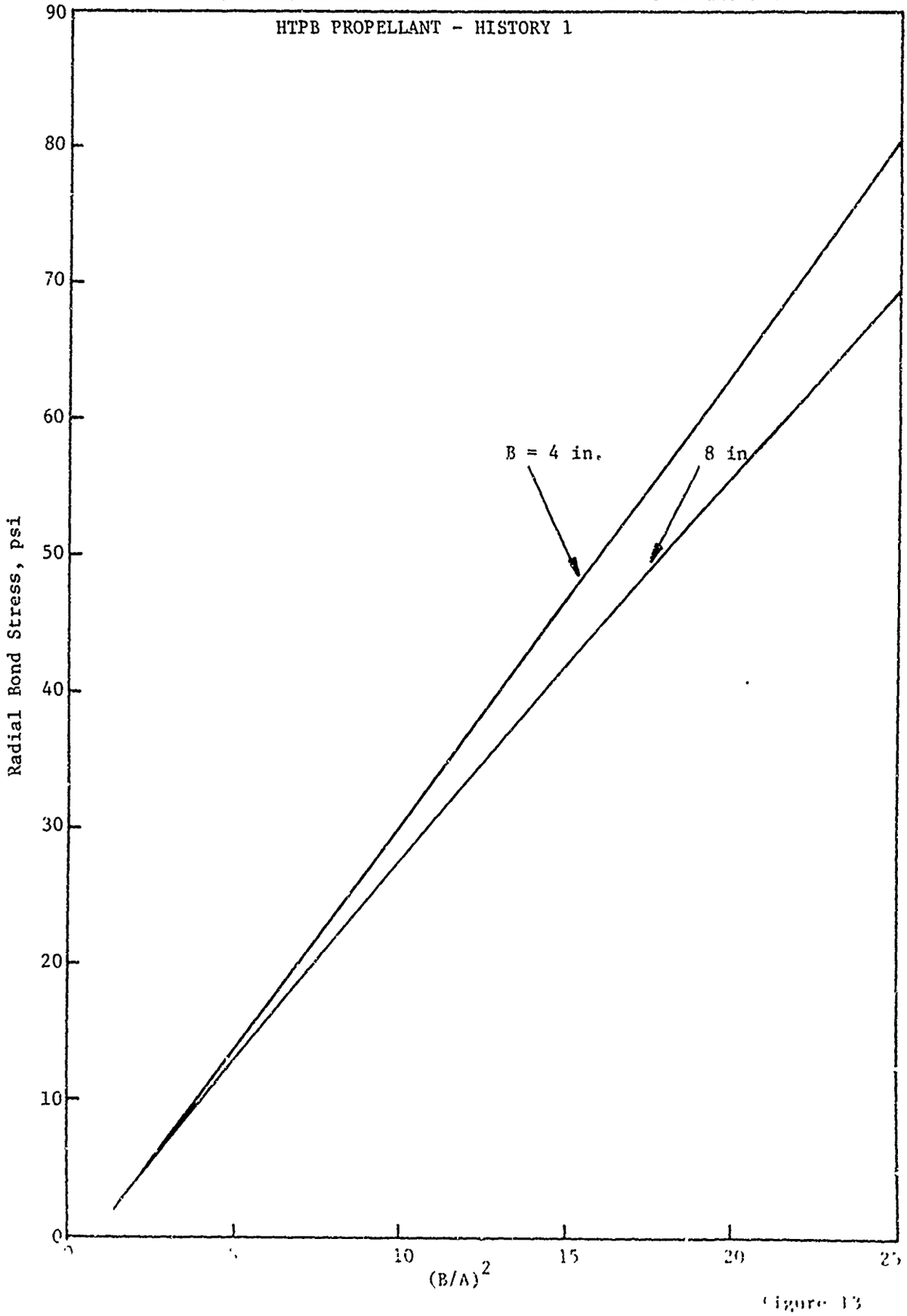

Figure 13

PARAMETRIC DESIGN CURVES GIVING CUMULATIVE DAMAGE PER 240 HOUR CYCLE BETWEEN 160° AND -65°F AND NUMBER OF CYCLES TO FAILURE FOR HTPB PROPELLANT

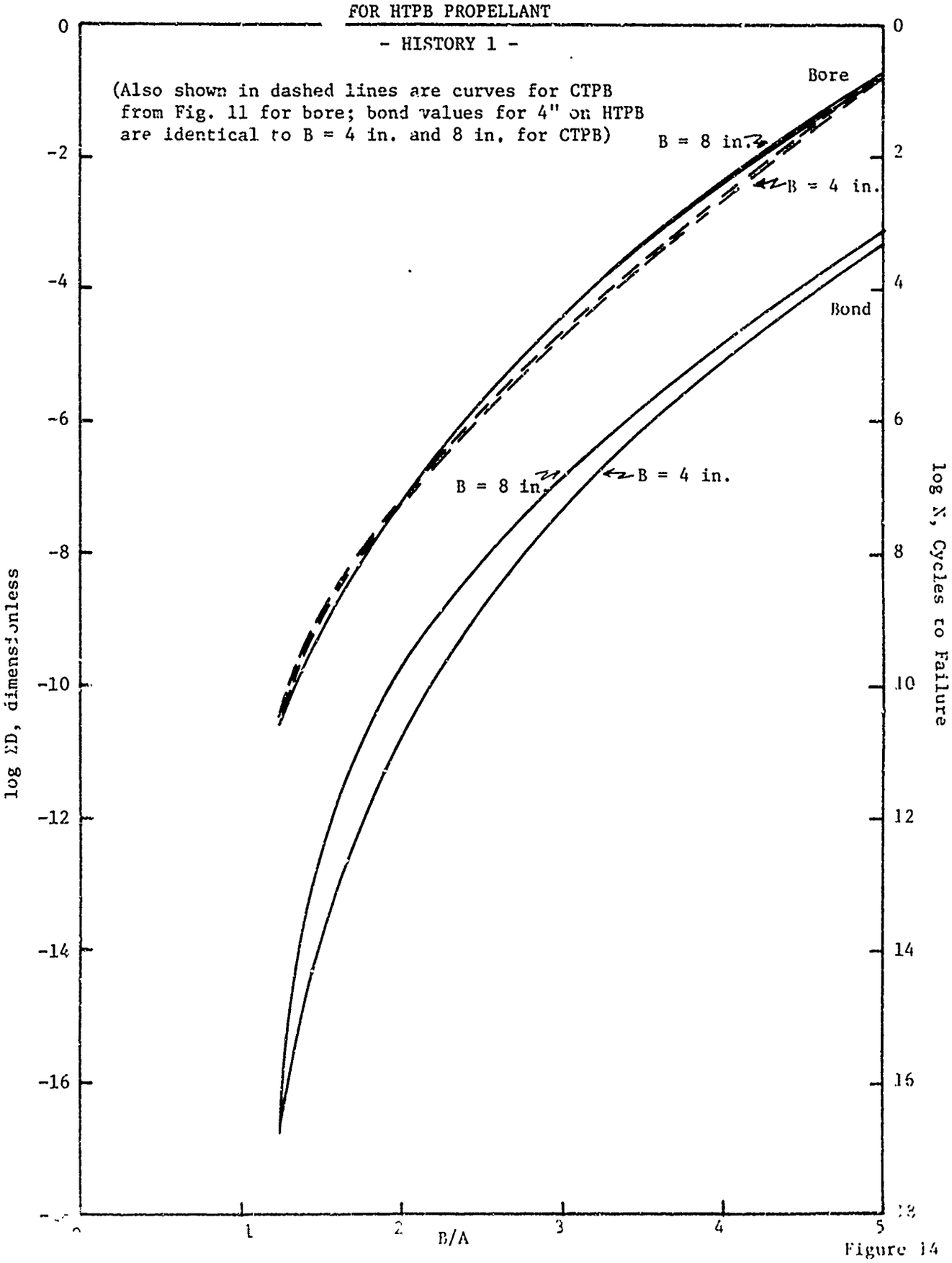

Figure 14

3. History 2

History 2 involves repeated thermal cycling between -65° and +160°F; the environmental temperature being changed instantaneously and held 48 hours at each temperature. The solutions to the thermoviscoelastic analyses are presented in Appendix C.

a. Parametric Design Curves for the CTPB Propellant - History 2

The parametric design curves for the CTPB propellant are given in Figures 15 to 17. The inner-bore hoop strains and the radial bond stresses were taken after 48 hours storage at -65°F, while the cumulative damage was taken for one complete thermal cycle beginning with 48 hours storage at -65°F followed by 48 hours at 160°F. Each of the subsequent thermal cycles duplicated this first one.

The inner-bore hoop strains are plotted in Figure 15 versus $(B/A)^2$. The results are very close to those observed for this propellant during thermal History 1.

The radial bond stress design curves are provided in Figure 16. As observed for History 1, the stresses are largest for the smaller diameter motor. These stresses for the 8 in. radius grains are almost identical to those for History 1, while the 4 in. diameter grain evinces much larger stresses when following History 2 (i.e., 98.3 psi versus 88.3 psi at $(B/A)^2$ equal to 25).

The cumulative damage results are given in Figure 17. They are relatively close to those obtained for History 1; see Figure 11. Again failures should be expected at the bore rather than at the bond.

The average number of cycles to failure is very important in this type of testing. From Figure 17 it is seen that at a B/A of 5 the 4 in. radius grain should endure on the average about 2.3 cycles while the 8 in. radius grain should hold 6.3 cycles.

b. Parametric Design Curves for the HTPB Propellant - History 2

These curves are presented in Figures 18 to 20. As with the CTPB propellant the inner-bore hoop strains, Figure 18, are negligibly affected by the change in thermal histories (History 2 compared to History 1). The radial bond stresses, Figure 19, show negligible differences for the 8 in. radius grains, while the 4 in. radius grains show a small increase in the bond stresses on following History 2 (i.e., about 3 psi at $(B/A)^2$ equal to 25).

PARAMETRIC DESIGN CURVES FOR INNER-BORE HOOP STRAIN AFTER 48 HRS. AT -65°F

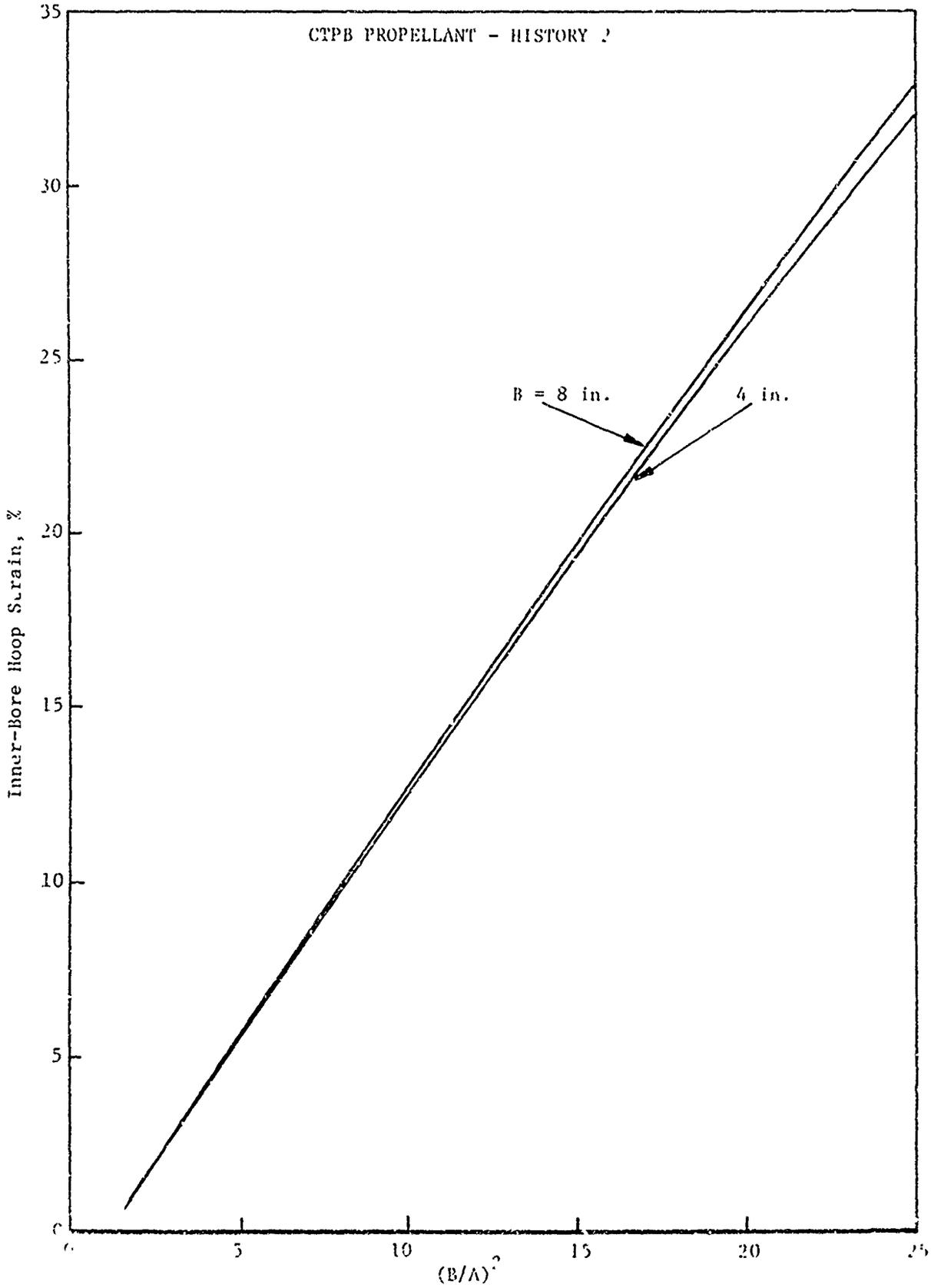

Figure 15

PARAMETRIC DESIGN CURVES FOR RADIAL BOND STRESS AFTER 48 HOURS AT -65°F

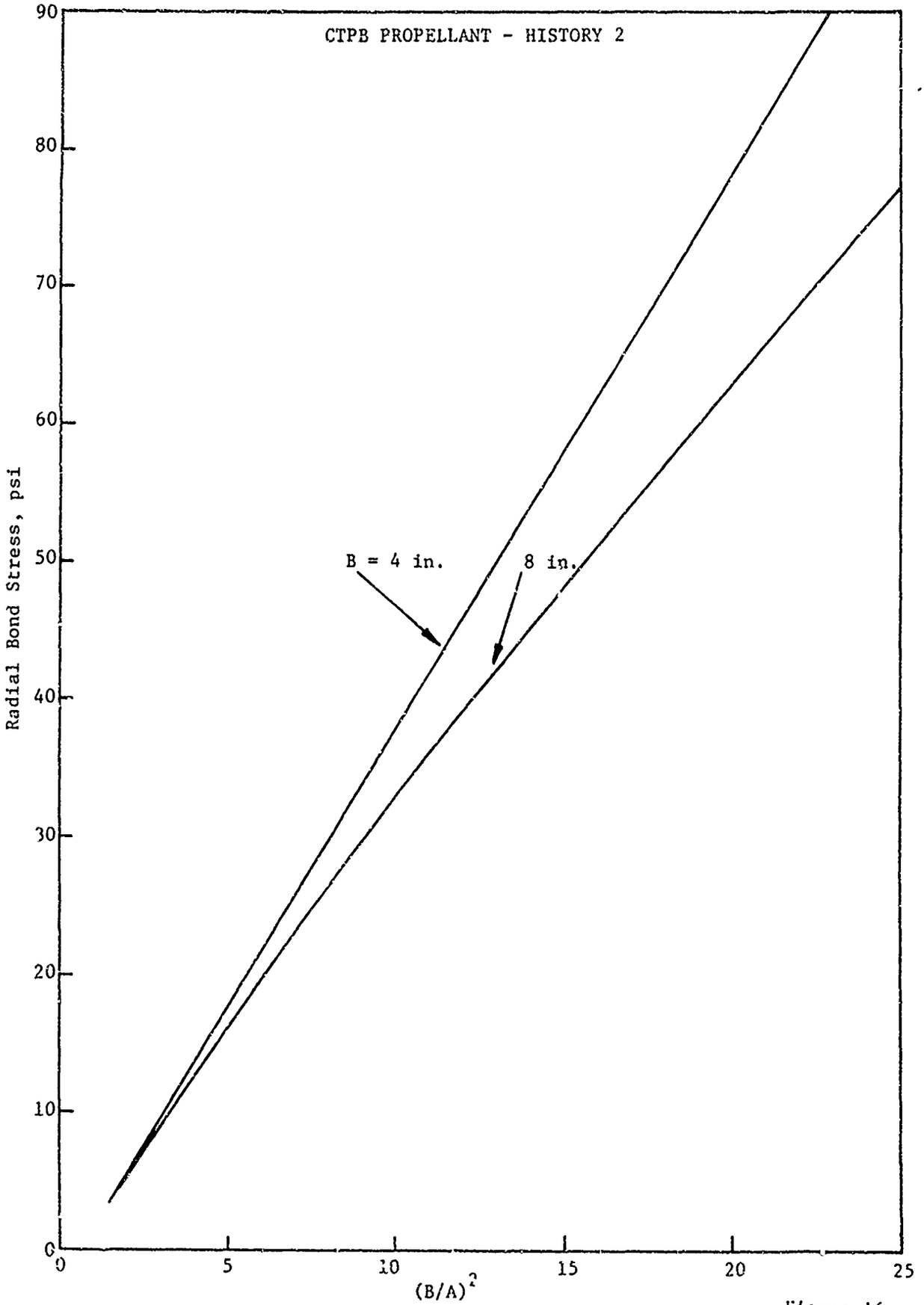

Figure 16

PARAMETRIC DESIGN CURVES GIVING CUMULATIVE DAMAGE PER 96 HOUR CYCLE BETWEEN -65° AND 160°F AND NUMBER OF CYCLES TO FAILURE FOR CTPB PROPELLANT
- HISTORY 2 -

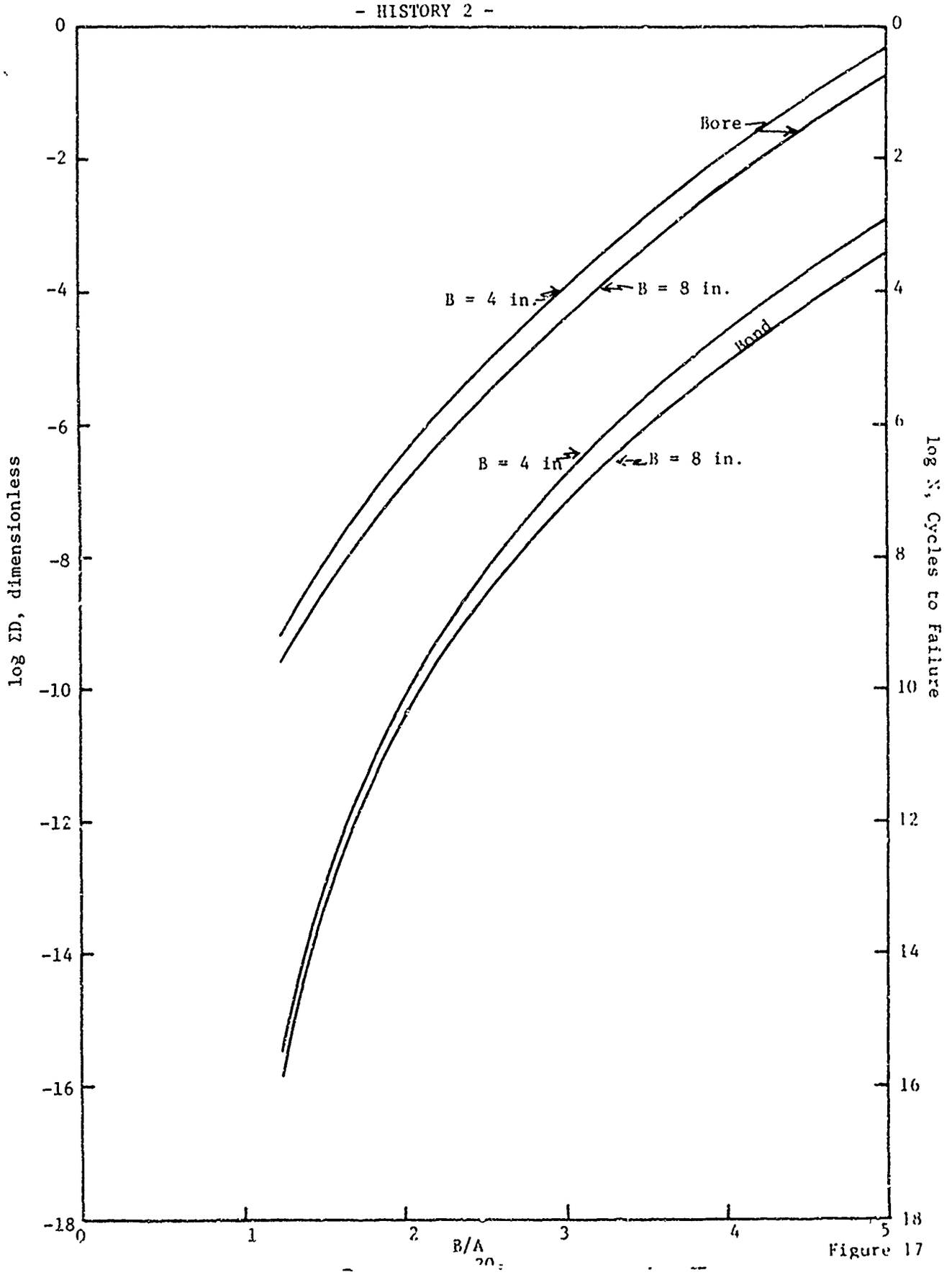

Figure 17

PARAMETRIC DESIGN CURVES FOR INNER-BORE HOOP STRAIN AFTER 48 HRS. AT -65°F

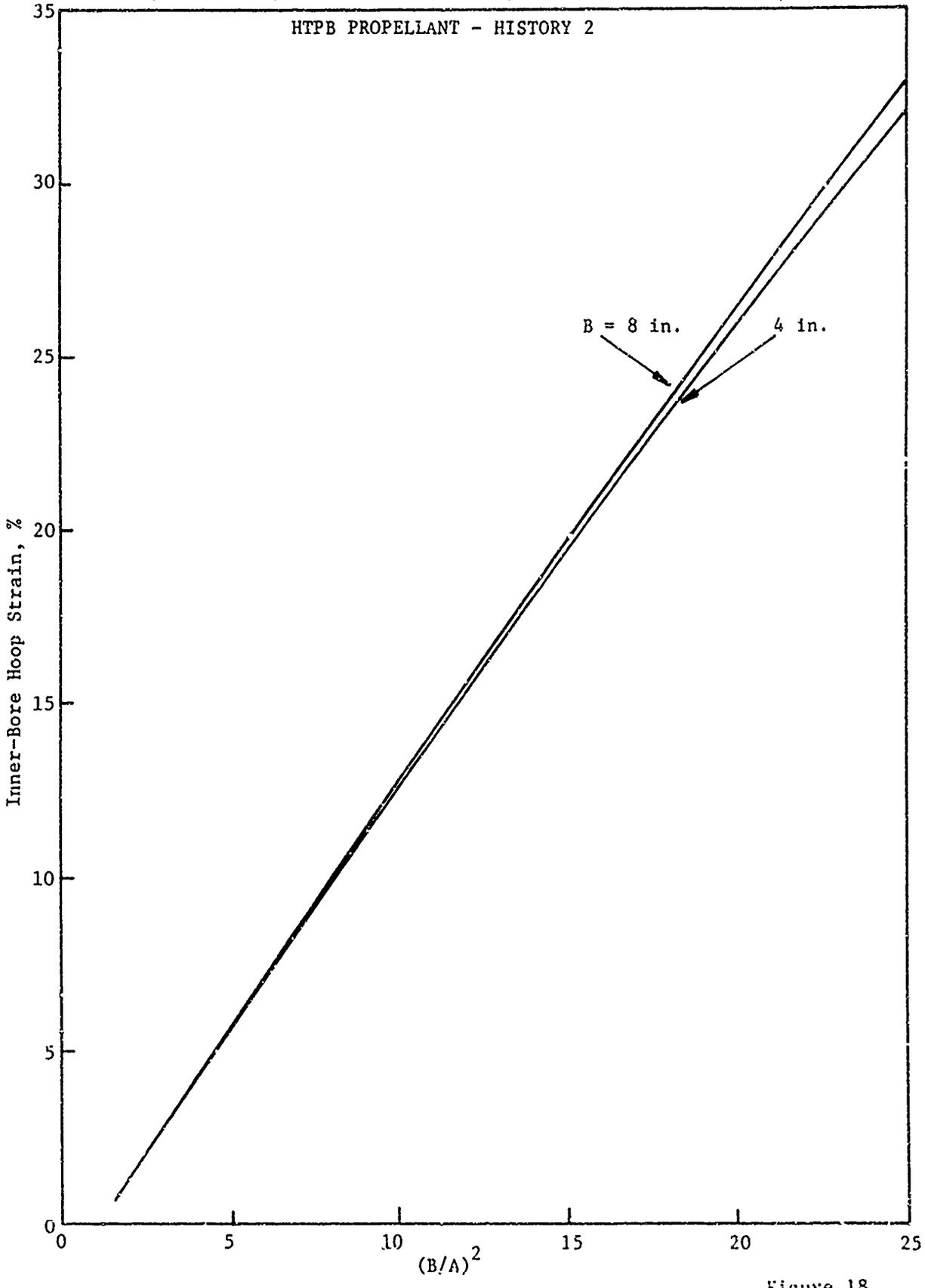

Figure 18

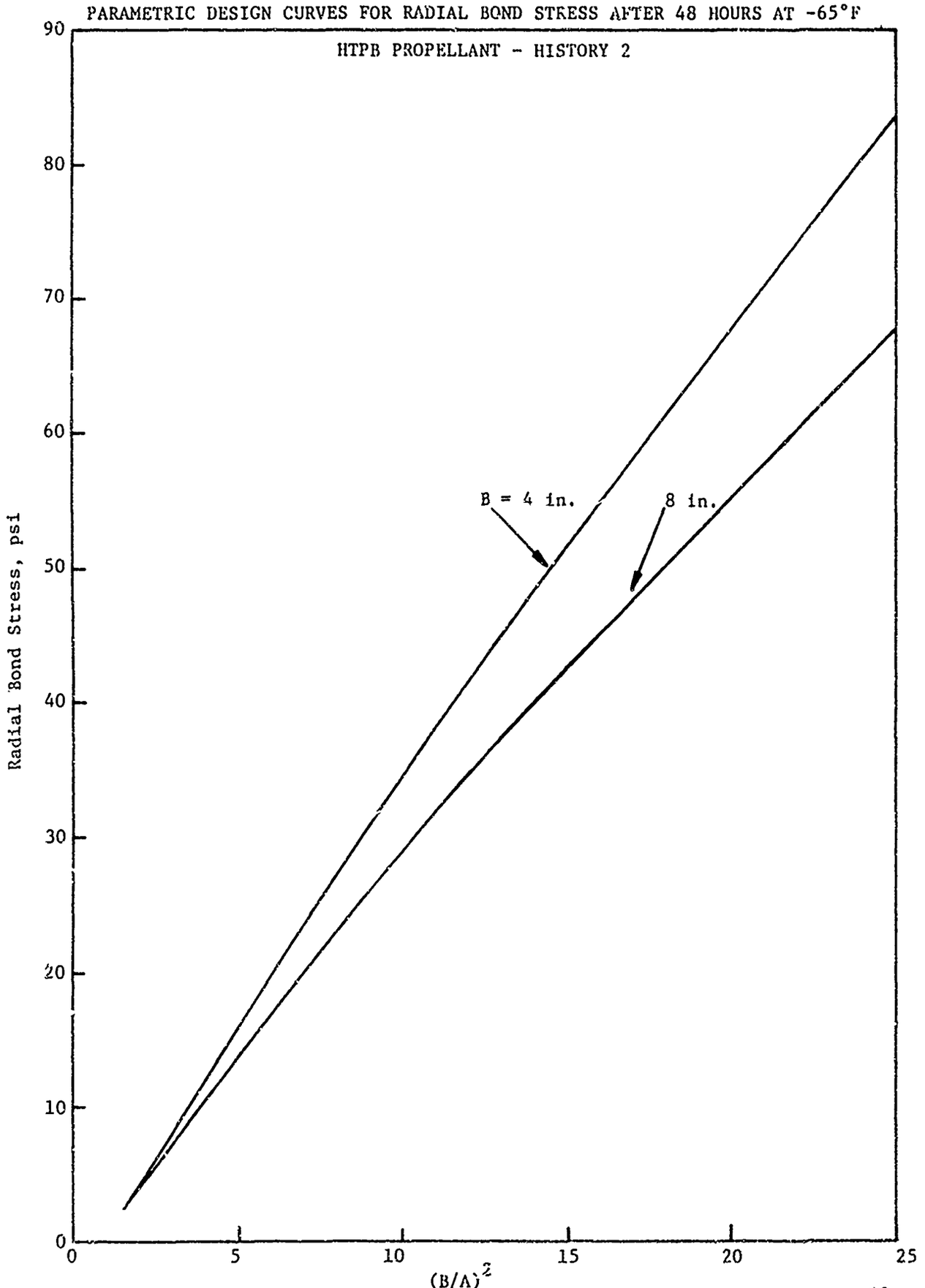
PARAMETRIC DESIGN CURVES FOR RADIAL BOND STRESS AFTER 48 HOURS AT -65°F
HTPB PROPELLANT - HISTORY 2
Radial Bond Stress, psi
90
80
70
60
50
40
30
20
10
0
B = 4 in.
8 in.
0
5
10
15
20
25
(B/A)²

Figure 19

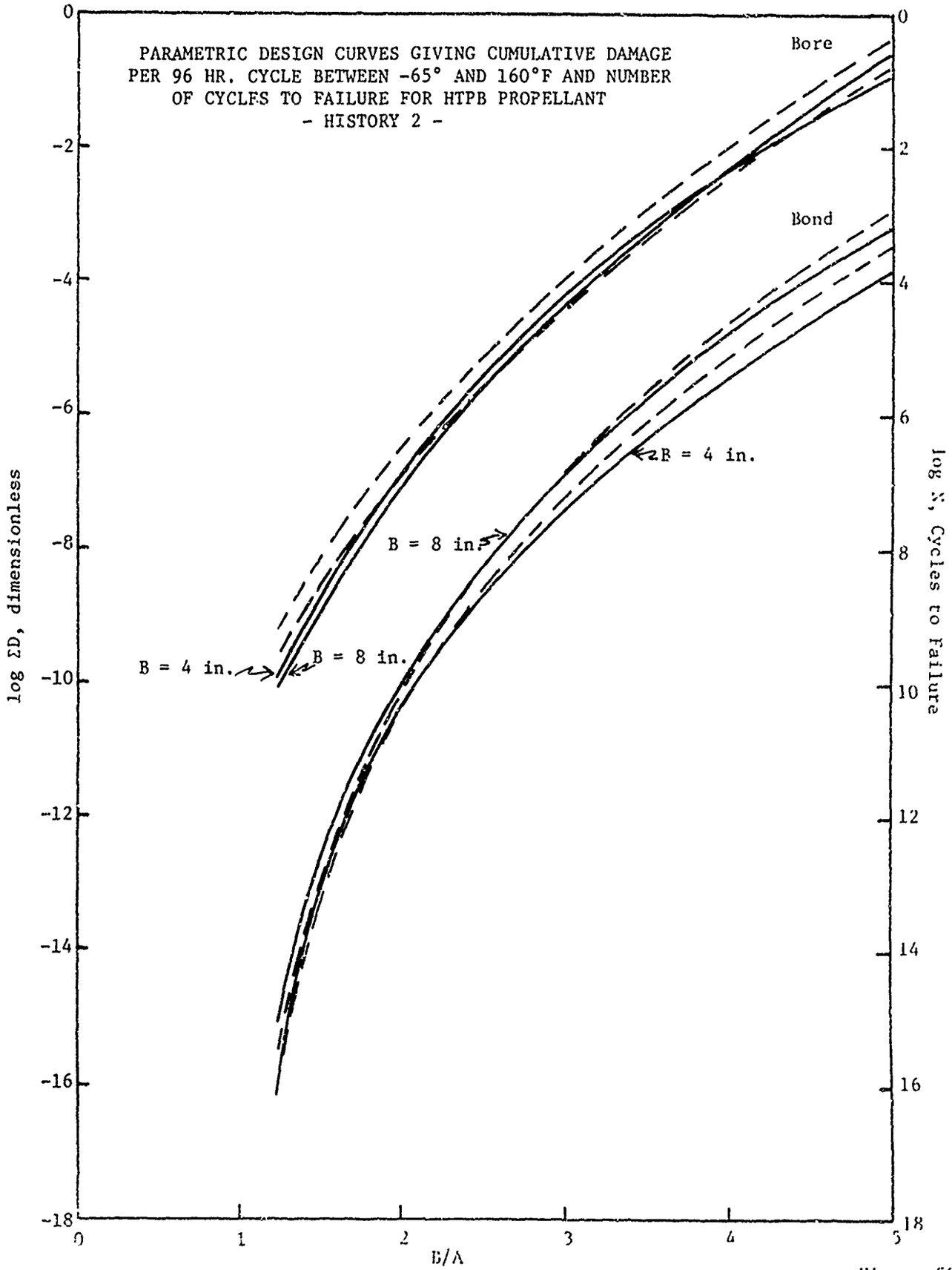
PARAMETRIC DESIGN CURVES GIVING CUMULATIVE DAMAGE
PER 96 HR. CYCLE BETWEEN -65° AND 160°F AND NUMBER
OF CYCLES TO FAILURE FOR HTPB PROPELLANT
- HISTORY 2 -
Bore
Bond
B = 4 in.
B = 8 in.
B = 4 in.
B = 8 in.
log ΣD, dimensionless
log N, Cycles to Failure
B/A
0
-2
-4
-6
-8
-10
-12
-14
-16
-18
2
4
6
8
10
12
14
16
18
1
3
5

Figure 20

The cumulative damage curves for HTPB show a greater difference from CTPB for History 2 than for History 1. This is illustrated by showing in dashed lines the CTPB values from Figure 17 on Figure 20.

The parametric design curves presented above were based upon analyses for given propellant systems. In the next section considerations are made for normalizing these analyses so that they can be applied to propellants with a range of properties.

E. NORMALIZING AND EVALUATING THE ANALYTICAL RESULTS

In any motor development program a propellant is selected, then evaluated to determine its suitability for the intended use. Structurally, the propellant is evaluated by stress analyses and some type of failure criterion. If the propellant proves to be unsatisfactory a new formulation is selected and the analyses repeated. These repetitions are costly and highly time consuming (so much so that frequently only a few alternatives are evaluated).

We have looked for, and found, methods to do the following: (1) structurally evaluate a typical propellant for a given application; (2) normalize the analytical results; and (3) simply evaluate a new formulation in terms of the normalized results without recourse to new analyses. Of course, the compositions of the new candidates should be similar to the one originally evaluated.*

To accomplish these objectives normalizations schemes for the relaxation modulus, inner-bore hoop strains and bore and bond stresses were developed. The damage relations were not so readily generalized, so, considerations for the interrelationships of strength and modulus were obtained and are provided here. These serve primarily as qualitative guides which may be useful in ranking expected structural performances.

The normalization procedures were established with the recognition that propellants employed for case-bonded grains are limited to a rather narrow range of moduli, when compared under any given test condition. This narrow range of modulus permits us to use some simplifying assumptions in defining the effects of key parameters.

The manner in which the range of propellant modulus is used will be described below. First, however, we shall consider a unique normalization procedure for describing propellant relaxation moduli. Our study depends directly upon this result.

---

* Specifically, the properties of the various candidates should follow the same a_T curves and the same normalized relaxation moduli (described next). Because of the production variabilities, identical values are not required, rather the values should be within the expected range for both the original and the alternate formulations.

1. Normalization of the Relaxation Modulus

It is conventional to express the tensile relaxation modulus in E(t), by the following general relation*:

$$E(t) = E_e + (E_g - E_e) \int_{-\infty}^{\infty} h_\ell^{-t/\tau} \, d\ell n\tau \qquad (1)$$

where E_g is the glassy tensile modulus

E_e is the equilibrium tensile modulus

h_ℓ represents a continuous distribution of relaxation times (normalized)

t is the time of the test

τ is a relaxation time

In general, it is very difficult to evaluate E_g experimentally. The value appears to vary significantly with the test conditions and with the method of testing, and most of the tests for this property are rather costly. Although it is conventional to use this quantity in basic studies we have found it to be unnecessary for practical engineering work.

A completely satisfactory substitute for E_g is the relaxation modulus evaluated at some experimentally convenient time. We have used the tensile modulus at one minute, E(1). The resulting relation using this parameter becomes (see Appendix D).

$$E(t) = E_e + (E(1) - E_e) \int_{-\infty}^{\infty} h'_\ell \, e^{-t/\tau} \, d\ell n\tau \qquad (2)$$

where h'_ℓ is a modified distribution of relaxation times

---

* The derivation is given in Appendix D. In that appendix we have used the shear modulus, $\mu(t)$, rather than the tensile modulus, E(t), since the stress analyses are specifically written around this quantity. However, the near incompressibility of propellants gives $E(t) \approx 3\mu(t)$. So, the two moduli can be used interchangeably.

This relation is simply derived as shown in Appendix D. It requires a minor modification in the function describing the distribution of relaxation times, h_ℓ'.

This equation permits us to define the relaxation modulus in terms of two constants, E_e and E(1), and the distribution of relaxation times, h_ℓ'. It is felt that h_ℓ' varies only slightly for propellants of a given type. Nevertheless, a broad range of relaxation curves can be represented for a given h_ℓ' by letting the two constants E_e and E(1) take on different values. Figure 21 shows a set of tensile relaxation modulus curves which differ only in the constants E_e and E(1).

The constant E_e usually falls outside the range of experimental observations, but few find it difficult to estimate. However, it too can be replaced by the relaxation modulus at some very long time, if desired. This can be seen by a further rearrangement of Equation (2). We did not consider that to be important to our parameter study, so it was not done here.

Equation (2) forms the technical basis for our normalization procedures. This normalization method defines the modulus in terms of two easily determined constants, E_e and $E(1) - E_e$. Also, as shown in Appendix D the same normalization applies to the Prony Series equation for the relaxation modulus. Since our engineering analyses depend directly upon the Prony Series relations it was expected that the calculated stresses and strains could be normalized using the same two modulus constants. Initial results considering these parameters are given below.

2. Normalization of Inner-Bore Hoop Strains

The inner-bore hoop strains are generally taken to be normalized already; and, in practice, we find this to be an adequate approximation. However, analytically the grain and case deflections vary inversely with the grain stresses, which, in turn, vary with propellant moduli. Accordingly, we considered the two principal strains at each time in the thermal histories described. Within a limited range of propellant moduli we found the principal strains to be stress dependent and to follow the

$$\left.\begin{aligned} \varepsilon_r\,(x, t, \sigma_r) &= \varepsilon_r\,(x, t, 0) - C\,(x, t, r)\,\sigma_r\,(x, t) \\ \varepsilon_\theta\,(x, t, \sigma_\theta) &= \varepsilon_\theta\,(x, t, 0) - C\,(x, t, \theta)\,\sigma_\theta\,(x, t) \end{aligned}\right\} \qquad (3)$$

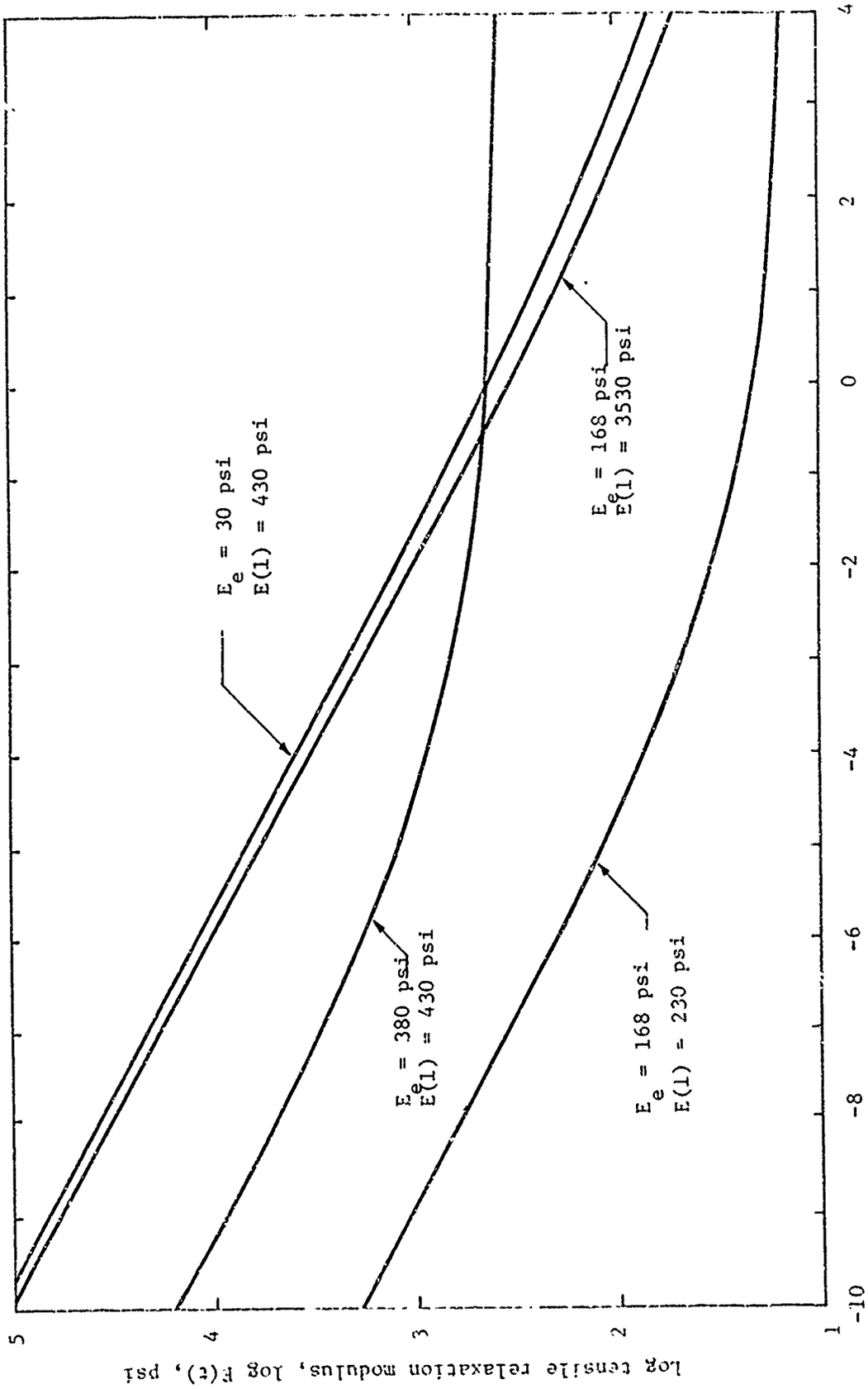

EFFECT OF VARIATION IN PARAMETERS UPON CURVES OF RELAXATION MODULUS WHICH ARE REPRESENTED BY THE SAME DISTRIBUTION OF RELAXATION TIMES

Figure 21

where

ε_r (x, t, σ_r) and ε_θ (x, t, σ_θ) are the principal strains in the radial and hoop directions expressed as functions of position, time and principal stress.

ε_r (x, t, 0) and ε_θ (x, t, 0) are the principal strains at zero stress.

σ_r (x, t) and σ_θ (x, t) are the principal stresses in the radial and hoop directions, respectively.

C (x, t, r) and C (x, t, θ) are position, time and orientation dependent functions which are analytically evaluated.

The analytically determined parameters C are obtained directly from corresponding solutions of elastic and viscoelastic stress analyses. When evaluated at a given time, $t = t_i$, Equations (3) become simple linear relations and their parameters C and ε (x, t_i, 0) become constants.

Three examples were prepared to show the variation of C (x, t, θ) at the inner-bore with time. These are given in Figure 22 for the CTPB propellant following History 1. The values show erratic behavior at very small strains (attributed to errors in significant figures) and when the stresses and strains are being rapidly changed. But, for the most part the C (bore, t, θ) values are nearly constant, depending only upon grain dimensions.

The inner-bore hoop strain at zero stress, ε_θ (bore, t, 0), varies regularly with step changes in the environmental temperature, Figure 23. The behavior is about as would be expected for this parameter.

3. Normalization of Grain Stresses

Examination of the analytical results for the grain stresses indicated the following relations to apply.

$$\left.\begin{aligned} \sigma_r\ (x, t) &= V\ (x, t, r)\ E_e + W\ (x, t, r)\ [E(1) - E_e] \\ \sigma_\theta\ (x, t) &= V\ (x, t, \theta)\ E_e + W\ (x, t, \theta)\ [E(1) - E_e] \end{aligned}\right\} \qquad (4)$$

COMPARISON OF VALUES OF C(bore, t, θ) FOR GRAINS FOLLOWING THERMAL HISTORY 1
- SELECTED DESIGNS -

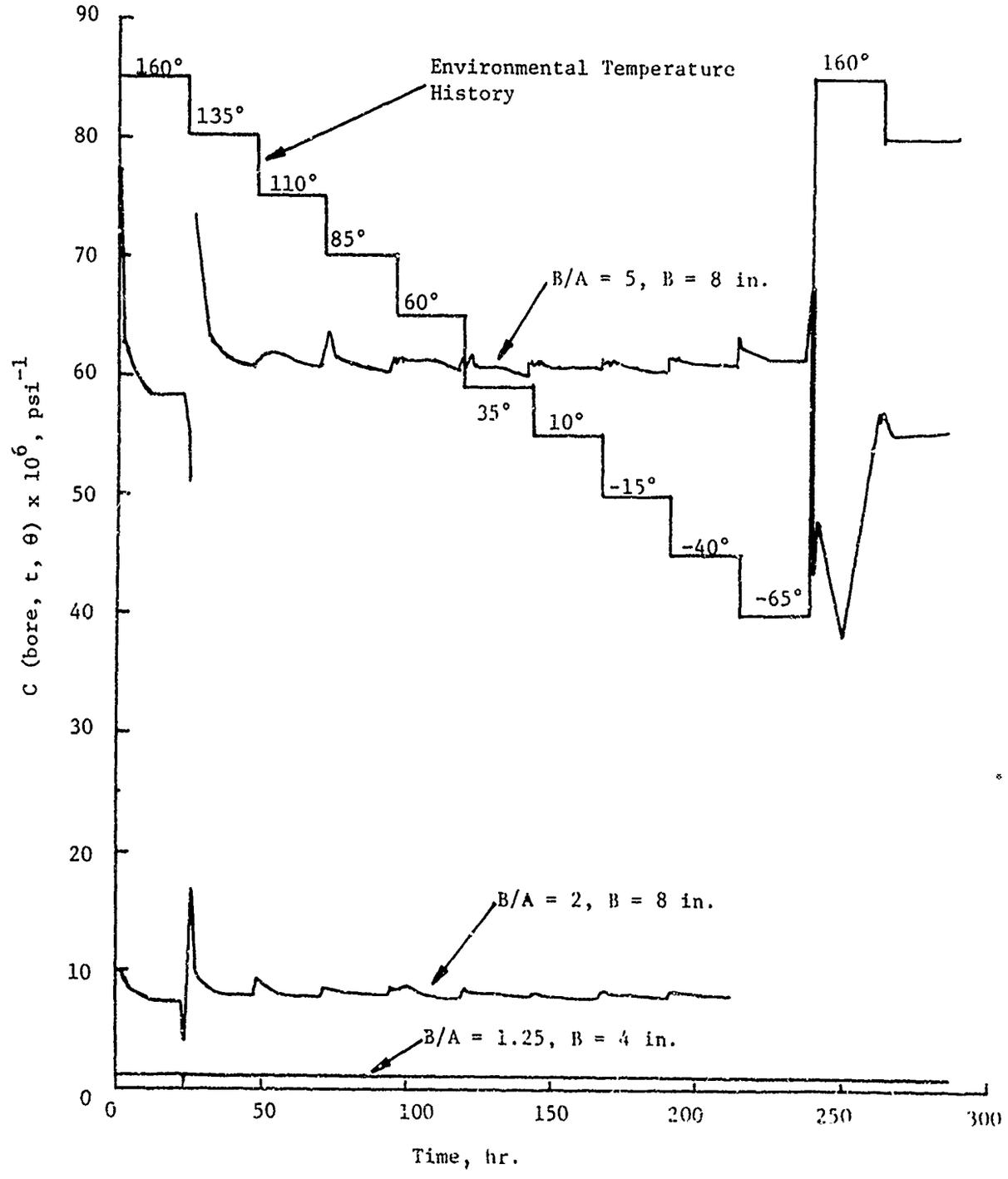

Figure 22

BORE STRAIN AT ZERO STRESS FOR CTPB PROPELLANT - HISTORY I
(B/A = 5, B = 8 in.)

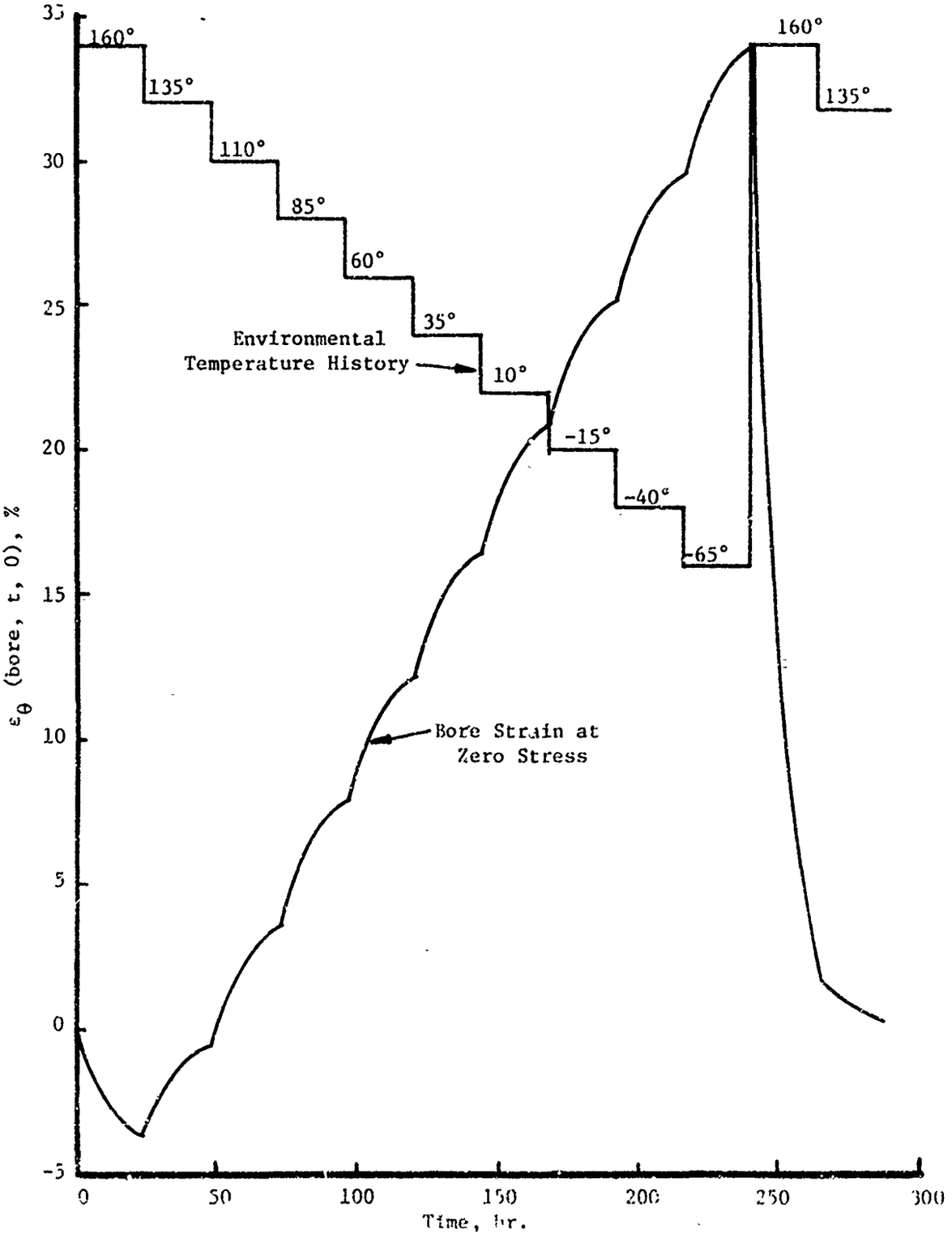

Figure 23

where $V(x, t, r)$, $V(x, t, \theta)$, $W(x, t, r)$ and $W(x, t, \theta)$ are position, time and orientation dependent functions requiring analytical evaluation.

At any given time V and W are constants and Equations (4) become simple linear relations. In use, V and W are evaluated for the initial candidate propellant only for the crucial times and locations. The corresponding grain stresses for a new propellant formulation are readily calculated given its equilibrium modulus, E_e, and the relaxation modulus at one minute, E(1).

This approach is limited to propellant formulations whose moduli are less than three times those of the initial candidate propellant. In general, this presents no serious difficulty since in a given application the moduli of most candidate propellants fall in a range that is within a factor of two of the lowest values.

Table 2 provides comparisons between the analytically calculated grain stresses and those estimated using Equations (4). The comparisons are made for various combinations of the propellant moduli, beginning with the elastic values ($E(1) - E_e = 0$) extending up to two times the moduli of the reference propellant.* The comparisons show a maximum difference of about 3.5% in Case 4 at B = 8 in., B/A = 5, for both the inner-bore and the cast-bond.

The effect of time on these comparisons is shown in Table 3. The comparisons are very good in all except Case 4, where during the rapid heating stage (from 240-264 hours) at 242.675 hours a very poor correlation exists. However, after 245.5 hours the comparison again becomes excellent.

From these considerations we see that the stress Equations (4) apply very well at moderate stresses and when the rate of change of stress is not great.

The stress relations (4) provide the best guide to propellant formulating developed to date. Also, because of the relationships of E_e and $E(1) - E_e$ to propellant physics we have a basis for evaluating the effects of polymer structure, the oxidizer-binder bond, and the filler factor. The details of these considerations are not appropriate to this report, but their development and potential application are clear.

* It was intended to compare the estimates with the calculated values for a propellant with moduli three times those of the reference propellant, but an erroneous input in the analysis invalidated the results.

COMPARISON OF ESTIMATED AND ANALYTICAL VALUES OF GRAIN STRESSES
FOR THE CTPB PROPELLANT FOLLOWING HISTORY 1 AT 240 HOURS

Case	Propellant Modulus E_e	Propellant Modulus $E(1) - E_e$	Stresses, Estimated/Analytical, psi B = 4 in. B/A = 1.25	B = 4 in. B/A = 2	B = 4 in. B/A = 5	B = 8 in. B/A = 1.25	B = 8 in. B/A = 2	B = 8 in. B/A = 5
			Inner-Bore Hoop Stresses					
1*	100	0	3.17/3.17	8.05/8.05	48.5/48.5	3.2/3.20	8.07/8.08	48.5/48.5
2*	100	310	11.8/11.9	29.6/29.6	172/172	11.8/11.9	28.8/28.8	153.3/153.3
3	200	310	15.0/-	37.7/-	221/-	15.0/15.1	36.9/36.8	202/199
4	200	620	23.7/-	59.2/-	345/-	23.7/23.7	57.6/57.2	307/296
			Radial Bond Stresses					
1*	100	0	0.566/0.567	3.08/3.08	24.7/24.7	0.574/0.574	3.06/3.06	24.0/24.0
2*	100	310	2.12/2.12	11.4/11.4	88.2/88.2	2.13/2.13	11.0/11.0	77.7/77.7
3	200	310	2.68/-	14.4/-	113/-	2.70/2.70	14.1/14.1	102/99.8
4	200	620	4.23/-	22.8/-	176/-	4.26/4.25	22.1/21.9	154/149

* Candidate propellants from which parameters V and W were determined.

- Stress analysis was not performed.

Table 2

COMPARISON OF ESTIMATED AND ANALYTICAL VALUES OF GRAIN STRESSES VERSUS TIME FOR THE CTPB PROPELLANT FOLLOWING HISTORY 1

Time, hr.	$E_e/[E(1) - E_e]$ =	Estimated Stress/Calculated Stress			
		Case 1 (100/0)	Case 2 (100/310)	Case 3 (200/310)	Case 4 (200/620)
120		17.4/17.4	27.2/27.2	44.7/44.2	54.5/53.8
120.425		17.6/17.6	27.7/27.7	45.3/44.8	55.4/54.7
122.675		18.8/18.8	30.6/30.6	49.4/48.9	61.2/60.4
125.5		20.0/20.0	33.1/33.1	53.1/52.6	66.2/65.3
144		23.6/23.6	40.3/40.3	63.9/63.3	80.5/79.4
168		29.8/29.8	56.1/56.1	85.9/85.0	112/110
192		36.1/36.1	75.7/75.7	112/111	151/149
216		42.3/42.3	105/105	147/145	209/204
240		48.5/48.5	153/153	202/199	307/296
242.675		38.2/38.2	-36.2/-36.2	1.97/2.38	-72.5/-37.5
245.5		29.5/29.5	-51.3/-51.3	-21.9/-21.3	-103/-85.9
252		15.6/15.6	10.5/10.5	26.1/25.9	21.0/21.4
264		2.64/2.64	1.10/1.10	3.74/3.66	2.20/2.14

Table 3

4. Parametric Design Curves Using Normalized Properties

The normalization relations generated above can be applied readily to the analyses prepared on this program. Note that the normalized strain curves are sufficiently well approximated by Figures 9, 12, 15 and 18. If further refinements are required, then Equations (3) may be employed.

Following Equation (2) the relaxation modulus is normalized, as shown in Figure 24, upon plotting $[E(t) - E_e]/[E(1) - E_e]$ versus t/a_T on a log-log scale. Figure 24 shows the normalized modulus curves for both the CTPB and HTPB propellants.

The normalized stress values, were prepared as parametric design curves with plots of V and W, following Equations (4), versus $(B/A)^2$. The design curves for History 1, taken at 240 hours, are given in Figures 25 and 26 for the CTPB propellant and in Figures 27 and 28 for the HTPB propellant. For History 2, at 96 hours, the design curves for the CTPB propellant are contained in Figures 29 and 30 and for the HTPB propellant in Figures 31 and 32. In each case separate graphs were prepared for the inner-bore hoop stresses and for the radial bond stresses.

The use of these curves is as follows: First, the relaxation modulus of the candidate propellant is normalized as shown in Figure 24, following Equation (2). If the curve of the normalized modulus is reasonably close to that of one of the propellants and if the a_T values are in reasonable agreement with those shown in Figure 2, then we can proceed to use the normalized values in Figures 25 to 32.

Next, the particular thermal history and grain design (radii A and B) are selected. With these parameters in hand the appropriate design graph is selected. The values of V and W are read from the curves at the given values of B and $(B/A)^2$. Then, using Equations (4), the grain stress at the bore (or at the bond) is calculated.

These normalized design curves greatly extend the utility of the viscoelastic analyses; thus, saving money. A number of ramifications of this approach should be investigated further.

Although this approach permits a number of simplifications, no straightforward normalization of the failure predictions is indicated. However, consideration of the relations leads to some interesting conclusions. These are discussed next.

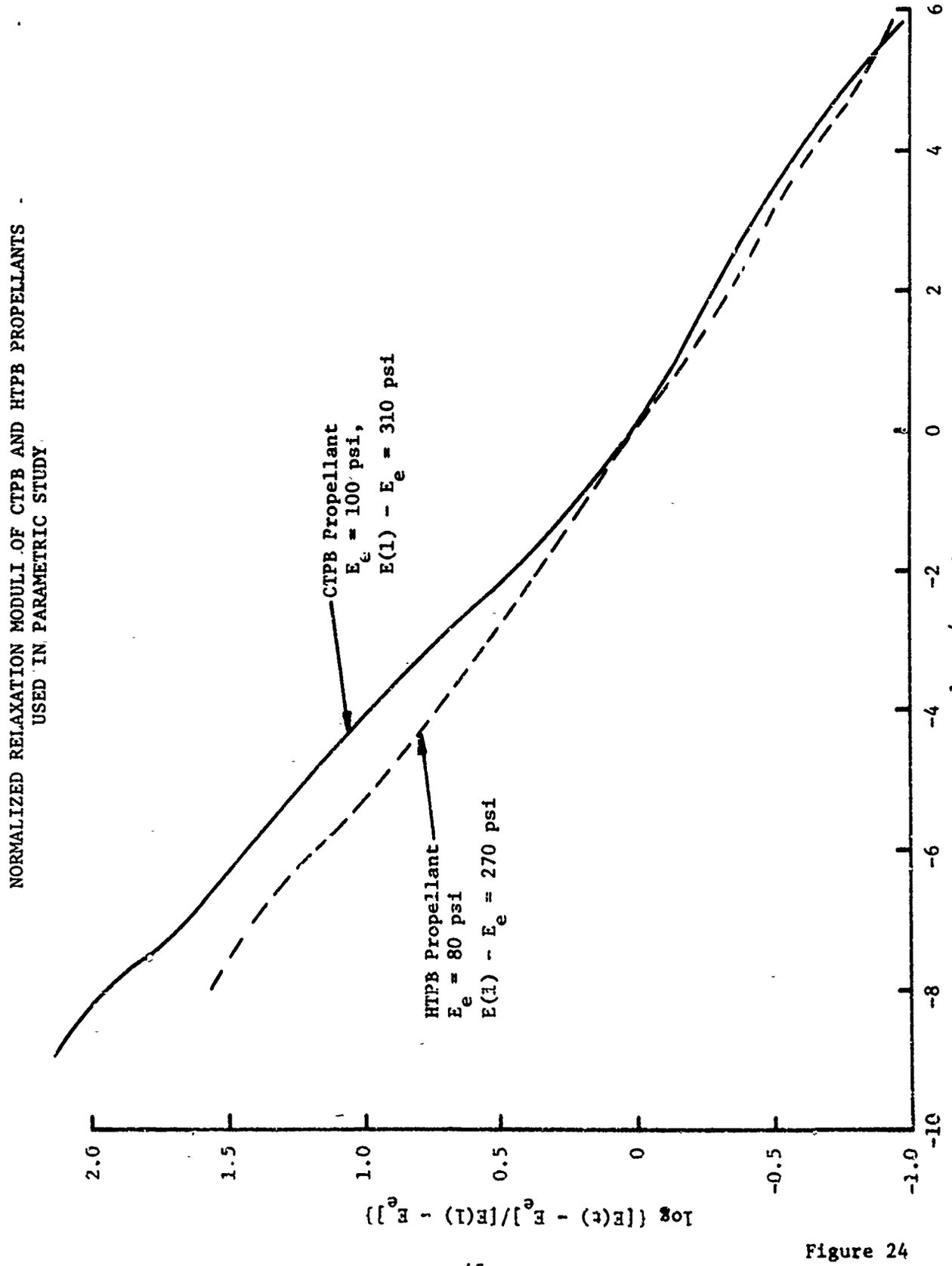
NORMALIZED RELAXATION MODULI OF CTPB AND HTPB PROPELLANTS
USED IN PARAMETRIC STUDY
CTPB Propellant
E_e = 100 psi,
E(1) - E_e = 310 psi
HTPB Propellant
E_e = 80 psi
E(1) - E_e = 270 psi
log t/a_T, min.
log $[[E(t) - E_e]/[E(1) - E_e]]$
2.0
1.5
1.0
0.5
0
-0.5
-1.0
6
4
2
0
-2
-4
-6
-8
-10

Figure 24

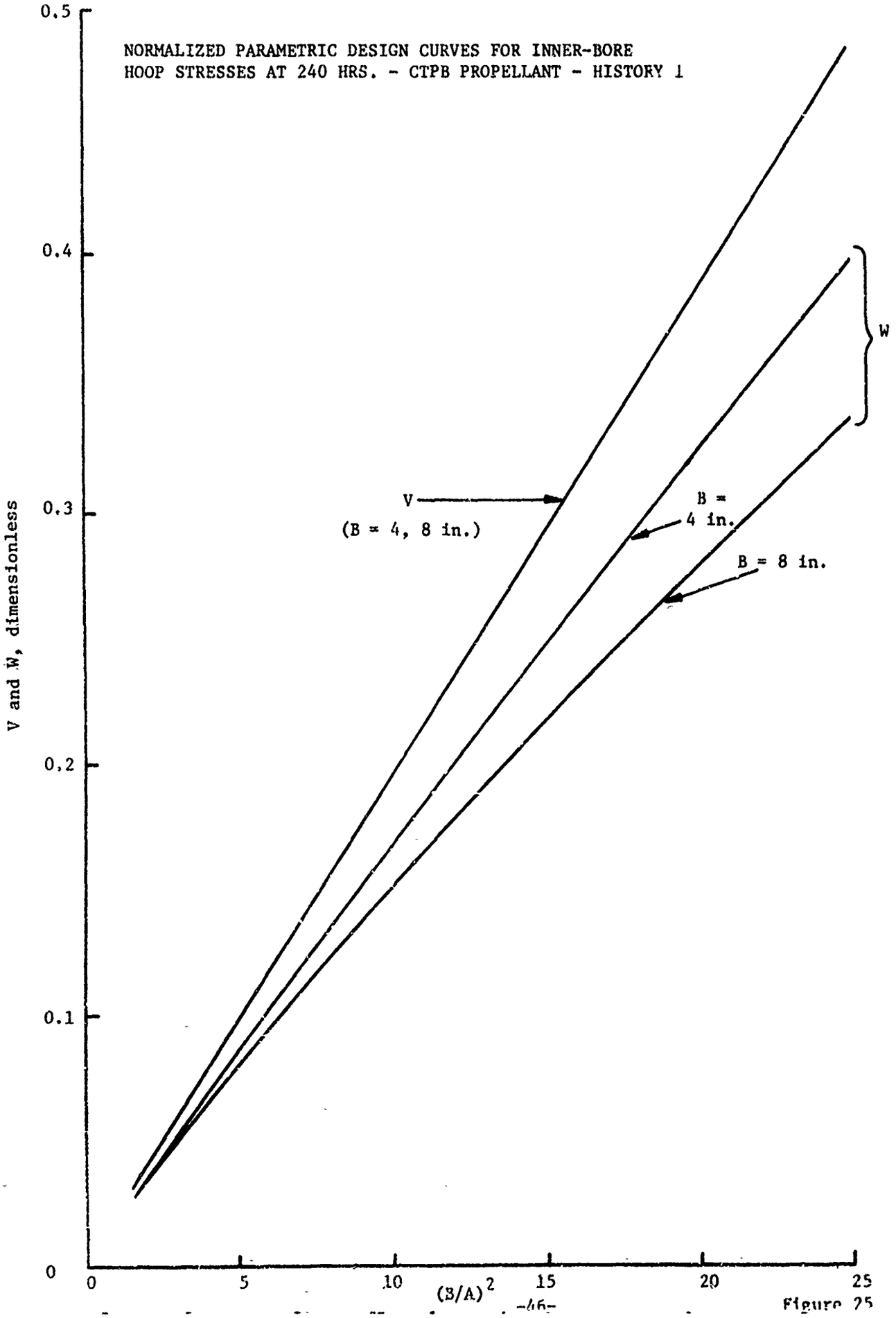
NORMALIZED PARAMETRIC DESIGN CURVES FOR INNER-BORE
HOOP STRESSES AT 240 HRS. - CTPB PROPELLANT - HISTORY 1
V and W, dimensionless
0.5
0.4
0.3
0.2
0.1
0
0
5
10
15
20
25
(B/A)2
V
(B = 4, 8 in.)
W
B = 4 in.
B = 8 in.

Figure 25

NORMALIZED PARAMETRIC DESIGN CURVES FOR RADIAL BOND STRESSES AT 240 HRS.
CTPB PROPELLANT - HISTORY 1

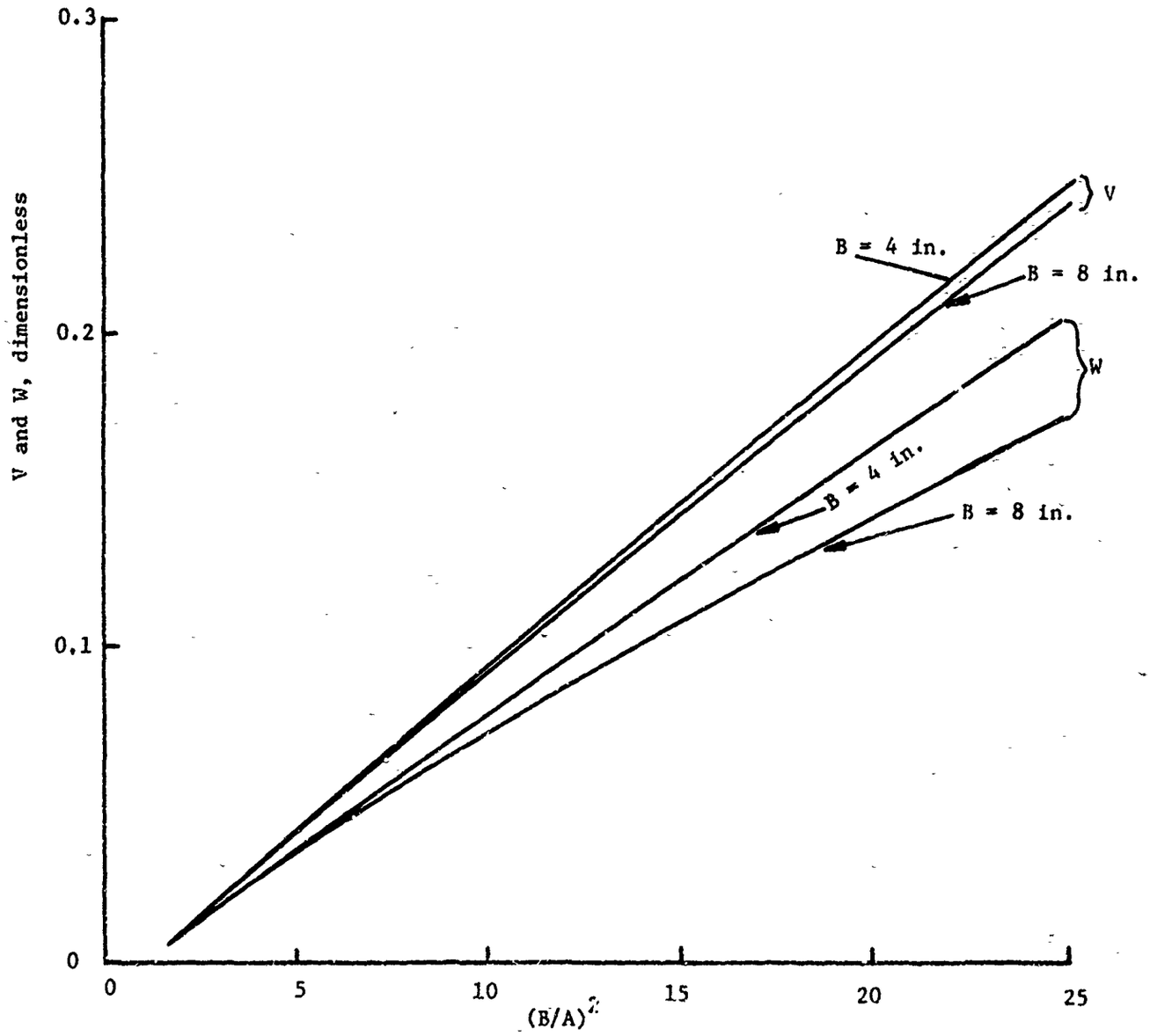

Figure 26

NORMALIZED PARAMETRIC DESIGN CURVES FOR INNER-BORE HOOP STRESSES AT 240 HRS.
HTPB PROPELLANT - HISTORY 1

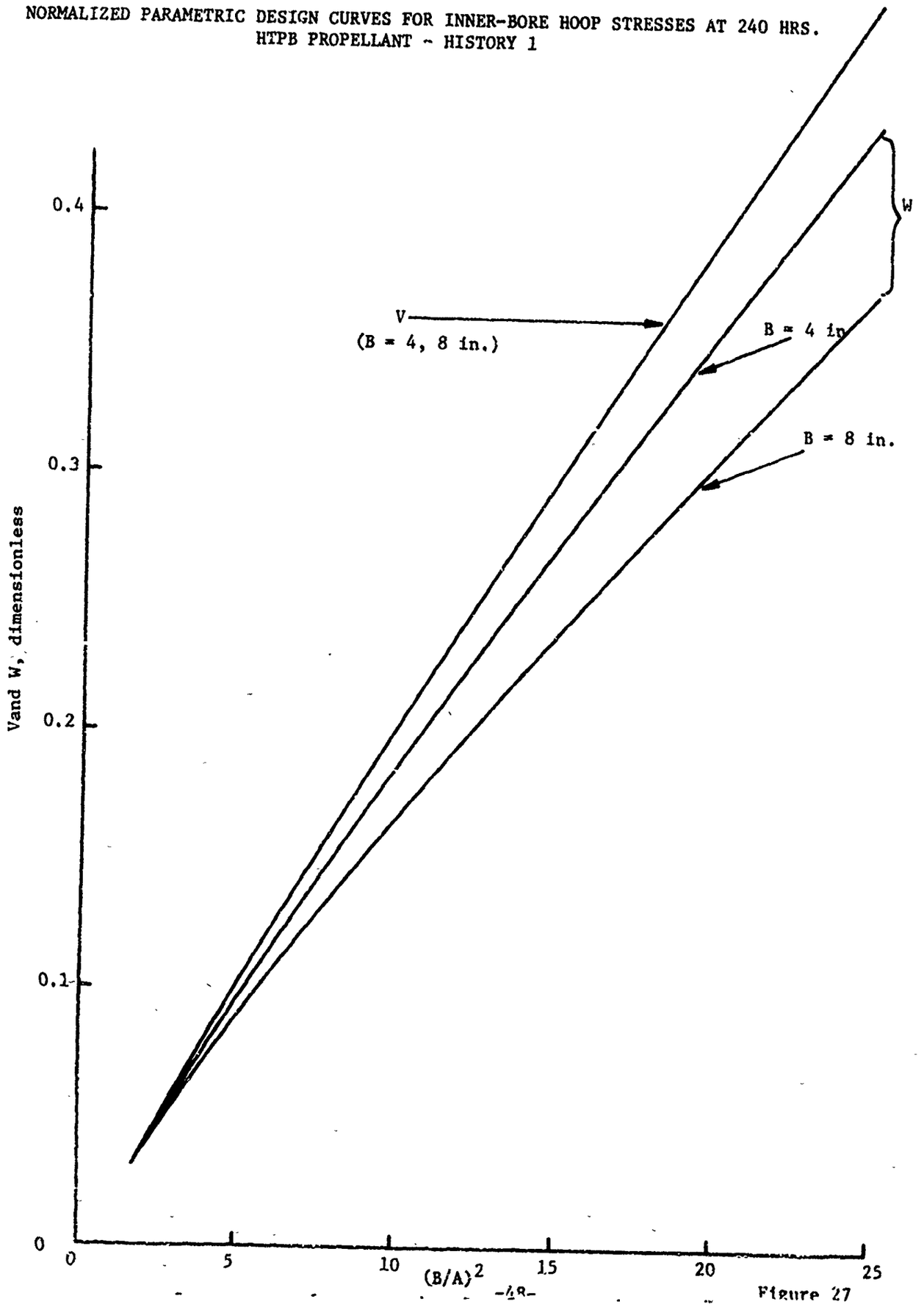

Figure 27

NORMALIZED PARAMETRIC DESIGN CURVES FOR RADIAL BOND STRESSES AT 240 HRS.
HTPB PROPELLANT - HISTORY 1

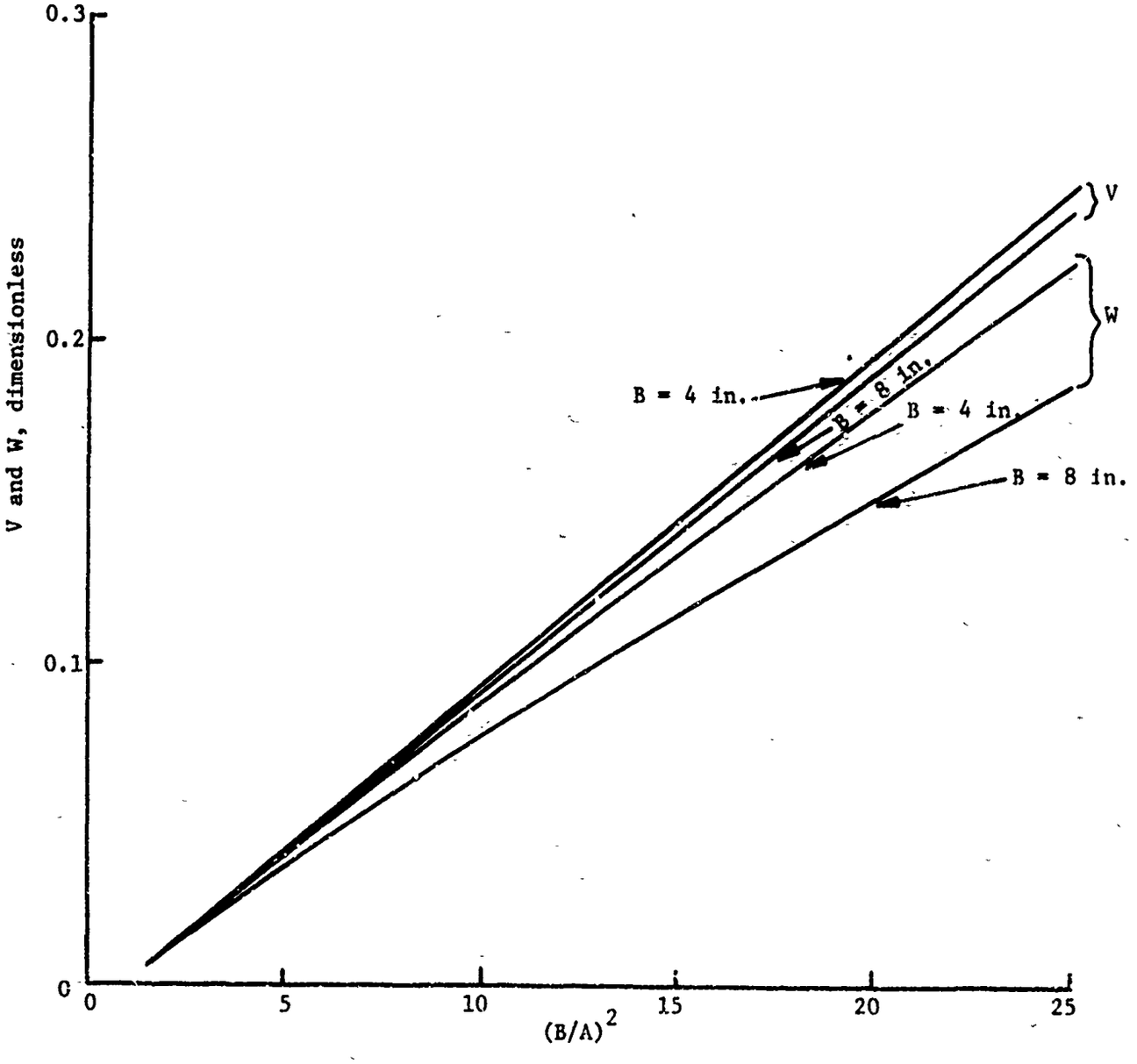

Figure 28

NORMALIZED PARAMETRIC DESIGN CURVES FOR
INNER-BORE HOOP STRESSES AT 96 HRS. CTPB PROPELLANT
HISTORY 2

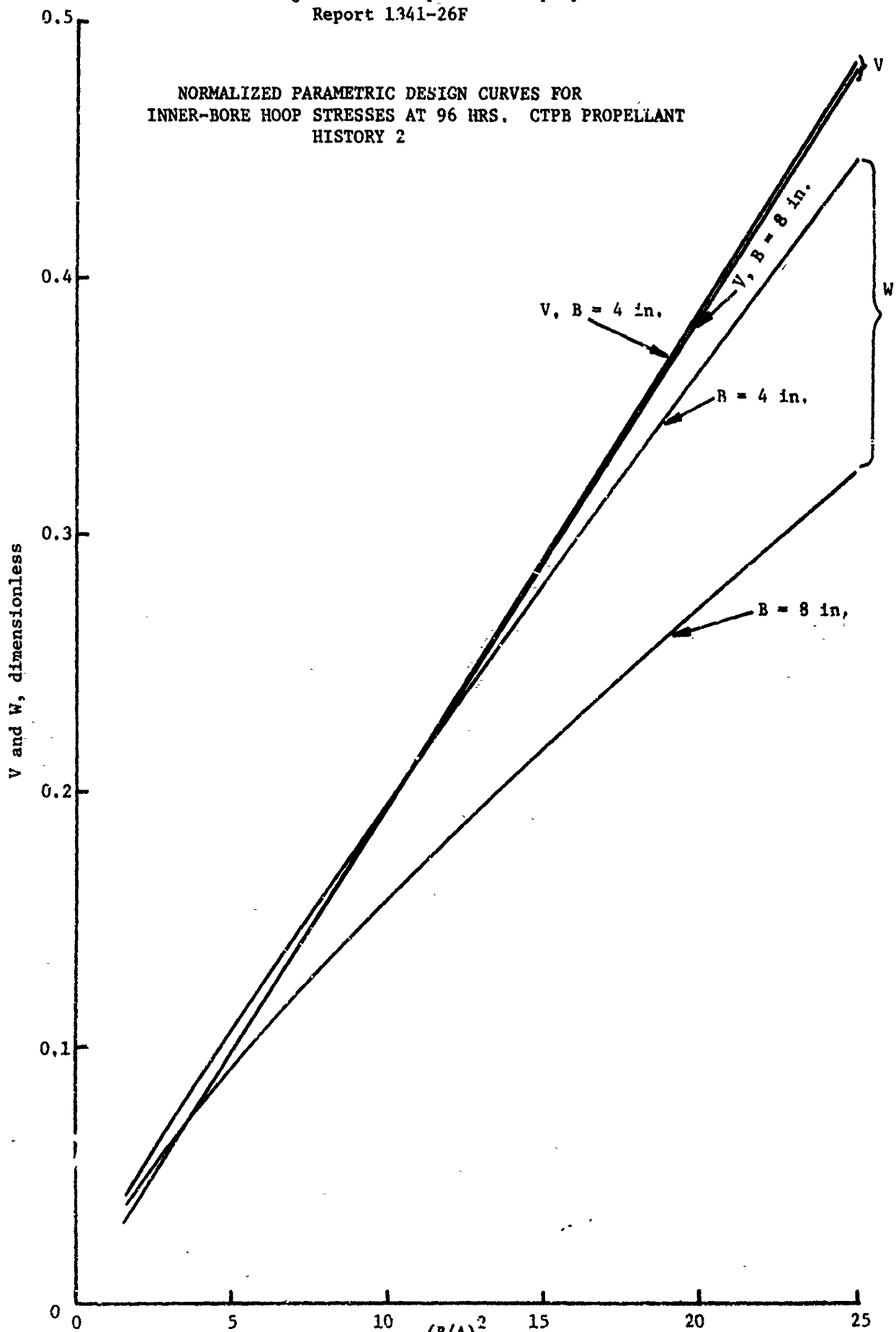

Figure 29

NORMALIZED PARAMETRIC DESIGN CURVES FOR RADIAL BOND STRESSES AT 96 HRS.
CTPB PROPELLANT - HISTORY 2

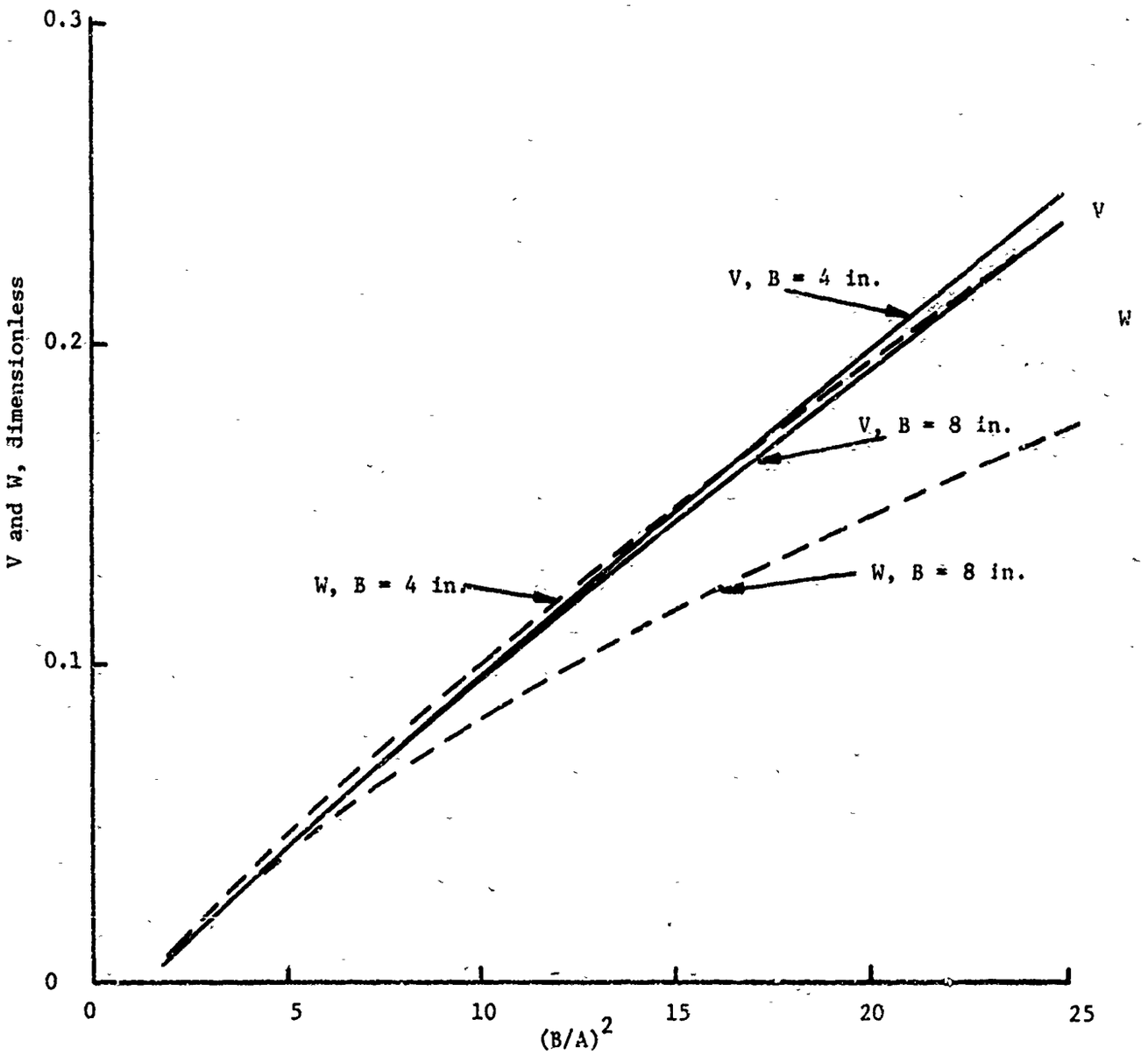

Figure 30

NORMALIZED PARAMETRIC DESIGN CURVES FOR INNER-BORE HOOP STRESSES AT 96 HRS. HTPB PROPELLANT - HISTORY 2

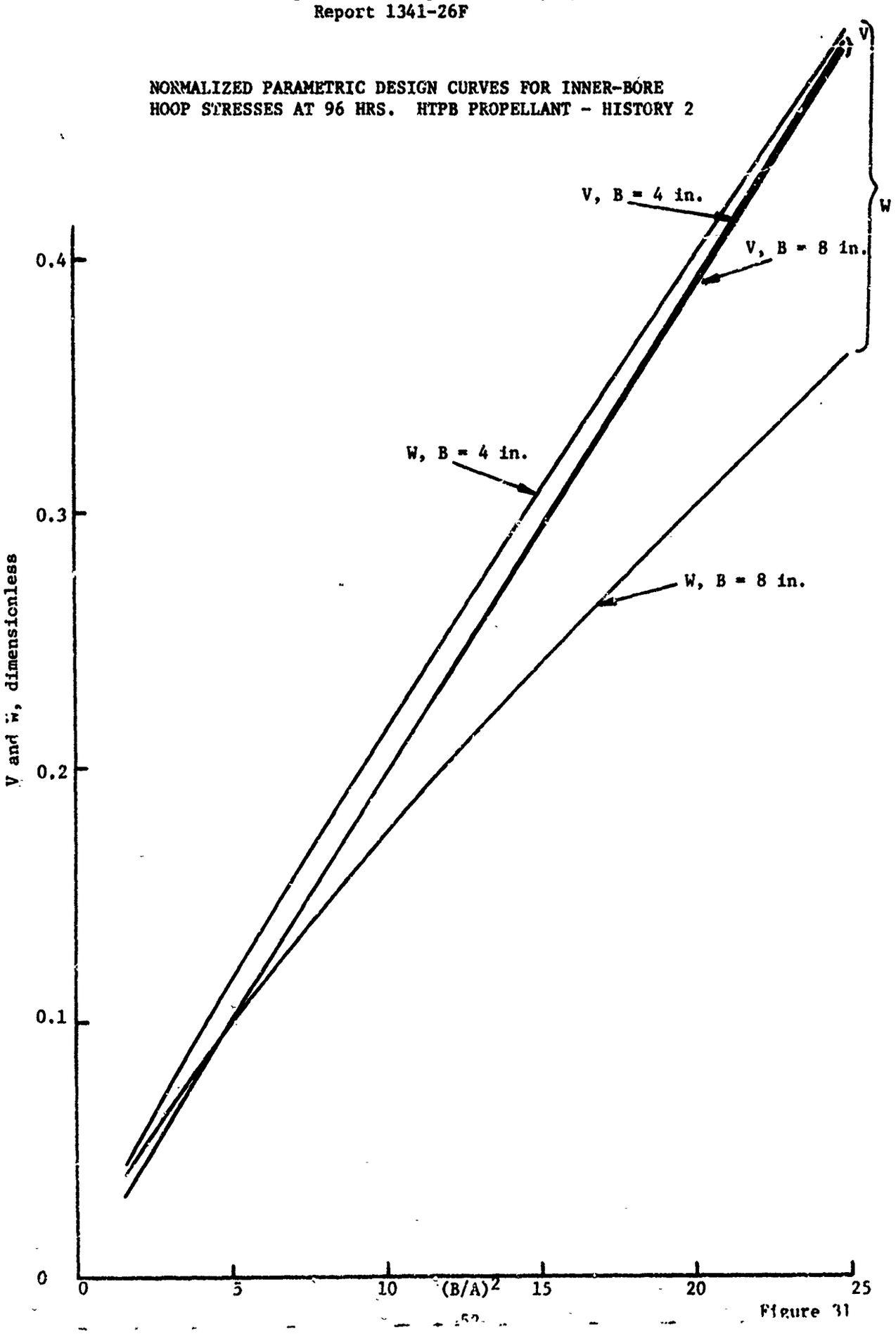

Figure 31

NORMALIZED PARAMETRIC DESIGN CURVES FOR RADIAL BOND STRESSES AT 96 HRS.
HTPB PROPELLANT - HISTORY 2

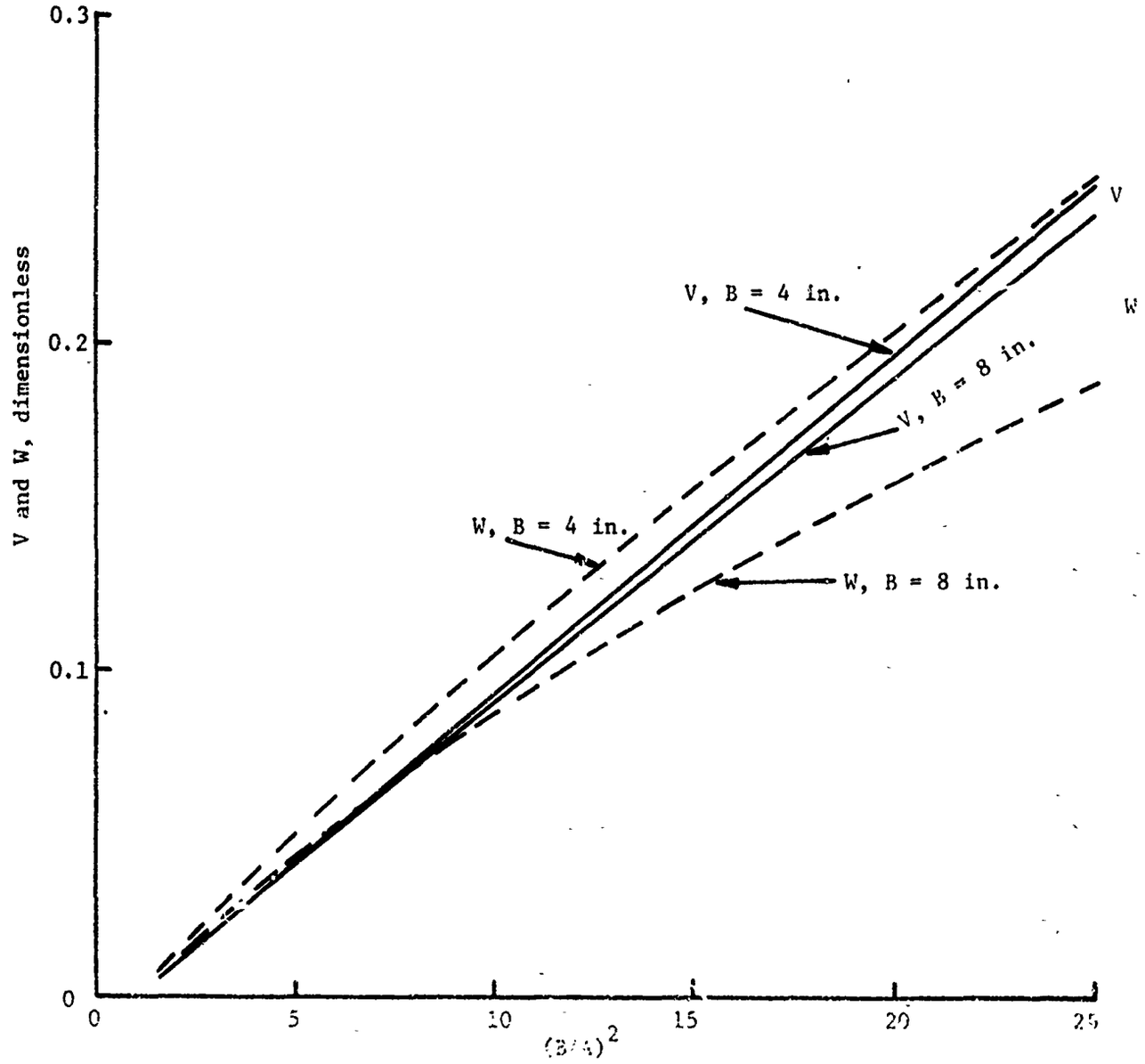

Figure 32

5. Strength-Modulus Interrelation

The previously described parametric design curves provide a simple and direct means for evaluating propellants with respect to given designs and thermal histories. At this point we would like to submit some very simple strength considerations which should apply to any motor use condition. They involve a somewhat different use of existing relationships between propellant strength, moduli, and grain stresses. These relations and their use are described below.

a. Basic Relations and Their Verification

Equation (22) of Reference (3) can be written:

$$\frac{\sigma_t(t_b) - \sigma_{cr}}{\sigma_g - \sigma_{cr}} = \left[\frac{E(t_b/q) - E_e}{E_g - E_e}\right]^{1/2} \qquad (5)$$

where

$\sigma_t(t_b)$ is the true stress expressed as a function of the time-to-break in a creep test

σ_g is the glassy strength

t_b is the time-to-break in a creep test

$E(t_b/q)$ is the relaxation modulus in tension at the time t_b/q.

q is an empirical constant

E_e is the equilibrium modulus in tension

Simply stated Equation (5) shows the creep strength to be related to the square root of a time-shifted modulus.

Following the procedures previously used in developing Equation (2), we see that both the right and left hand portions of Equation (5) can be rewritten so that the glassy modulus and the glassy strength are replaced by their values at t_b = 1 min. Thus,

$$\frac{\sigma_t(t_b) - \sigma_{cr}}{\sigma_{t(1)} - \sigma_{cr}} = \left[\frac{E(t_b/q) - E_e}{E(1/q) - E_e}\right]^{1/2} \tag{6}$$

Being truly pragmatic, we recognize that at longer times, (i.e., not near the glassy region) propellant relaxation moduli approximate a simple power-law relation. That is

$$E(t) - E_e \approx k\ (t/t_o)^{-n} \tag{7}$$

where k and n are constants

t_o is a reference time

The term inside the brackets in Equation (6), when combined with Equation (7), can be written

$$\frac{E(t_b/q) - E_e}{E(1/q) - E_e} \approx \frac{(t_b/q\ t_o)^{-n}}{(1/q\ t_o)^{-n}} = (t_b/1)^{-n} \tag{8}$$

But, solving Equation (7) directly for $t = t_b$ and $t = 1$, and taking ratios, gives

$$\frac{E(t_b) - E_e}{E(1) - E_e} = (t_b/1)^{-n} \tag{9}$$

Thus, the left hand terms of Equations (8) and (9) must be equivalent. Using this equivalence in Equation (6) gives

$$\frac{\sigma_t(t_b) - \sigma_{cr}}{\sigma_t(1) - \sigma_{cr}} = \left[\frac{E(t_b) - E_e}{E(1) - E_e}\right]^{1/2} \qquad (10)$$

We have tested Equation (10) and found it to work quite well. Of course, the wide variability observed in measuring both strength and modulus properties must be taken into account. To show the correlation we will replace the exponent 1/2, which is on the bracket in Equation (10) with an undefined constant m. As shown below, the quantity m reflects the variability in the strength and modulus data, but the quantity certainly varies around the value m = 0.5.

The first correlations involve creep-to-failure strength data and relaxation moduli for three propellant types. The results are listed below.

Propellant Type	Exponent m
CTPB	0.49
HTPB	0.59
Polyurethane	0.44

Wiegand[6], using nominal tensile strength and initial tensile modulus data, obtained results which are better analyzed according to Equation (10). His data give the following values for m.

Propellant Type	Exponent m
ANP-2830 BI	0.57
ANP-2969 KHI	0.58
Polybutadiene, aged and unaged	0.67
ANP-2639	0.4
ANBS-104	0.58
ANP-2862JM	0.5
ANP-2935HY-2	0.44

Bersche, et al[7], commenting on Wiegand's results noted that constraints were required on the interrelationship. We believe that the necessary constraints are provided by Equation (10).

Table 1 of Reference (7) provides the following values for m.

Propellant Type	Exponent m
Acrylate	0.56
CTPB	0.46
PBAN	0.47
PVC	0.71
NC	0.66

Although Wiegand's and Bersche's data might have been more rigorously analyzed, we feel that they give reasonable support to Equation (10).

Now that we have a satisfactory strength-modulus relationship we must find ways to use it. This we have done below in a preliminary way only.

b. Applications

The primary application intended here is to rank the structural capabilities of candidate propellants with respect to a given motor use.

The use of Equation (10) requires two additional sources of information. First, we need to recognize as a rule of thumb that the grain stress, $\sigma(x,t)$ at any time and position in the grain is proportional to the modulus, thus, we obtain

$$\sigma(x, t) \approx k\, E(t) \qquad (11)$$

(NOTE: For precise work, Equations (4) should be used.)

The second information requirement is a viscoelastic stress analysis of a representative propellant under the given structural use conditions.

Using Equations (10) and (11) (or Equation (4) when appropriate) together with the existing structural analysis permits us to rank a number of propellant candidates. For example, consider a design in which the moduli of the new propellant were exact y double those of the reference propellant. By Equation (11) the new grain stresses would be approximately doubled. But, by Equation (10) (assuming $\sigma_{cr} = 0$) the propellant strength increases only 41%. Thus, the relative strength to grain stress for the new candidate propellant is inferior to that of the reference propellant, which gives the former a lower rank.

A tabulation is given below to show the relative effects of changes in propellant moduli upon propellant strength, grain stresses and the relative strength to stress ratios. These comparisons are based upon Equations (10) and (11) and assume propellants of a single binder type.

TABLE 4

RATIOS OF PROPERTIES: NEW CANDIDATE/REFERENCE PROPELLANT

Ratio of Moduli	Ratio of Propellant Strengths	Ratio of Grain Stresses	Relative Strength/Stress
0.2	0.45	0.2	2.25
0.4	0.63	0.4	1.57
0.6	0.77	0.6	1.28
0.8	0.89	0.8	1.11
1.0	1.0	1.0	1.00
1.2	1.10	1.2	0.92
1.4	1.18	1.4	0.84
1.6	1.26	1.6	0.79
1.8	1.34	1.8	0.74
2.0	1.41	2.0	0.71

This tabulation shows that the softer (lower modulus) propellants should perform better from the point of view of relative strength to stress ratios (of course the propellant chemist has known this for years). The only restrictions on this being resistance to slump and some necessary safety margins to account for possible degradative chemical changes. In particular, where postcure is a problem, the effect can be seen to lower the relative strength/stress ratio. Thus, the initial modulus at cure should be targeted at the low end of the possible modulus scale, even though extended cure might be required for some small portion of the production, in order to improve the safety margin.

III. IMPROVED ANALYTICAL METHODS

Any prediction of grain failure, regardless of the failure criterion used, is limited by the accuracy of the predicted stresses, strains, or strain energies employed in making the prediction. Therefore, in the development of the linear cumulative damage analyses it was necessary to make basic improvements in the stress and thermal analyses of propellant grains. At the beginning of the current program we had the most advanced one-dimensional and two-dimensional, thermal, viscoelastic stress analysis capability. In addition, the linear cumulative damage analyses were provided in conjunction with the automated thermal and stress analyses.

Although these analytical methods gave us advanced capabilities, they were, nevertheless, limited. The two-dimensional analysis gave numerical difficulties after 500 calculation-time points. Also, they were limited to circular bore grains. In addition, the non-linear viscoelastic effects of strain-dilatation in propellants were ignored. The current program was designed to extend the present analytical methods in these areas.

The work reported in the following section involves: (1) modification and extension of the two-dimensional (linear), thermoviscoelastic analysis; and (2) investigation of the means for, and importance of, accounting for non-linear propellant behavior.

A. EXTENSION OF TWO-DIMENSIONAL THERMOVISCOELASTIC ANALYSIS

1. Increased Number of Calculation-Time Points

During the previous program[3], a time marching procedure for the axisymmetric thermoviscoelastic analysis of propellant grains was developed. The analysis functioned satisfactorily when applied to relatively short time one- and two-dimensional thermal problems and to long time one-dimensional thermal cycling problems. It was subsequently observed, however, that for two dimensional analyses which covered a long period of real time, the solution procedure became unstable due to the accumulation of numerical error. The numerical difficulties were associated with the short word length of the IBM 360/65 computer. With the 32 bit word, used in the 360/65 computer, a real number can be represented to only 7 decimal digits of accuracy. The result of an operation (addition, multiplication, etc.) is truncated (not rounded) which causes a one-sided, building error when numerous operations are performed for the final result. The observed numerical error is attributed to the summation of truncation errors during the solution and history accumulation procedures. Dr. Herrmann reformulated the method of solution in an attempt to alleviate this difficulty. Previously,[3] the problem was solved with the total loads acting on the system at each solution time point. In the new formulation only the

incremental loads are used and the solution then gives the incremental stresses and strains. These are summed for each solution time point to give the final answers. The "incremental analysis" equations are very similar to those previously reported[4,9] with the exceptions noted in Appendix E.

This method results in initially encouraging results, but near-capacity problems were found to have unstable solutions at later times. The problem was improved further by performing calculations in double precision arithmetic. The combined effect of these two steps was to nearly double the useful number of calculation-time points.

To minimize computer core requirements the present analysis, Appendix H, selectively performs only the critical calculations in double precision.

The one item that merits additional investigation is the possibility of developing a procedure that would permit the systematic determination of the optimum size time increments. Such a development should substantially improve the accuracy and economy of the analysis.

The two-dimensional, transient, thermo-viscoelastic, finite element, computer program was given the number E11902. Due to a recent policy decision the available core capacity of the IBM 360/65 computer was drastically reduced. The E11902 program as described in Appendix H, which required a core capacity of 490K to run a maximum capacity problem, was therefore cut down in size so that it could be run with only 364K core capacity. This, of course, reduced the size of the maximum problem which could be handled. The new program limits are now: 195 node points, 168 elements and 8 Prony Series Terms. All other limitations are as described earlier.

2. Prony Series Curve Fit Analysis

The shear relaxation modulus is represented by a Prony series. This series forms the basis of the one- and two-dimensional, viscoelastic stress analyses.

The evaluation of the constants of the Prony series has been simplified using a straightforward computer solution. Appendix F provides both the mathematical relations involved and a "Users Manual" for the computer program.

Now that we have developed the basic, two-dimensional, thermo-viscoelastic, stress analysis capability, it is imperative that we put it to good use. As part of this use, Aerojet has put the program "on line" to solve its problems. But there are a number of problems where we require still more information, so further extensions of our analytical capabilities were required. Some of our more successful efforts are considered next.

3. Two-Dimensional Planar Analyses

The current analysis was designed to analyze case-bonded cylindrical grains. For arbitrary solids of revolution, a complete analysis would entail a three-dimensional capability. Since this is a remote possibility we must limit ourselves to practical approaches where limited factors, of immediate concern, are examined. The thermoviscoelastic analysis of planar sections will permit us the opportunity of real grain cross-sections, but without considering the influence of the end conditions. This capability should permit the evaluation of propellant specimens, which had been made in thin slabs, and relate their behavior to available analyses. Thus, we could better assess new grain designs and propellants, before making them in full-scale grains.

The description of this program is given next followed by examples showing a few applications of the program.

a. Description

The two-dimensional thermo-viscoelastic analysis program was originally restricted to axisymmetric analyses; during the current phase of the program the analysis was extended to plane problems. The extension is straight forward and well documented for other analyses and thus only the unusual features of this analysis will be noted in this report. The plane strain option includes the possibility of generalized plane strain (i.e., the value of axial strain is permitted to be non-zero, however, it must be constant throughout the body) by permitting the requirement that the grain cross-section experience an axial strain equal to the average axial thermal strain in the case. The generalized plane stress option was modified so that the stress throughout the thickness of the body, may be specified as a constant rather than zero. The values of the thickness stress constitutes one of the input parameters. The inclusion of a non-zero thickness stress required the modification of the governing variational equation. This modification is described in Appendix C.

b. Test Cases

To check out the planar options, three analyses were performed. All were analyzed using the CTPB propellant described in Appendix A. The analyses were performed for grains subjected to cooling from 135°F, the stress free temperature, to -65°F.

Problem No. 1

A generalized plane strain problem was prepared and run on the modified program. The gridwork used is shown in Figure 33. This gridwork represents a 30° segment of a perforated propellant grain bonded to a steel case.

Problem No. 2

A plane stress problem was run. The gridwork is identical to that used in Problem No. 1, Figure 33.

Problem No. 3

The final problem is a generalized plane strain problem and similar to Problem No. 1 except that the slot width is halved and the finite element mesh is finer for better resolution of the stresses and strains. The gridwork used in this problem is shown in Figure 34.

Figure 35 shows stresses and strains vs. time for the three problems of an inner bore element. Figure 36 shows the damage and damage rate vs. time for Problems No. 1 and 3 of the same elements. Problem No. 2 is not shown in this figure because at no time did the damage or damage rate become high enough to be shown on the scale used on the figure.

An interesting question relating to these problems is the effect of grid size. As is well known the stresses and strains increase rather rapdily as the surface is approached at the end of a slot. Consequently, Problem No. 3 rerun with a finer mesh would result in a greater cumulative damage.* The question is what element size should be used to ensure that the cumulative damage computed is the appropriate value. Studies concerning this effect are beyond the scope of the present work, but could be investigated using this computer program.

Table 5 summarizes the size of the three problems together with the computer time for each solution.

* The stress values used are for the element centroids. An extrapolation, or averaging, procedure to obtain surface stresses would help alleviate this problem. Of course, the accuracy of the analysis is also related to the grid size; which is a separate problem.

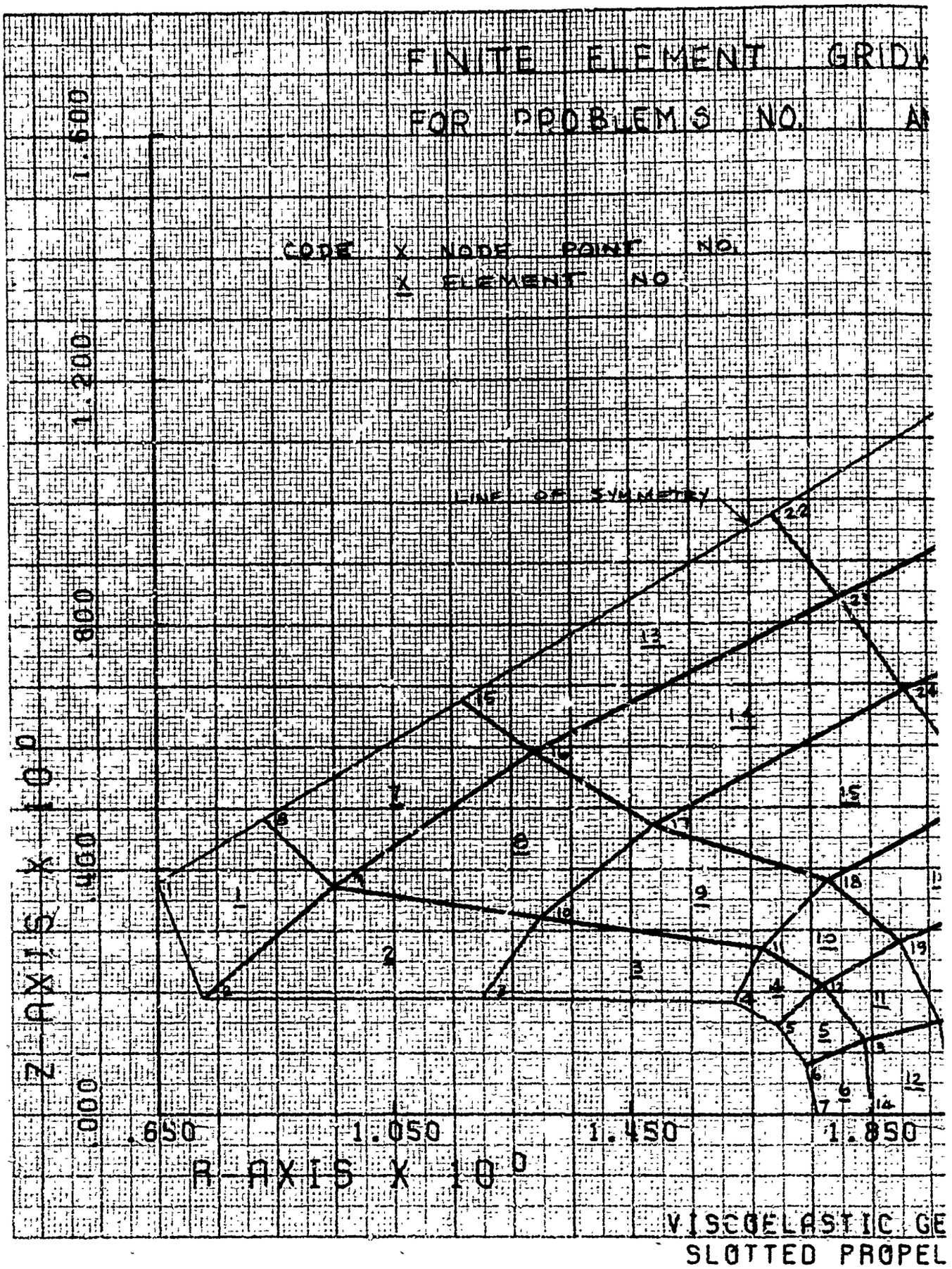
FINITE ELEMENT GRID
FOR PROBLEMS NO. 1 A
CODE X NODE POINT NO.
X ELEMENT NO
LINE OF SYMMETRY
Z-AXIS X 10^0
.000
.400
.800
1.200
1.600
.650
1.050
1.450
1.850
R-AXIS X 10^0
VISCOELASTIC GE
SLOTTED PROPEL

A

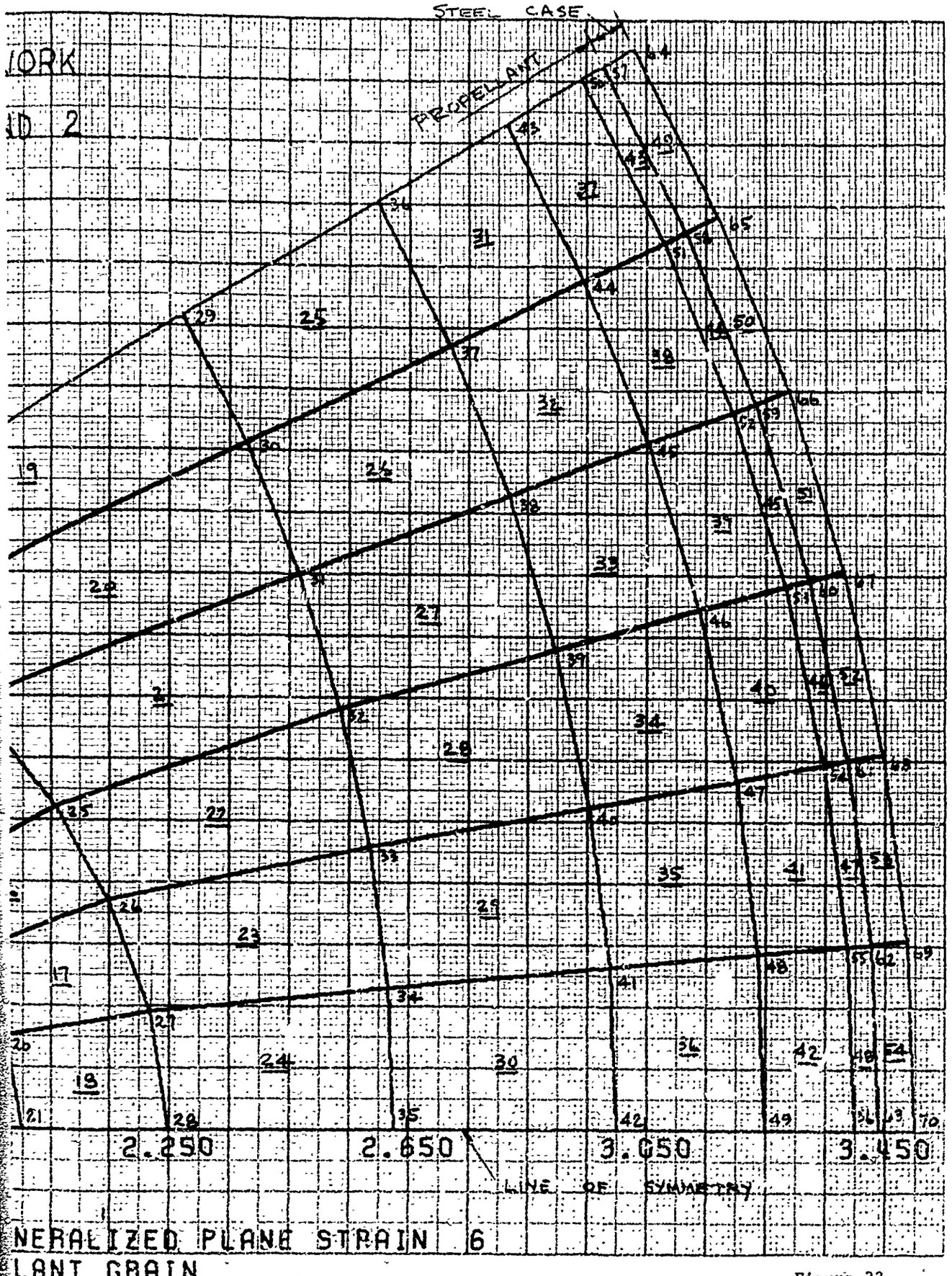

Figure 33

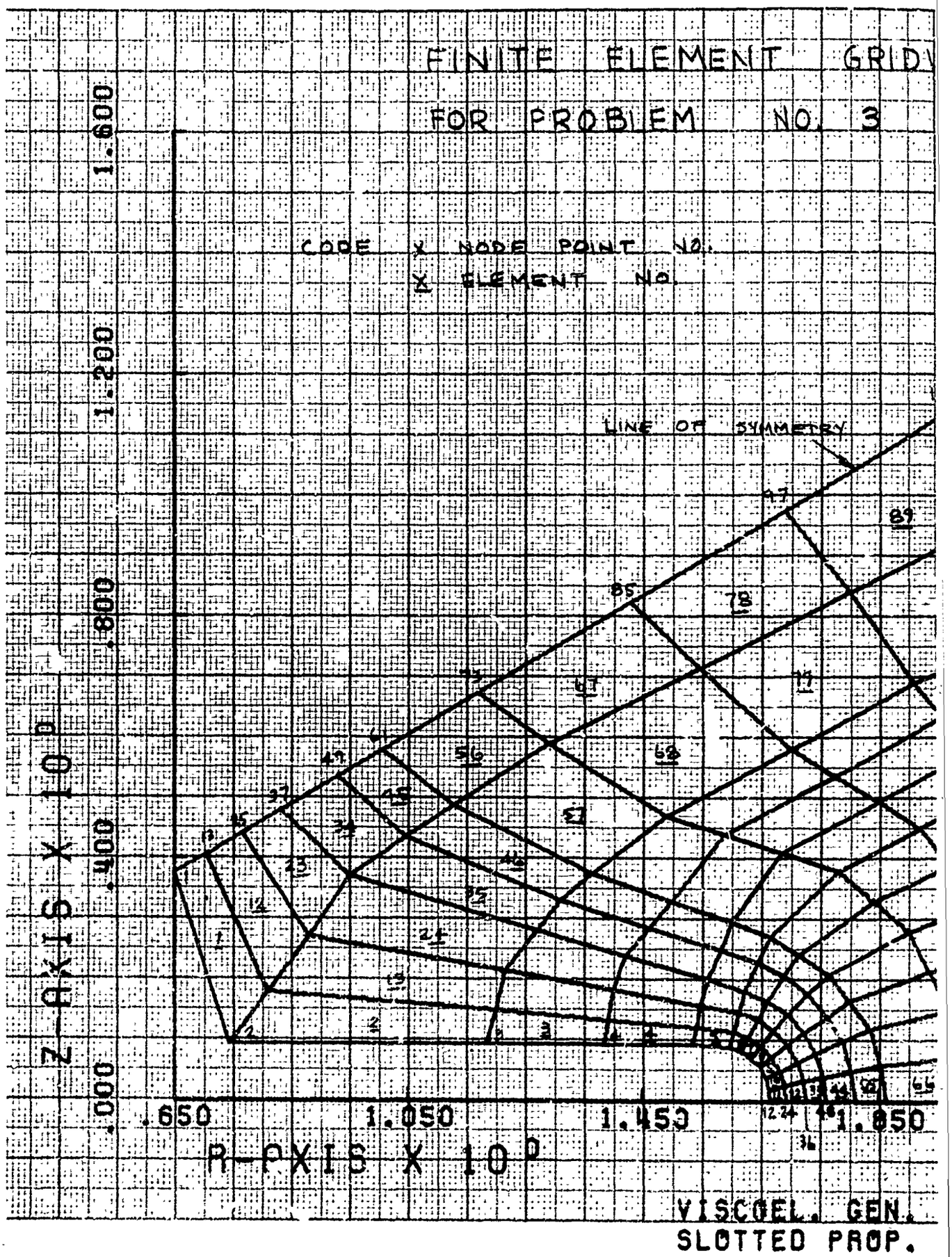
FINITE ELEMENT GRID
FOR PROBLEM NO. 3
CODE X NODE POINT NO.
X ELEMENT NO.
LINE OF SYMMETRY
Z-AXIS X 10
.000
.400
.800
1.200
1.600
.650
1.050
1.450
1.850
R-AXIS X 10
VISCOEL. GEN.
SLOTTED PROP.

A

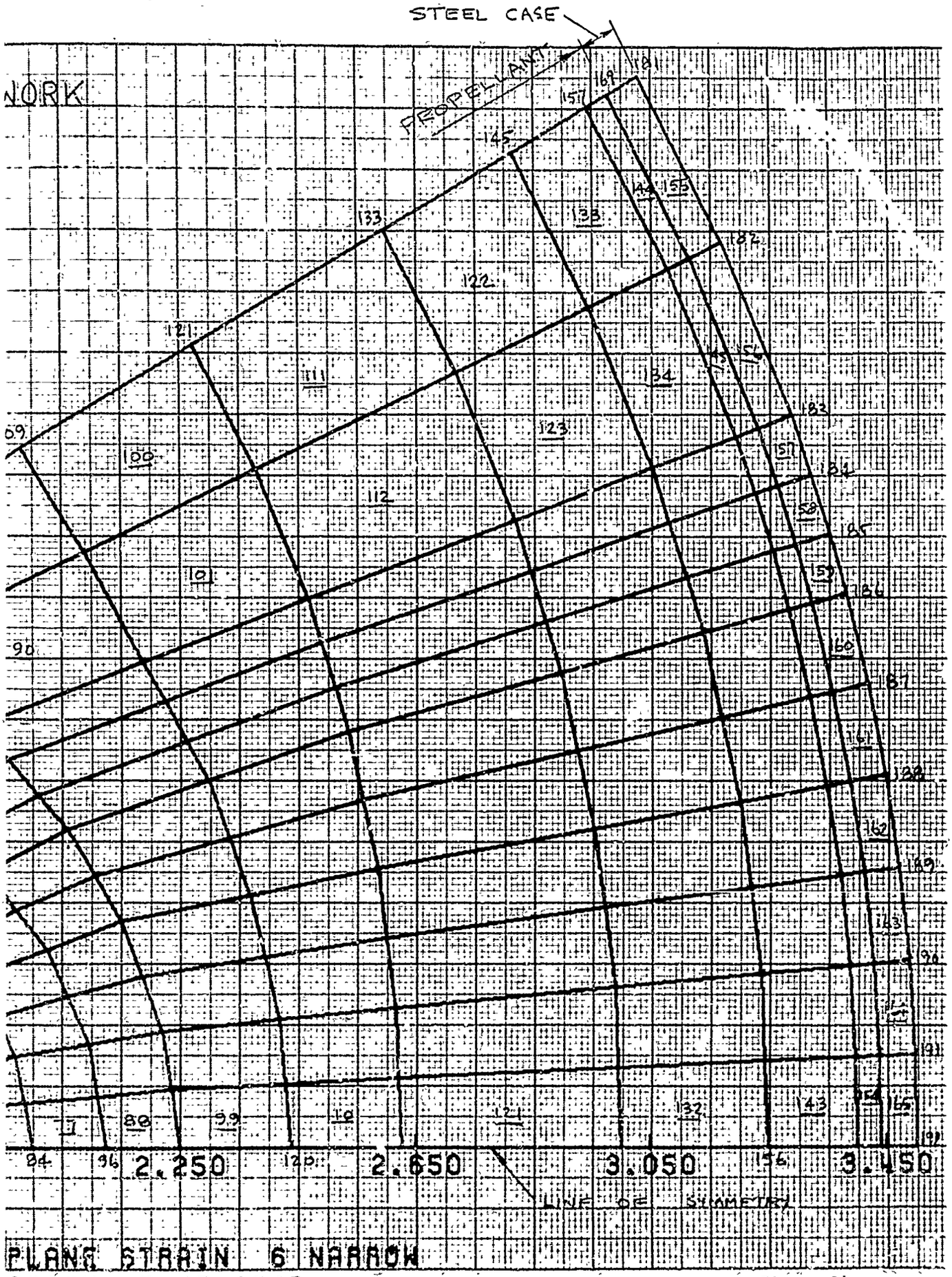
STEEL CASE
PROPELLANT
NORK
2.250
2.650
3.050
3.450
LINE OF SYMMETRY
PLANE STRAIN 6 NARROW
GRAIN FINE GRID

Figure 34

STRESS AND STRAIN VS. TIME FOR PROBLEMS NO. 1, 2 AND 3

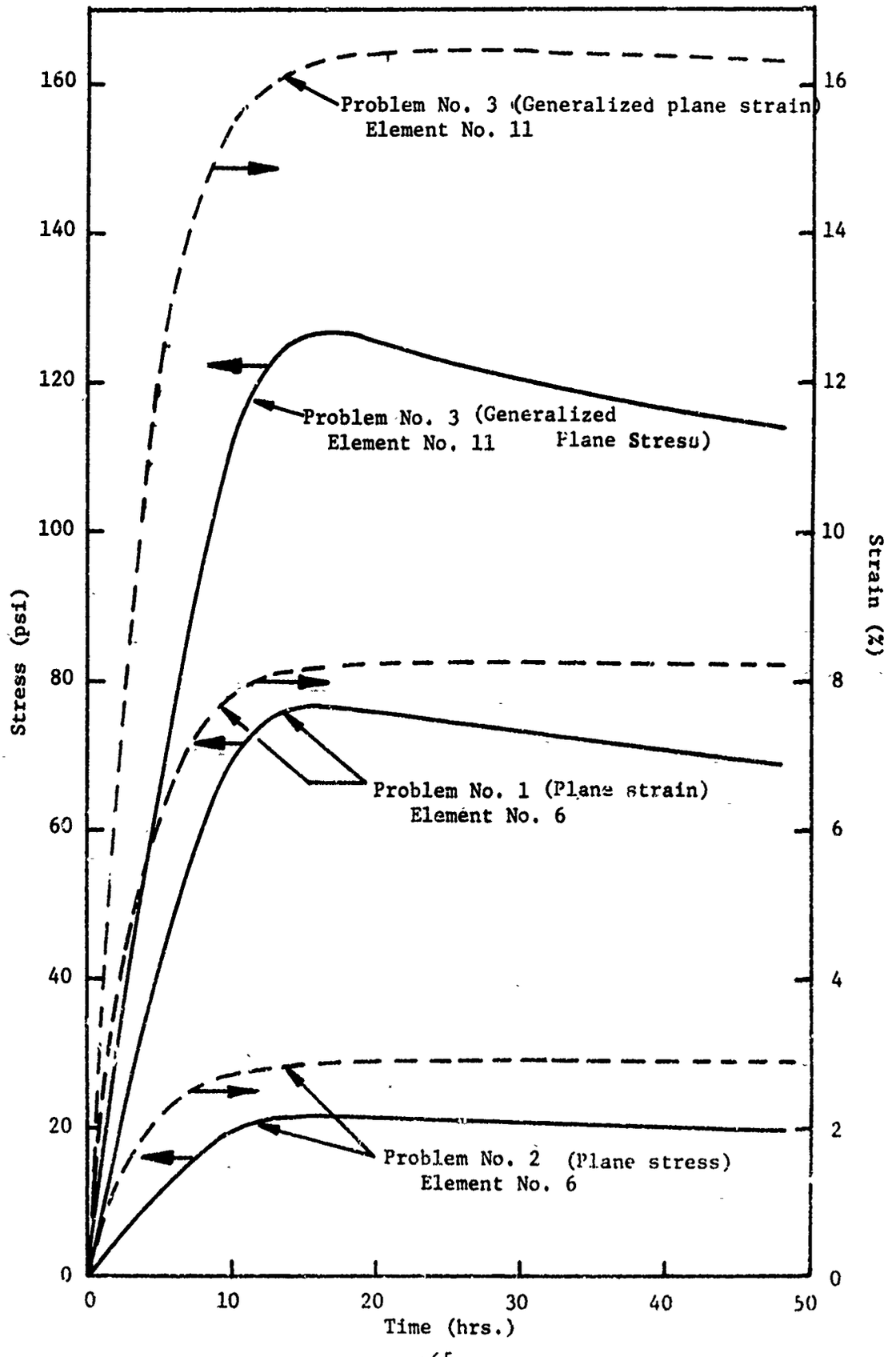

Figure 35

DAMAGE AND DAMAGE RATE VS. TIME FOR PROBLEMS NO. 1 AND 3

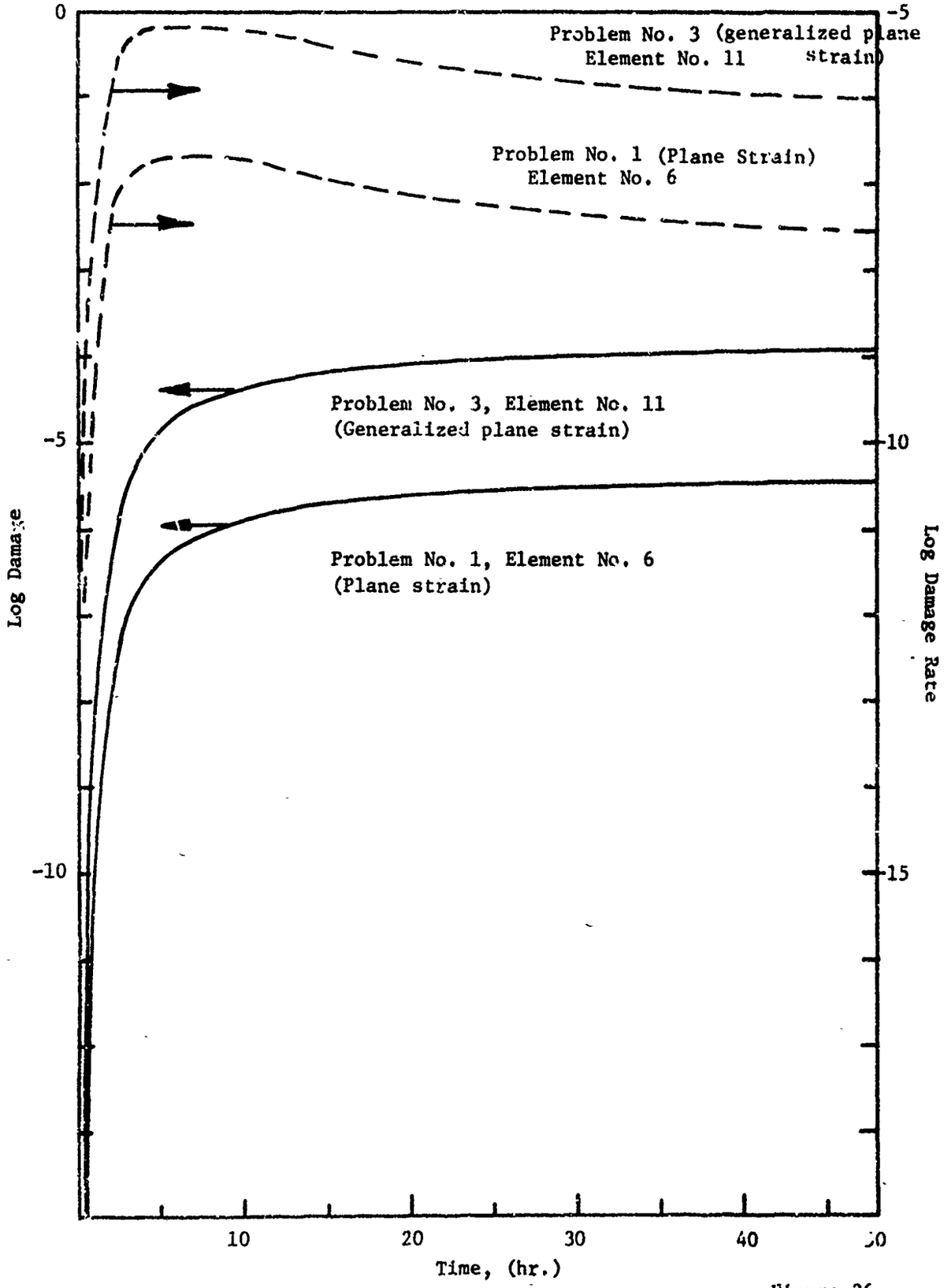

Figure 36

SUMMARY OF SIZE AND COMPUTER TIME FOR THE THREE PROBLEMS ANALYZED

	Node Points	Elements	Solution Time Points	Central Processing Unit, Time, min.	Billed Time, min.
Problem No. 1: Generalized Plane Strain	70	54	40	2.685	4.394
Problem No. 2: Plane Stress	70	54	40	2.577	4.146
Problem No. 3: Generalized Plane Strain	192	165	40	11.352	17.694

Table 5

B. NON-LINEAR ANALYSIS

The fact that the viscoelastic response of solid propellants is highly non-linear has been established by numerous investigators. However, a characterization of this non-linear behavior has not been firmly established. The purpose of this investigation was to attempt to determine qualitatively whether or not these nonlinearities negate stress analysis predictions based upon linear theory.

In general, the response of grains to various loading conditions is mainly determined by the dilatational behavior of the propellant, hence, it would appear that accounting for the non-linear dilatational response of propellants is of primary importance.

The grossness of linear characterizations presently employed in analysis is illustrated by the fact that they assume that the volume change in the propellant is a linear function of the mean pressure (they assume the dilatation to be linear elastic). Thus, whenever the mean pressure is negative, the dilatation is predicted to be negative.[10] It has been observed, however, that under certain conditions a negative mean pressure can be accompanied by a very substantial positive dilatation (see Figure 1 of Reference (11). Although insufficient experimental data are available to permit a comprehensive characterization of the nonlinear dilatational effects, it was felt that an evaluation could be obtained by utilizing a description which qualitatively accounts for the behavior reported for a limited class of stress states in References 11 and 12, and which predicts reasonable results for other stress states. Because of the tentative nature of the characterization it was deemed desirable to approximate the non-linear behavior by an equation which could be incorporated into the existing analysis with a minimum amount of effort. The details of the analytical approach and the assumed dilatational behavior are given in Appendix I.

The resulting analytical evaluation appeared to be very straight forward and useful. Therefore, it was programmed for the computer (at UCD) and simple problems evaluated. The accuracy of the procedure was verified for a simple problem.

To ascertain the importance of the non-linear dilatational behavior two plane strain analyses were performed for the grain configuration shown in Figure 37. The shear relaxation function and the shift function for a real propellant were used in conjunction with the non-linear dilatational relationship developed herein. Two temperature histories were considered: (a) $T = 70° \rightarrow -10°$ and (b) $T = 70° \rightarrow 150°$, Figures 37 and 38 are plots of the bore hoop stress, the interface stress and the bore hoop strain. These plots indicate that when the propellant experiences a temperature increase causing a compressive stress state the non-linearities are of little consequence. However, for a temperature drop the non-linear effects are significant; the maximum discrepancies for the example being of the order

Report 1341-26F

COMPARISON OF LINEAR AND NON-LINEAR PREDICTIONS FOR THE STRESS

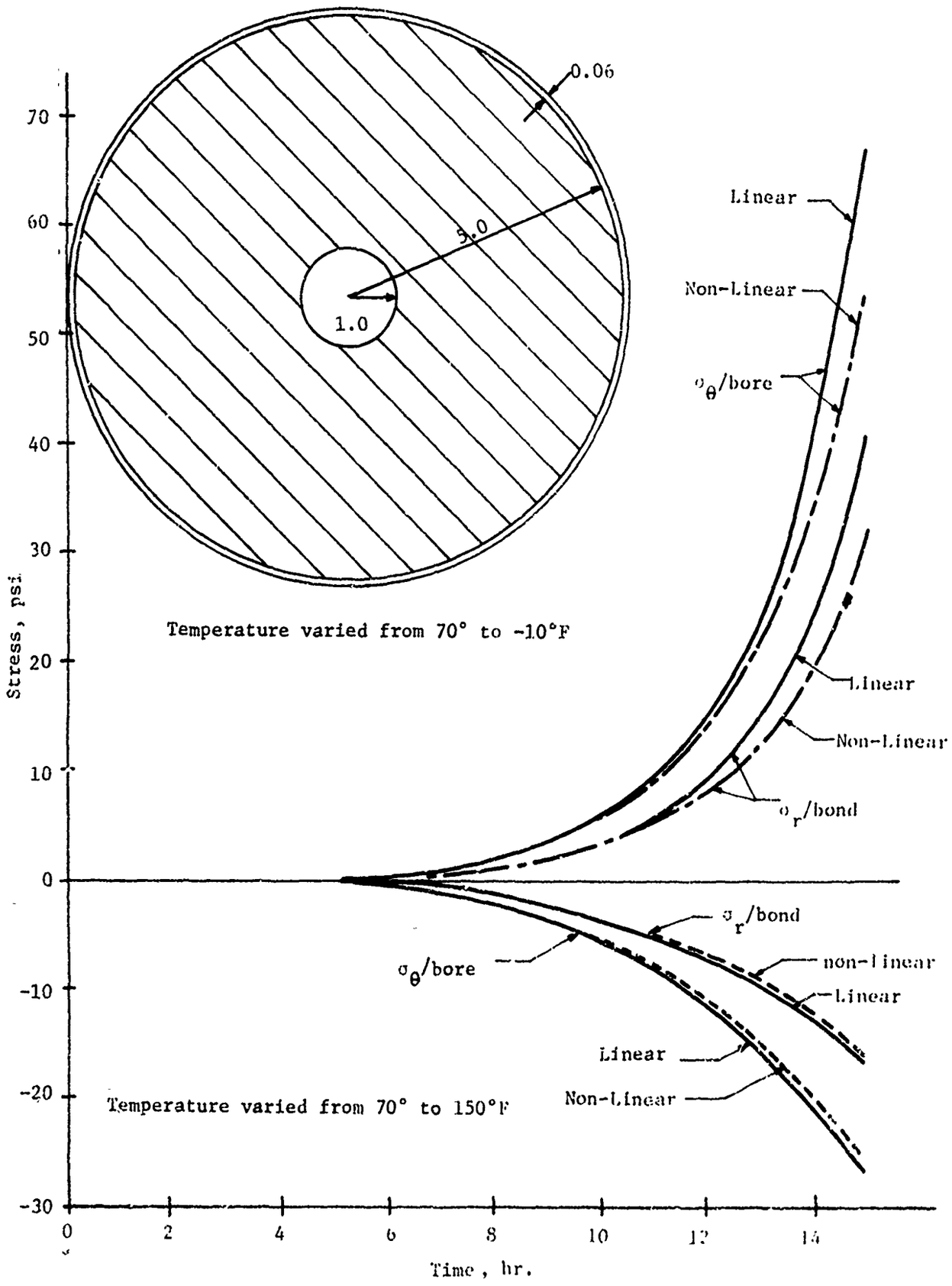

Figure 37

Aerojet Solid Propulsion Company
Report 1341-26F
COMPARISON OF LINEAR AND NON-LINEAR PREDICTIONS
FOR STRAIN

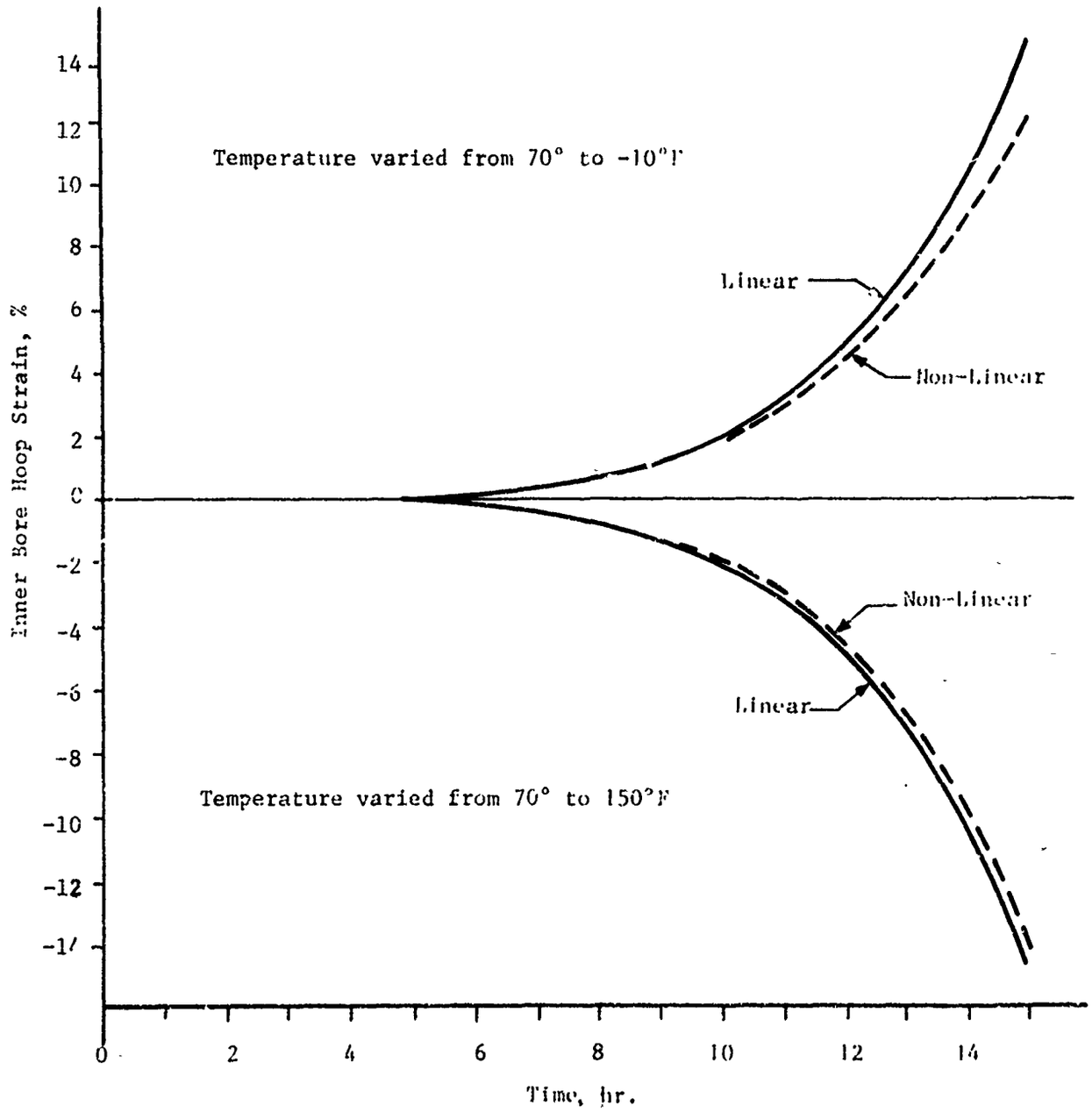

Figure 38

of 20% - 25%*. It is expected that if the dilatational equation included viscoelastic effects, thus permitting consideration of temperature cycling, the effects would be even more dramatic.

It is felt that the above results demonstrate the importance of accounting for the nonlinear dilatational effects and the feasibility of including such a description into existing two-dimensional propellant analyses. A rigorous consideration of the nonlinear effects will depend upon the determination of a nonlinear viscoelastic characterization for propellants which not only qualitatively but also quantitatively describes the observed propellant behavior.

A rigorous determination of a nonlinear dilatational law will require extensive testing for other stress states, e.g., biaxial stress, strip biaxial, and simple shear (with superimposed hydrostatic pressure). Additionally several different types of tests will need to be performed, e.g., constant strain rate, relaxation (various strain levels) and creep. The loading histories will need to include loading, loading-unloading, multi-step loading and unloading, etc. Lastly the effect of variable temperature upon the above tests will need to be determined.

C. REVIEW OF NON-LINEAR ANALYSIS EFFORTS AND RECOMMENDATIONS FOR FUTURE WORK

R. J. Farris, acting as a consultant to Aerojet, reviewed the analytical progress noted above and made a number of suggestions for future studies. These comments and suggestions are summarized below.

1. Current Status and Its Value

Aerojet and other facilities currently have the ability to perform complex linear-thermo-viscoelastic stress analysis for materials exhibiting an equivalence between time and temperature. These computed stress-time histories are then substituted into linear cumulative damage relations which in turn are used to predict failure. How these operations are carried out, whether by finite element, finite difference, or other means, is of no importance assuming all yield accurate results.

Dr. Herrmann has recommended extending this linear method of analysis to account for the non-linear dilatational effects present in all propellants at larger strains. He has proposed a simple modification to the linear viscoelastic constitutive equation wherein all of the non-linearity is contained in dilatational terms. I have learned that even at small strains composite solid propellants are not linear viscoelastic materials.

---

* This is of the order experienced by grains of similar design and measured in thermal cycling, see References 1 and 2.

It is true that at large strains when dilatation and dewetting are present, the material behavior is markedly non-linear. However, it was non-linear before the dilatation was present. Hence, the proposed correction cannot bring the analysis into line.* The problem is quite basic, before obtaining accurate analysis with dilatational non-linearities one must first be able to obtain accurate analysis without the dilatational non-linearities.

2. Solution

This problem has been solved[13] for materials having non-linear homogeneous constitutive equations, eq., scalar multiplication holds while superposition does not. For this class of constitutive equations, correspondence principles have been obtained for proportional boundary value problems, e.g., problems separable in space and time. Here, half of the solution, either the stresses or the strains, can be obtained from a linear solution and the other half is obtained by substituting the linear solution into the non-linear constitutive equation. For displacement boundary value problems such as thermal cooling, the strains are given by a linear solution, and the stresses are obtained by substituting this linear strain solution into the non-linear constitutive equation. The opposite situation exists for stress boundary value problems. Application of this theory to propellant stress analysis should yield accurate results so long as the material has not dewetted, since considerable evidence exists indicating the homogeneity condition is destroyed when dewetting occurs.

For the range of strain where dewetting dilatation becomes important, the constitutive equation described above would require further modification to yield accurate results. This is the place for Herrmann's suggested modification; but, applied to the non-linear homogeneous constitutive equation rather than to the linear constitutive equation.

3. Recommendations

a. Verify that propellants have homogeneous but non-linear constitutive equations below dewetting.

b. Use the non-linear constitutive equations of Farris[13] in stress-analysis for stress or strain states where dilatation will not be important.

c. After this has been accomplished and verified, then modify the theory to account for dilatation in the manner Herrmann recommends.

---

* Editor's Note: By way of a counter-argument there is no reason why the "new" constitutive relation based only on dilatation could not adequately represent observed behaviors at all strain levels.

IV. GRAIN FAILURES ON PRESSURIZATION

The linear cumulative damage, LCD, and maximum principal stress, MPS, failure relations for solid propellants have been thoroughly developed and verified in application to the thermal cycling of motors.[1-3,14] The next logical application of these relations is the prediction of failures of grains on motor pressurization. The MPS relation has been verified in the laboratory for uniaxial and strip-biaxial tensile testing under superimposed hydrostatic pressures. However, analytical and theoretical difficulties existed for the case of a three-dimensional test with superimposed hydrostatic pressure.

To put this problem in perspective we prepared a brief summary of the LCD and MPS relations applicable to the pressure problem. Following this, we examined the basis of the time-pressure shift factor, a_p, and its application in a three-dimensional grain problem.

Then, we addressed ourselves to the problem of evaluating the effects on propellant failure properties of the damage accumulated from some past history. This is an important problem when considering firings of motors after they have seen severe handling or prolonged thermal cycling histories.

An especially successful effort was the development of a grain pressurization analog test. This test permits the direct evaluation of a propellant in determining its ability to function as a grain during motor pressurization. A detailed description of the test is given, followed by a presentation of test results obtained on a PBAN propellant.

A. EFFECT OF PRESSURE ON BASIC DAMAGE EQUATIONS

The linear cumulative damage relation merely states the manner in which damage can be added. To apply the relation in a three-dimensional stress field requires a time-dependent, stress failure criterion. An empirical approach showed that the applicable relation is a time-dependent, maximum principal stress failure criterion.

Combining the LCD and MPS criteria leads to integral relations which take full account of the past stress-time-temperature history at a point in the grain. We have found that a simple power-law approximation of the MPS criterion makes the history integrals quite simple to use. The pertinent equations are reviewed in Appendix J, which provides the basic equations for stress and temperature changes. Beginning from that point we can consider the effects of pressure changes on these relationships.

Equation (J-5) is the most general form of the linear cumulative damage relation for thermal histories. It permits the summation of damage for any type of thermal or mechanical loading history. The equation is given here for reference.

$$\Sigma D = \frac{1}{P(n)\ (\sigma_{to} - \sigma_{cr})^{B} t_o} \int_0^t \frac{(\sigma_t - \sigma_{cr})^{B}}{a_T(t)}\ dt \qquad (J\text{-}5)$$

where

ΣD is the accumulated damage fraction

σ_t is a true stress which varies with the time

σ_{cr} is the critical true stress below which no failures are observed.

t is the time

t_o is the unit value of the time for whatever units are used in measuring t.

σ_{to} is the true stress required to fail the specimen in the time t_o.

$a_T(t)$ is the time-temperature shift factor with the temperature expressed as a function of the time,

$P(n)$ is a statistically related parameter which relates the n^{th} test specimen in the population to the mean of the propellant.

This basic relation can now be extended to include considerations of pressurization effects.

In homogeneous elastomers and plastics, the effects of superimposed hydrostatic pressures upon viscoelastic properties is accounted for by a time-pressure shift, a_p.[15-16] This shift factor is used in precisely the same manner as a_T and arises from the same molecular nature of the polymer.

Based on the above interpretation, we should expect that the MPS failure relation, Equation J-3 could be made to account for the effects of pressure by the insertion of a_p to give

$$\bar{t}_f = t_o a_p a_T \left(\frac{\sigma_t - \sigma_{cr}}{\sigma_{to} - \sigma_{cr}} \right)^{-B} \qquad (12)$$

This relation has proved to hold for all the solid composite propellants tested thus far, as shown in References 1, 2, 3, 4 and 17. However, in using this relation the reader should understand that there is also an effect of pressure on the stress terms. The true stress, σ_t, is given as follows

$$\sigma_t = \frac{F}{A} - P \qquad (13)$$

where F is the applied force
A is the actual area of the cross-section
P is the superimposed pressure

The effect of pressure on σ_{cf} and upon $\sigma_t - \sigma_{cr}$ leads to an interesting result. At a pressure of 0 psig we have observed σ_{cr} to be quite small and have approximated it to zero. However, for the purpose of generalization, let σ_{cr} be a term whose value at atmospheric pressure is equal to $(F/A)_{cr}$. The critical stress at other hydrostatic pressures follows the approach given by Equation (13). Thus, we obtain

$$\sigma_{cr} = \left(\frac{F}{A}\right)_{cr} - P \qquad (14)$$

Subtracting Equation (14) from Equation (13) gives

$$\sigma_t - \sigma_{cr} = F/A - (F/A)_{cr} \qquad (15)$$

This relation shows that the stress difference term ignores the superimposed pressure. Only the time-pressure shift factor, a_p, changes with the pressure.

When Equation (12) is combined with the LCD relation, a more generalized relationship than Equation (J-5) is obtained. Thus,

$$\Sigma D = \frac{1}{P(n)\ (\sigma_{to} - \sigma_{cr})^B t_o} \int_o^t \frac{(\sigma_t - \sigma_{cr})^B}{a_{T(t)}\ a_{p(t)}}\ dt \qquad (16)$$

where $a_{p(t)}$ is the time-pressure shift factor expressed as a function of the time.

Equation (16) gives the most general history relation permitting time variations in the loads, temperatures and pressures acting at a point in the grain. It has been verified in the laboratory for uniaxial and strip-biaxial tensile test specimens under superimposed pressures.(1,2 and 4)

Although the relation had been verified in the laboratory, the reasons for its existence were not adequately understood. Also, the structural application of a_p was unknown. These questions are examined in the next section.

B. UNDERSTANDING AND USE OF THE TIME-PRESSURE SHIFT FACTOR

The use of a_p requires a definition of the appropriate value to be used for the pressure when three-dimensional stresses are involved. In a grain, near the propellant-liner bond, physical restraints by the case significantly reduce the effective superimposed pressure. Thus, the pressure imposed at the inner-bore cannot be the reference pressure required for the selection of a_p.

To understand this problem and to provide a basis for evaluating appropriate values of a_p we reviewed the literature and reevaluated current and past laboratory data. We arrived at a workable solution with some important theoretical implications. These are presented in Appendix K.

The failure mechanisms discussed in Appendix K give further evidence that the MPS criterion holds for solid propellants. A competing criterion, the maximum shear stress criterion, was found to be greatly in error when applied to failures of Poker Chip tensile specimens.

From the failure mechanisms of propellants it was concluded that a_p must be a function of σ_{cr}. Also, both of these quantitites provide a measure of the suppression of vacuoles by the superimposed pressure. Thus, using Equation (14) the value of σ_{cr} can be known at any point within a grain, assuming the appropriate value of P is known (as obtained analytically). Then, as indicated by Equation (K-2) the appropriate value of a_p can be obtained from laboratory characterization data.

$$a_p = f\ (\sigma_{cr}) \qquad (K\text{-}2)$$

Curves of a_p vs. σ_{cr} can be obtained from failure tests on uniaxial tensile specimens. For most propellants, $(F/A)_{cr}$ will be very small so that

$$\sigma_{cr} \approx -P \qquad (17)$$

In this case the previously reported approach of plotting a_p versus the pressure is eqivalent to plotting it versus σ_{cr}.

We have examined the use of a_p and found it to depend upon σ_{cr}. Now we would like to digress a bit and examine the effects of a previous damage history upon the simple ultimate properties of a propellant,

C. EFFECTS OF PREVIOUS DAMAGE

The cumulative damage relations provide a simple, direct means for evaluating the effects of previous damage histories upon propellant failure. This is important when considering the firing of a motor after a period of storage, thermal cycling, transportation and handling. To be sure, these damage histories limit motor firing capabilities, but until now we did not know the extent.

The relations applicable to this study are provided in Appendix L. They give a direct approach for evaluating the effects of damage upon the failure properties of propellants or propellant-liner adhesive bonds. Using the approach given in Appendix L we prepared the curves given in Figure 39 for a PBAN propellant. They show the dependence of the maximum true stress and the strain at maximum true stress upon the previous damage, ΣD_p, for specimens tested at 77°F, 0.74 min^{-1} strain rate under 1000 psi superimposed stress.

The application of these curves is essentially that for using uniaxial tensile data to predict motor firing capability. But, from a purely qualitative view, one can see that propellant strength is not greatly affected at values of ΣD_p less than 0.9. The strain at maximum true stress falls off at a higher rate than the strength but remains more than 75% of its original value at $\Sigma D_p = 0.8$. Since any <u>practical</u> motor design must have low values of ΣD_p (i.e. because of broad statistical ranges values are limited to less than 0.1, even after severe usage) then we can disregard previous damage histories when predicting motor firing behaviors.

Following this reasoning, it was concluded that motor firing performances generally ignore any previous damage history. That is, if a set of motors would fire successfully before thermal cycling or handling treatments then they should fire essentially as well after them; providing there are no failures produced by the pre-firing histories*

Actually, this behavior (that the motor tends to ignore its previous damage history) is well known experimentally, but it had not been shown analytically before this.

* It is implicit in these discussions that chemical damage is not being considered in calculating the damage history.

EFFECT OF PREVIOUS DAMAGE UPON THE TENSILE FAILURE PROPERTIES OF A PBAN PROPELLANT
(Tested at 77°F under 1000 psig superimposed hydrostatic pressure
and 0.74 min^{-1})

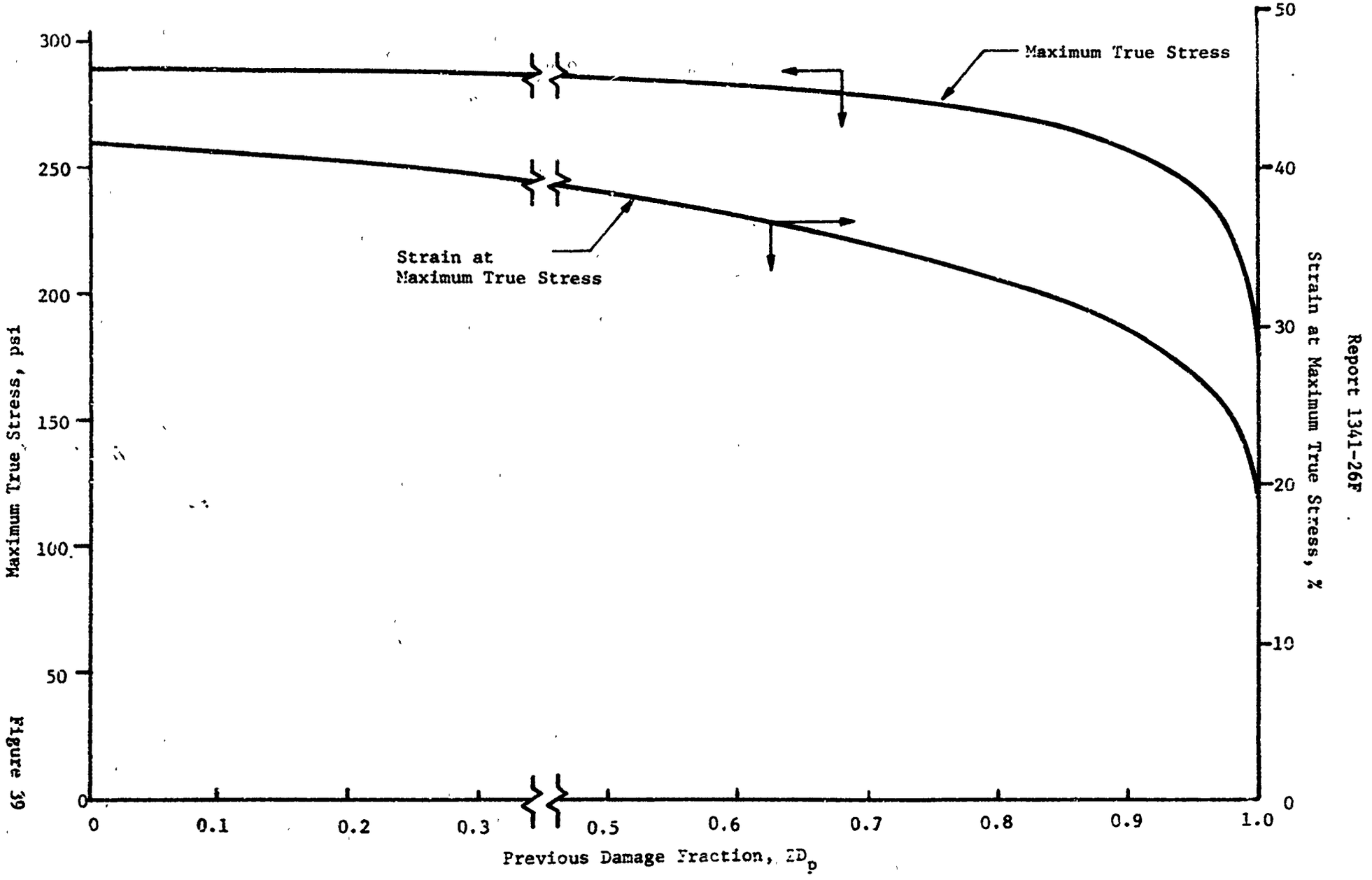

Figure 39

We have considered the effects of previous damage and found that the ultimate properties are significantly affected only when the grain is nearing failure ($\Sigma D_p = 1.0$). Now we are prepared to consider the development and use of a new analog test. This test can be used to evaluate the ability of a grain to withstand the stresses and strains produced in motor firings.

D. GRAIN PRESSURIZATION ANALOG TEST

A new test method, which is both easy to use and versatile, was devised to evaluate our cumulative damage predictions for motor pressurization failures. After evaluating the results of this testing we feel that the analog test offers a great potential for evaluating propellants in general. Like the analog tests for grain thermal storage and cycling, this test provides rapid, easily obtained data. The tests can be used to evaluate the propellant in some standard test mode, or in a test condition simulating a given motor application. In any event, we recommend that the test be evaluated by the Special Test Procedures Committee of the JANNAF Mechanical Behavior Wroking Group.

The design of the device is shown schematically in Figure 40. Basically it is a closed bomb with windows at both ends. The windows permit a view of the inner-bore of the grain, Figure 41, which is end-bonded to metal plates and these, in turn, are attached to the end plates of the bomb. The grain is caseless with a gap designed between the outer diameter and the sidewall of the bomb. The inner-bore and this outer port are pressurized separately according to a previously planned schedule. The outer pressure, P_o, is selected to give an "equivalent case stiffness". The value of P_o must be selected with respect to the given inner-bore pressure, P_i. (If desired, the inner-bore deflection can be limited by allowing the outside diameter of the grain to meet, and stop at, the heavy sidewall of the bomb.)

An exploded view of the test chamber and the grain, with the metal end-plates attached, is given in the photograph of Figure 42. Figure 43 is a photograph of the test set-up ready for operation. Here the light source is at the left and the lens of the camera on the right. The small canisters sitting on top of the test cylinder are the pressure transducers which are connected to the inner and outer port areas of the grain.

The grain, Figure 41, is a simple cylinder 9.5 in. long by 4.0 in. outside diameter with small flanges at both ends. The inner-bore can be of any practical design currently envisioned. The only limitation is that the expected failure area be visible through the windows in the bomb end-plates.

FLOW CIRCUIT DIAGRAM FOR GRAIN
PRESSURIZATION ANALOG TEST SET-UP

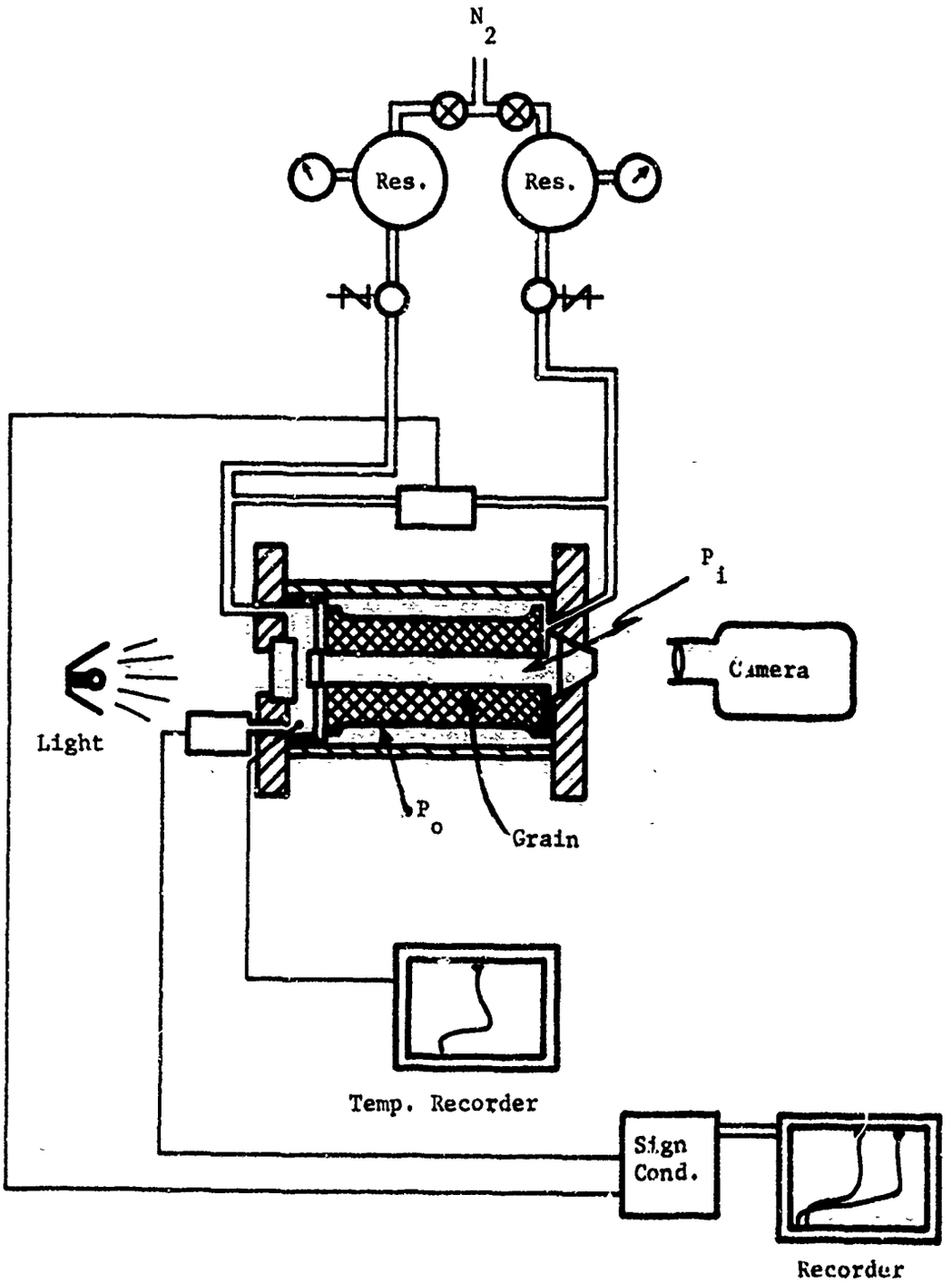

Figure 40

DESIGN OF GRAIN FOR PRESSURIZATION ANALOG TEST

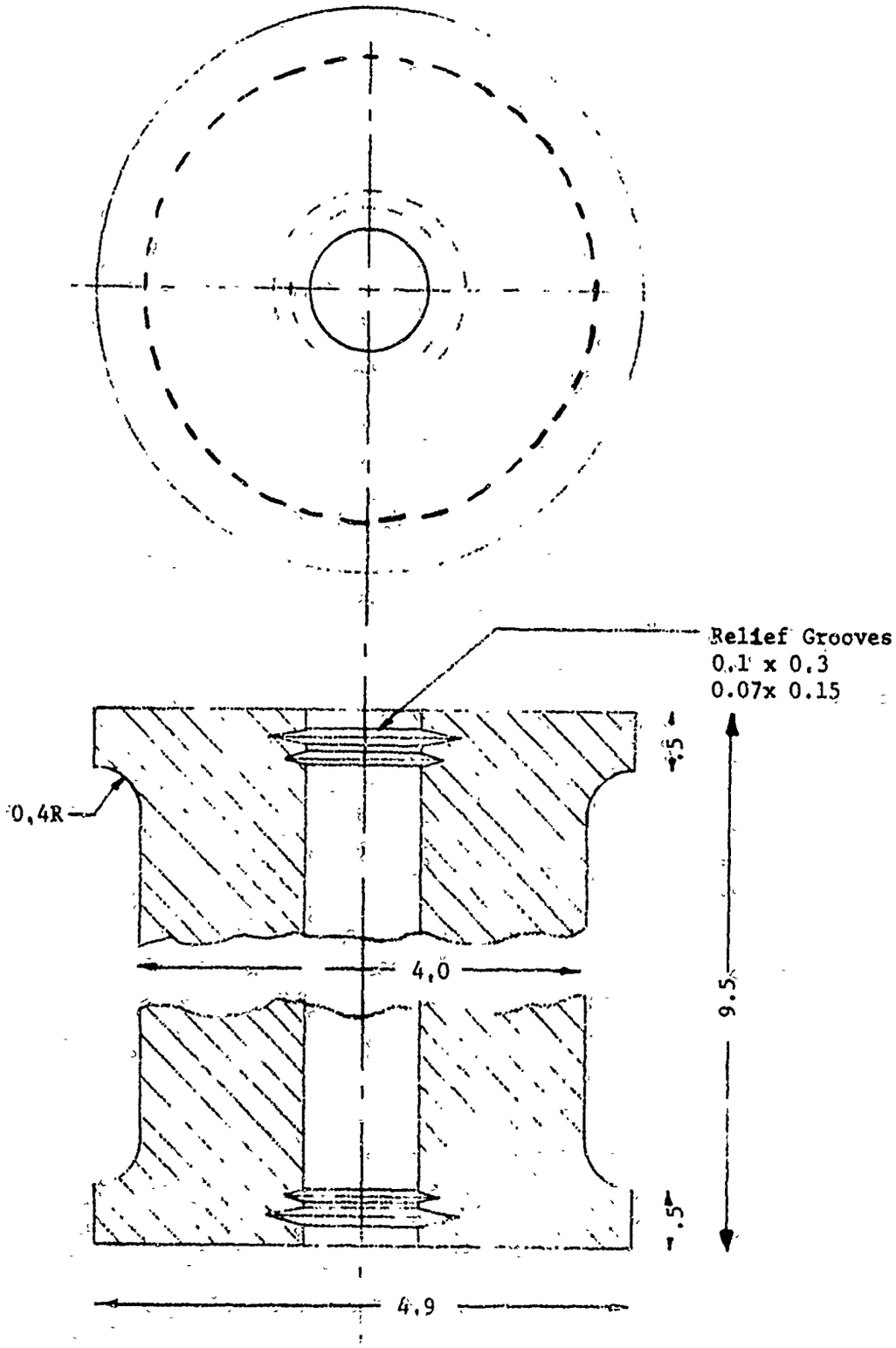

Figure 41

FIGURE 42. EXPLODED VIEW OF PRESSURIZATION ANALOG TEST CHAMBER AND GRAIN

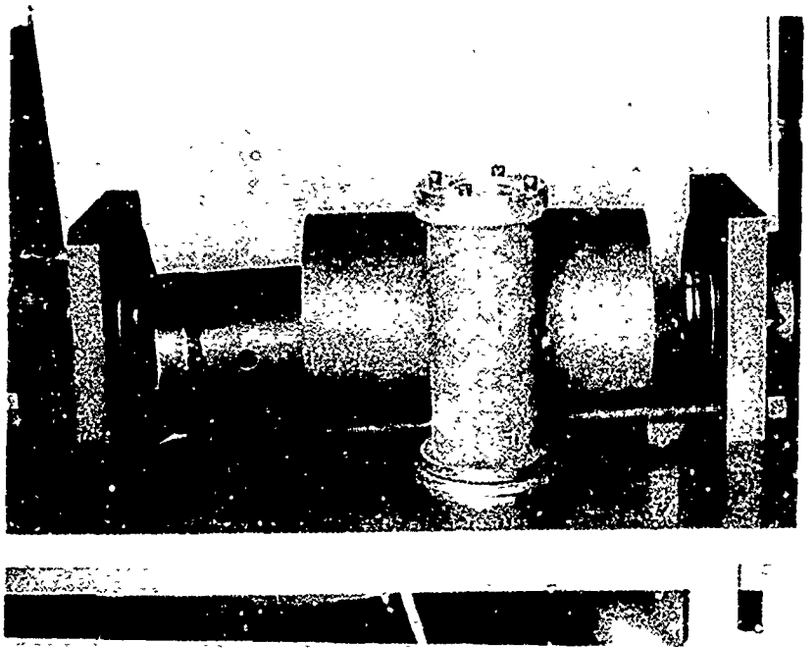

FIGURE 43. PRESSURIZATION ANALOG TEST READY FOR USE

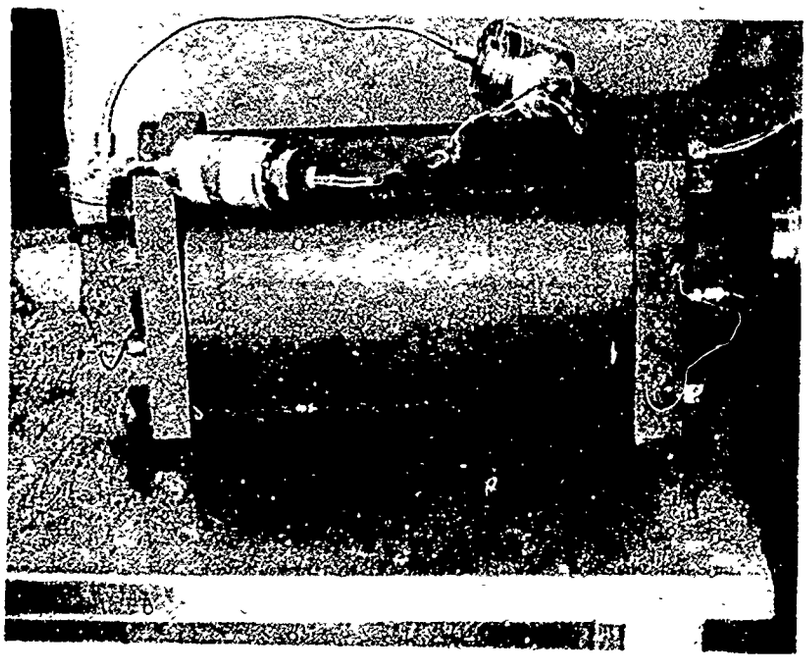

Figures 42 and 43

To prevent bond failures along the interface to the metal plates two stress-relieving grooves were machined into the bore at both ends of the grain, see Figure 41. This design was arrived at empirically. Although some bond failures were observed, most of the grains show initial failures along the inner-bore.

The bomb is pressurized at moderate rates (e.g., around 100 psi/sec) with nitrogen gas. At this low rate the gas temperature increases about 40°F on pressurizing to 250 psig. For very high pressurization rates (i.e., above 1000 psi/sec) it will be necessary to use oil, because of the excessive temperature rises expected.

Cracking or tearing of the inner-bore is photographically recorded. The inner-bore displacements may also be monitored in this fashion, or by other suitable instrumentation.

Initial testing with this device, at a low pressurization rate of 50 psi/sec., was carried out using wooden cylinders, dummy polyurethane propellants and a live PBAN propellant. The inner-bore was monitored with a 70mm Hulcher camera at 25 frames/second.

Unfortunately, the Hulcher camera has a very shallow depth of focus, about 1/2 in. at the distances involved here. This meant that the grain failures had to initiate at, or move into, this 1/2-in. deep field of view. We were successful in capturing a crack in this area for only one of our tests, Test E. This is shown in Figure 44 as a small black line at the bottom of the bore.

Obviously, better optical procedures will have to be used before this test can be used routinely; the equipment for this being commercially available. We believe this test to be sound and the experimental methods simple to follow.

The next section describes five tests on this device using a PBAN propellant.

E. COMPARISON OF PREDICTIONS WITH TESTS TO FAILURE ON GRAIN PRESSURIZATION

1. Approach

A total of ten grains were tested using the pressurization analog test. Five were tested after the stress relieving notches were devised. For these last tests a PBAN propellant, from a 44 in. diameter casting was used. All the grains were tested to failure.

PHOTOGRAPH OF INNER-BORE CRACKING DURING PRESSURIZATION
ANALOG TEST E

Frame #51

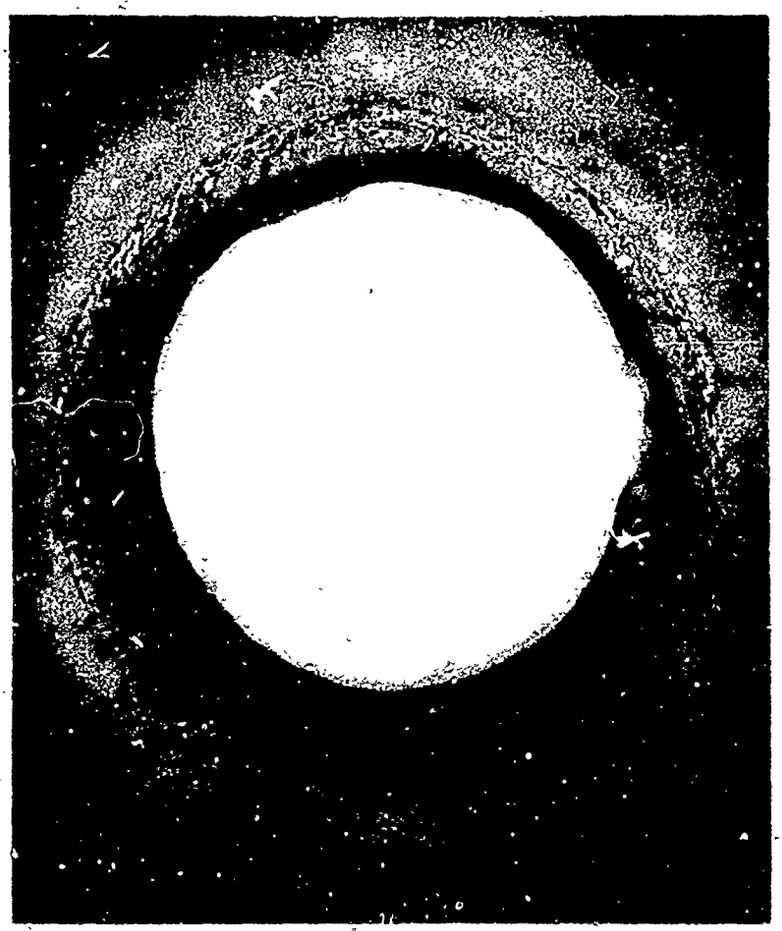

Crack

Figure 44

The stresses, strains and damage fractions were calculated using a planar analysis option of the two-dimensional viscoelastic computer program. The observed failure conditions were compared with those calculated by the LCD analysis and by a simple strain failure criterion.

The material properties used in the analyses are given in Appendix M. The cumulative damage parameters for the PBAN propellant are provided in Appendix M also.

Figures 45 and 46 provide two different forms of a strain failure criterion. Both of these use the values of a_p used in fitting the stress failure data.

The response and failure data in Appendix M show the propellant to be weak and to have relatively low moduli; while the ultimate strain data, Figures 45 and 46, are highly time dependent and poorly reproducible. The test specimens were soft and showed a number of surface defects. This may partially account for the apparently superior performance of the test grains to that of the tensile specimens. The actual test results on grains are described next.

2. Pressurization Analog Tests

Five grains were tested, but only four of them were analytically evaluated because of fund limitations. The four analyzed grains had bore diameters of one inch. The fifth had a 1.8 in. bore diameter.

The five grains were pressurized at moderate rates to pre-selected pressures at which the grains would be until they failed. A pressure differential between the bore and the case was varied to simulate a range of case stiffnesses. Table 6 shows the initial pressurization rates, maximum pressures before failure and the pressure differentials actually produced.

The failure-time data given in Table 6 were obtained from a differential pressure measurement. When this value began to fall rapidly the grain was considered to have cracked through the web. This time is somewhat later (by an unknown amount) than the time for failure initiation. Since the cracks progress slowly, propagation times of the order of one second, or more, might be expected for these cases. Test E is a good example of a grain exhibiting a bore crack without propagating the failure. No failure was observed after 85 seconds, yet the photo in Figure 44 shows that a crack existed at 62.5 seconds.

The detailed test pressures and photos of the bore cracks are presented below for each analog test.

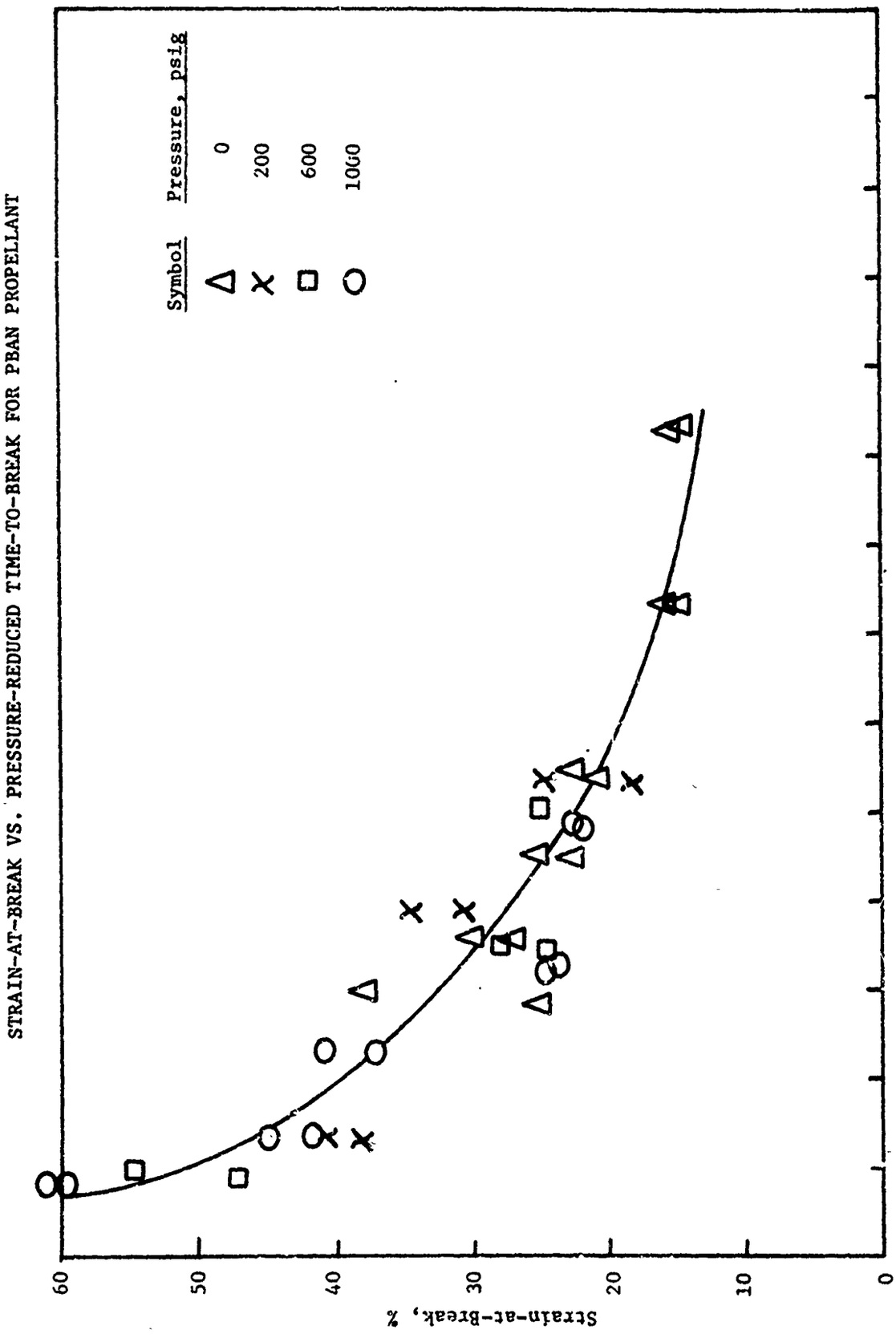
STRAIN-AT-BREAK VS. PRESSURE-REDUCED TIME-TO-BREAK FOR PBAN PROPELLANT
Symbol
Pressure, psig
0
200
600
1060
Strain-at-Break, %
60
50
40
30
20
10
0
-5
0
5
log t_b/a_p, min.

Figure 45

STRAIN-AT-BREAK VS. PRESSURE-REDUCED STRAIN RATE FOR A PBAN PROPELLANT

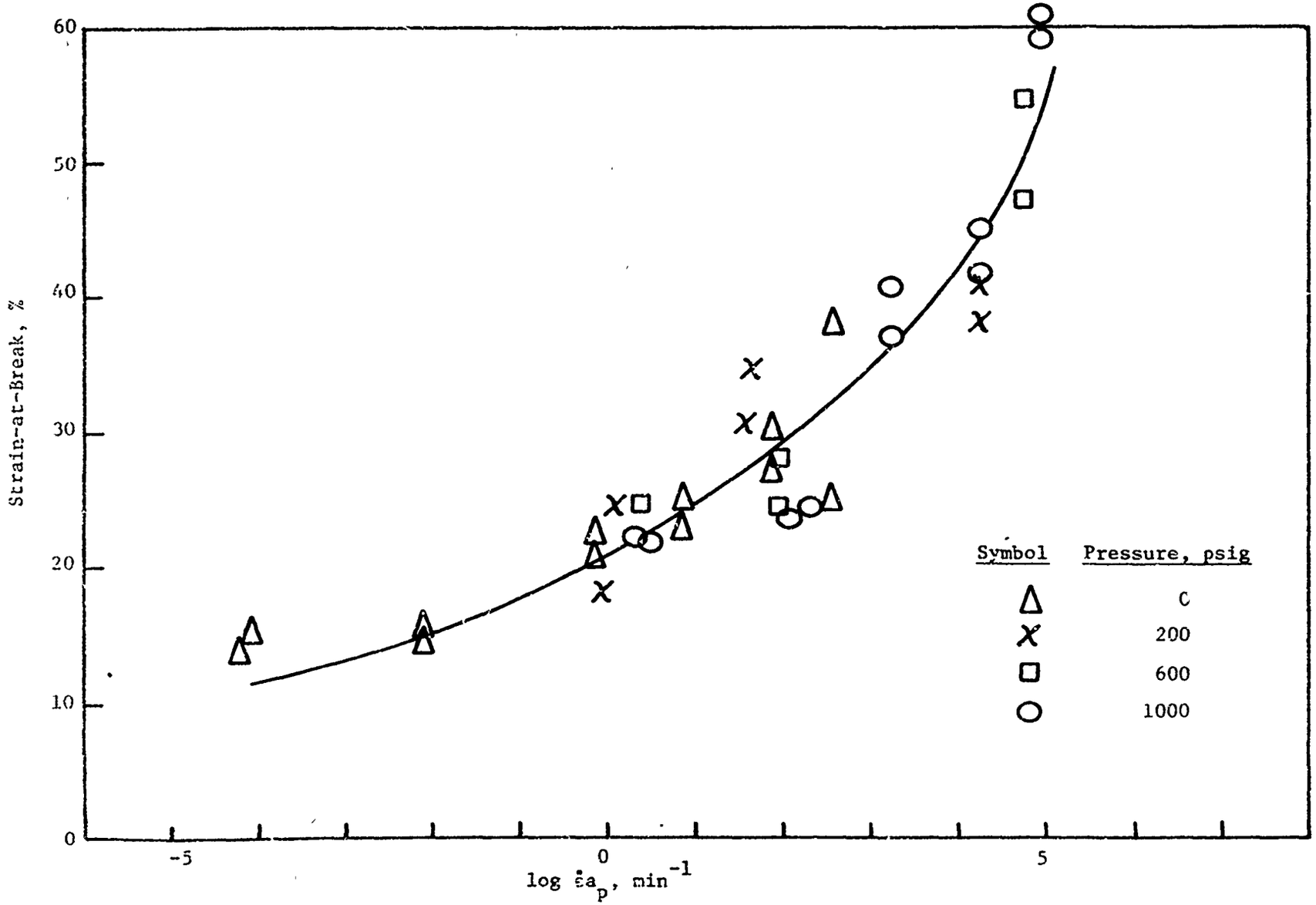

Figure 49

PRESSURIZATION ANALOG TEST CONDITIONS AND FAILURE DATA
(4 in. O.D. Grains)

Test	I.D., in.	Initial $\dot{P}$ psi/sec. Bore	Initial $\dot{P}$ psi/sec. Case	Max. Press. psig Bore	Max. Press. psig Case	Diff. Pressure, psi	Time-to-Failure sec.	Failure Description
A	1.0	113	50	207	104	103	2.25	Small crack + Unbonding
B	1.0	109	52	248	135	113	2.7	1-1/2" long crack + dewetting + unbonding
C	1.0	84	52	352	226	126	6.3	Very long cracks thru grain web
D	1.0	107	55	338	234	114	16.6	Very long cracks thru grain web
E	1.8	43	35	218*	200*	18	?	Small bore crack

* At pt. where max differential obtained

Table 6

Figure 47 shows the pressure-time traces for analog Test A. Figures 48 and 49 show the inner-bore failures which occurred before the grain unbonded from the metal plates. These bore cracks are small and shallow. These photos also show large tooling markes which show the difficulty of working with this soft propellant. These tooling marks did not appear to affect the failure behavior of this grain.

Figure 50 gives the pressure-time traces for Test B. While Figure 51 shows the inner-bore cracks produced before unbonding at the grain ends. Figure 52 shows some minute cracks which, in actuality, meet the requirements of failure as predicted by most propellant failure criteria.

Figure 53 presents the pressure-time traces for Test C. Figures 54 and 55 show the large, deep cracks produced. Figure 56 shows the crack which penetrated through the web.

The pressure-time trace for Test D is provided in Figure 57. Figures 58 and 59 show the very large bore cracks, one of which propagated through the web, Figure 60.

The pressure-time trace for Test E is given in Figure 61. No photos were made of the bore cracks, which were small and shallow, except for the bore photo given previously in Figure 44.

The laboratory results described above were prepared for comparison with cumulative damage failure predictions. These comparisons are made next.

3. Comparisons with Failure Predictions

The four analog tests A to D were evaluated analytically for the stresses, strains and damage fractions. The results of the analyses are summarized in Table 7, which compares the observed times to failure with the average times obtained from the damage analyses.

As shown by Table 7 the calculated times are significantly less than those observed. A portion of this is attributed to the low crack propagation rate. That is, the crack could initiate and slowly propagate into the photographic field of view or it could slowly tear through the web, finally affecting the pressure differential. Had the inner-bore optics and photography been more effective the questions about the crack initiation time would have been eliminated. The greater error obtained for largest bore strains in Table 7 appear to be from underestimating the effect of pressure. The non-linear properties afforded by finite deformations can be quite large. Add to this the dilatational effects and we can easily reduce the bore stresses by 20% or more, see Section III.B. Since the damage is calculated using bore stresses to the 8.75 power, a simple reduction of 20% in these stresses would reduce the damage to 13.5% of that calculated here. These reductions in the stresses and damage fractions are about that needed to resolve the discrepancies between the

PRESSURE-TIME TRACES FOR ANALOG
TEST A - DIMENSIONS: B = 2.0 in., A = 0.5 in.

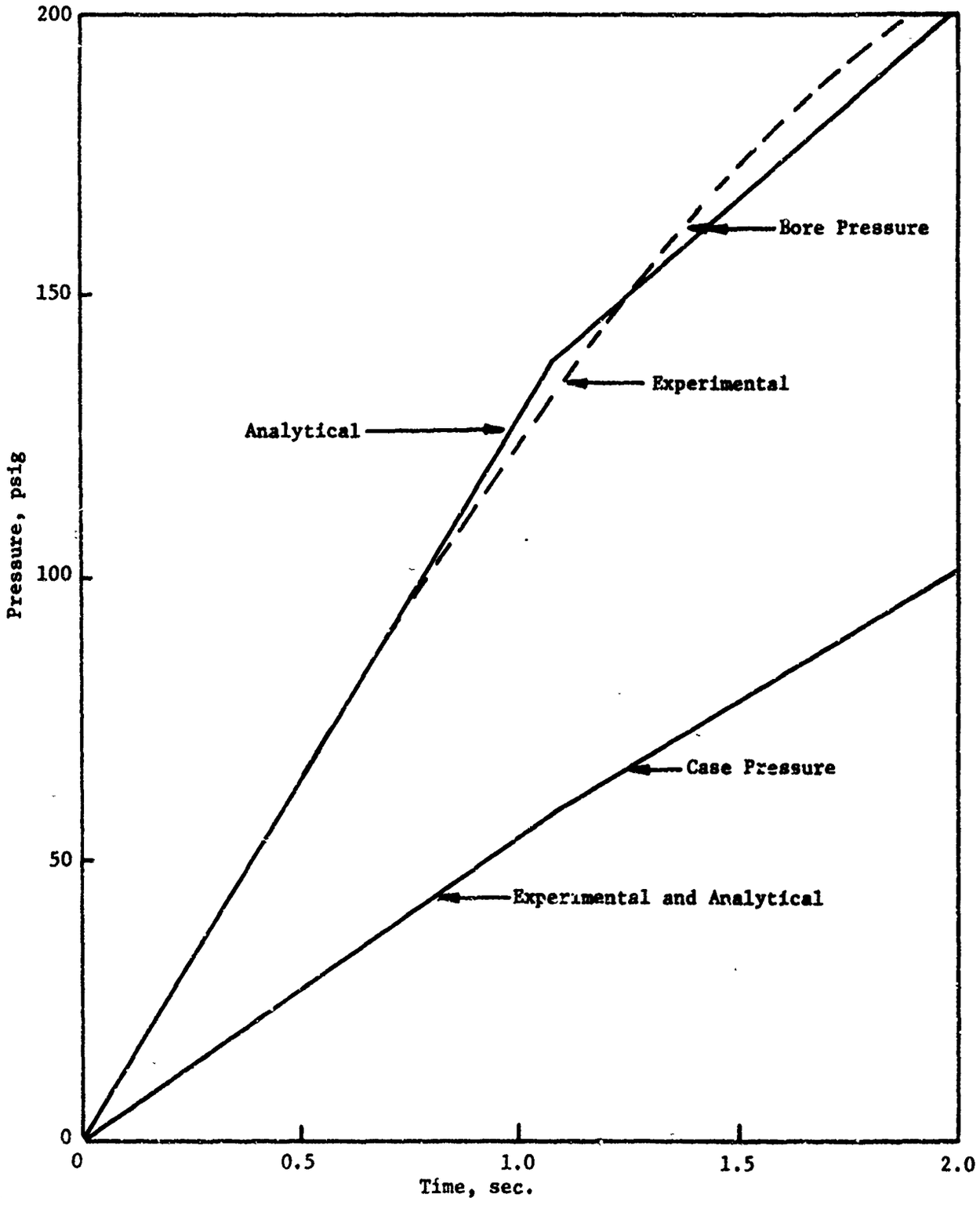

Figure 47

FIGURE 48. CLOSE-UP OF BORE FAILURES OF PRESSURIZATION ANALOG TEST A

FIGURE 49. CLOSE-UP OF BORE FAILURES OF PRESSURIZATION ANALOG TEST A

Figures 48 and 49

PRESSURE-TIME TRACE FOR ANALOG
TEST B - DIMENSIONS: B = 2 in., A = 0.5 in.

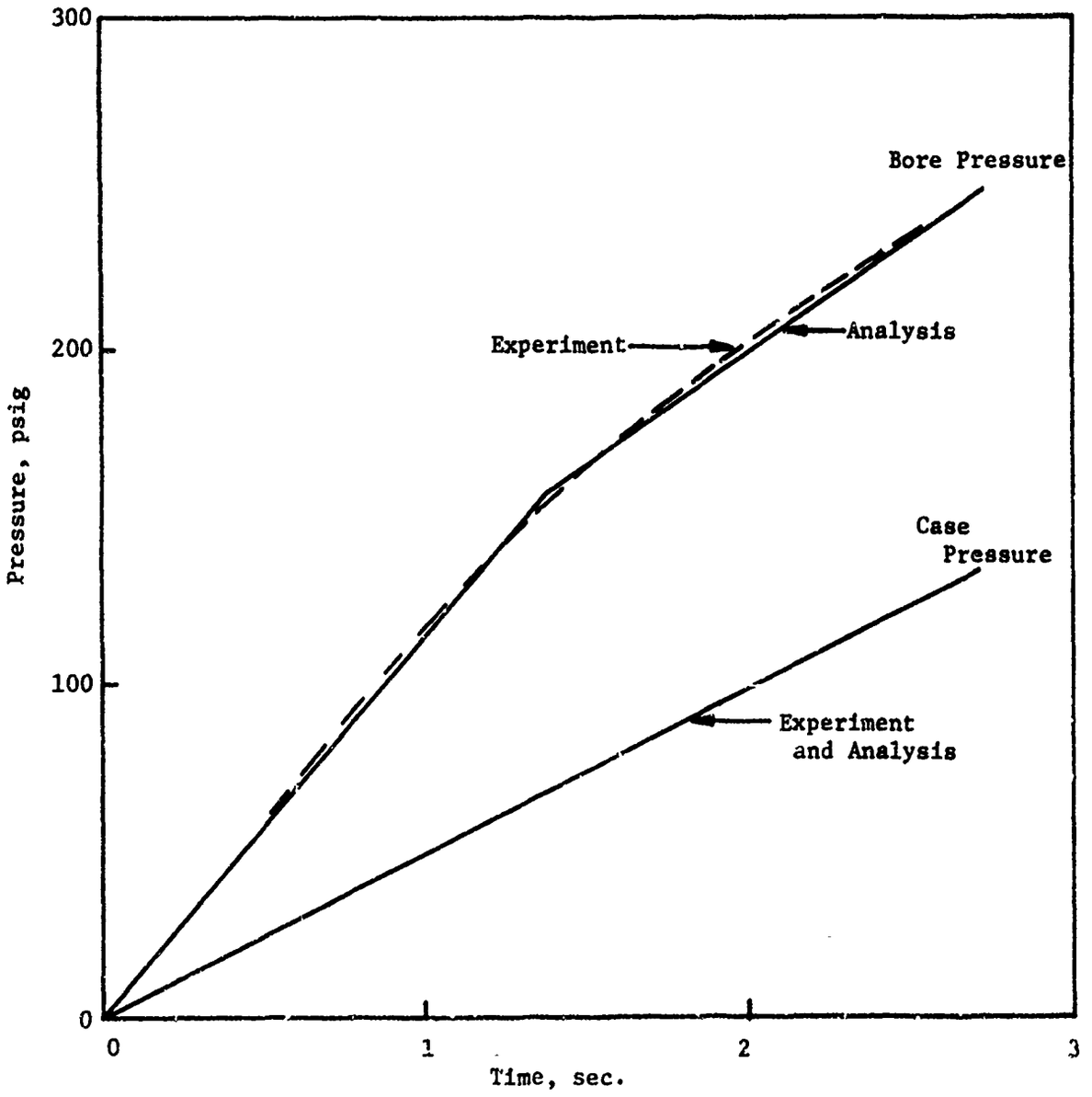

Figure 50

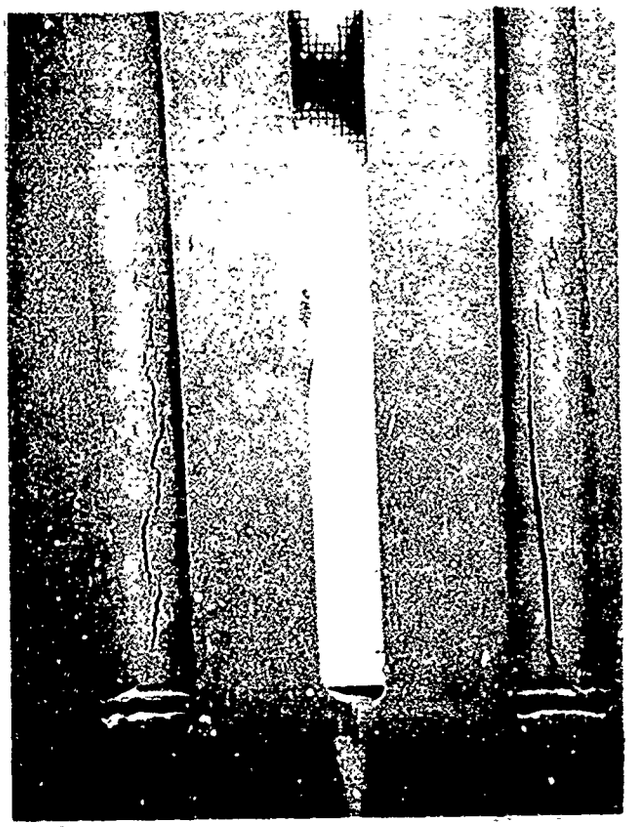

FIGURE 51. BORE FAILURES OF PRESSURIZATION ANALOG TEST C

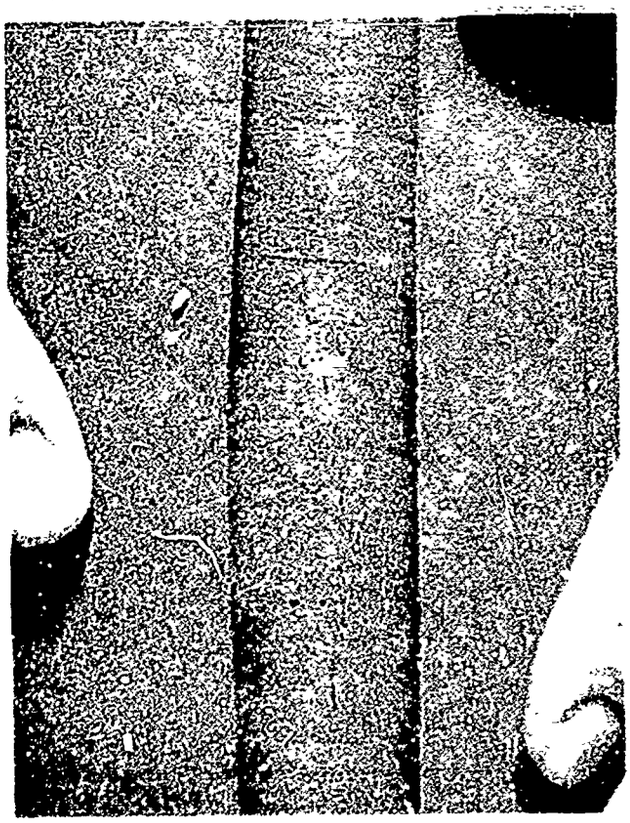

FIGURE 52. CLOSE-UP OF TINY BORE FAILURES OF PRESSURIZATION ANALOG TEST B

Figures 51 and 52

PRESSURE-TIME TRACE FOR ANALOG

TEST C - DIMENSIONS: B = 2.0 in., A = 0.5 in.

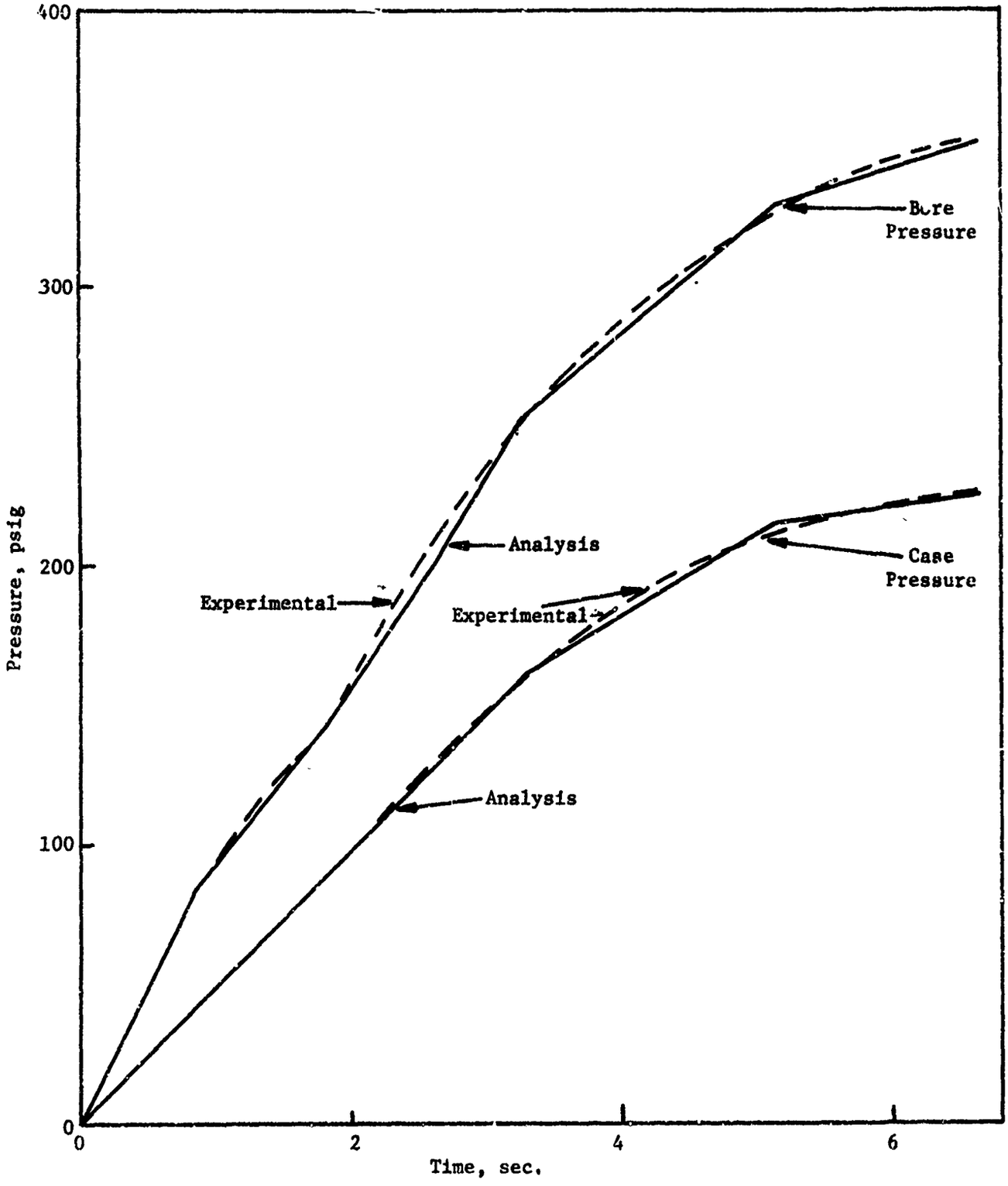

Figure 53

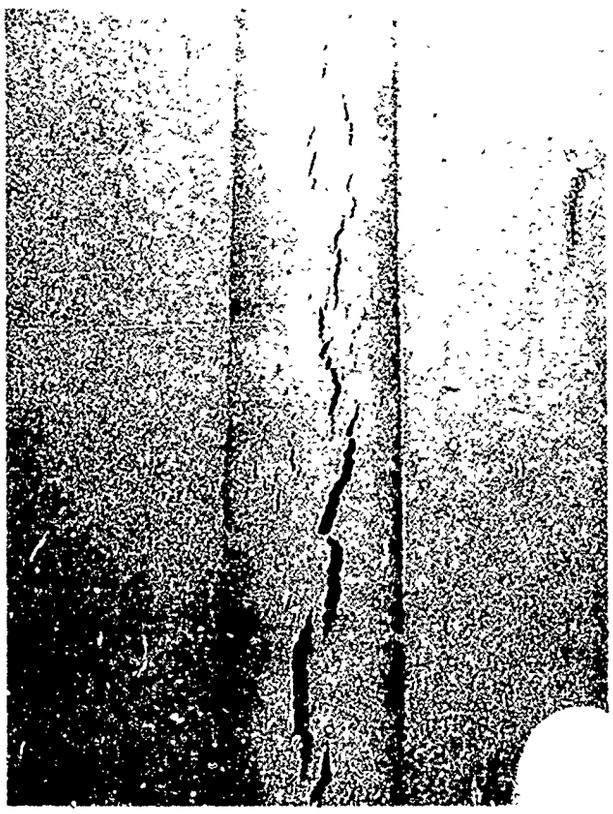

FIGURE 54. CLOSE-UP OF BORE FAILURES OF PRESSURIZATION ANALOG TEST C

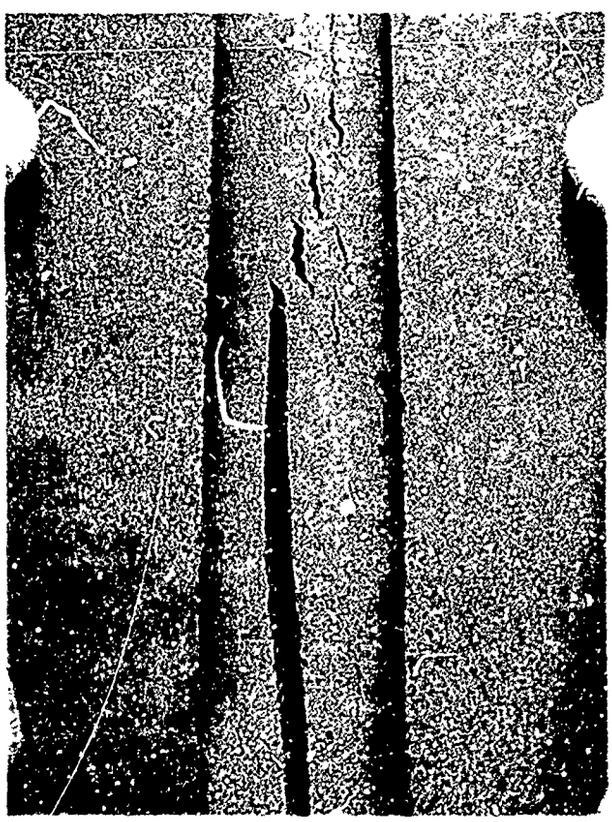

FIGURE 55. CLOSE-UP OF BORE FAILURES OF PRESSURIZATION ANALOG TEST C

Figures 54 and 55

EXTENSION OF BORE CRACK THROUGH SIDEWALL OF PRESSURIZATION
ANALOG TEST C

Figure 56

PRESSURE-TIME TRACE FOR ANALOG
TEST D - DIMENSIONS: B = 2.0 in., A = 0.5 in.

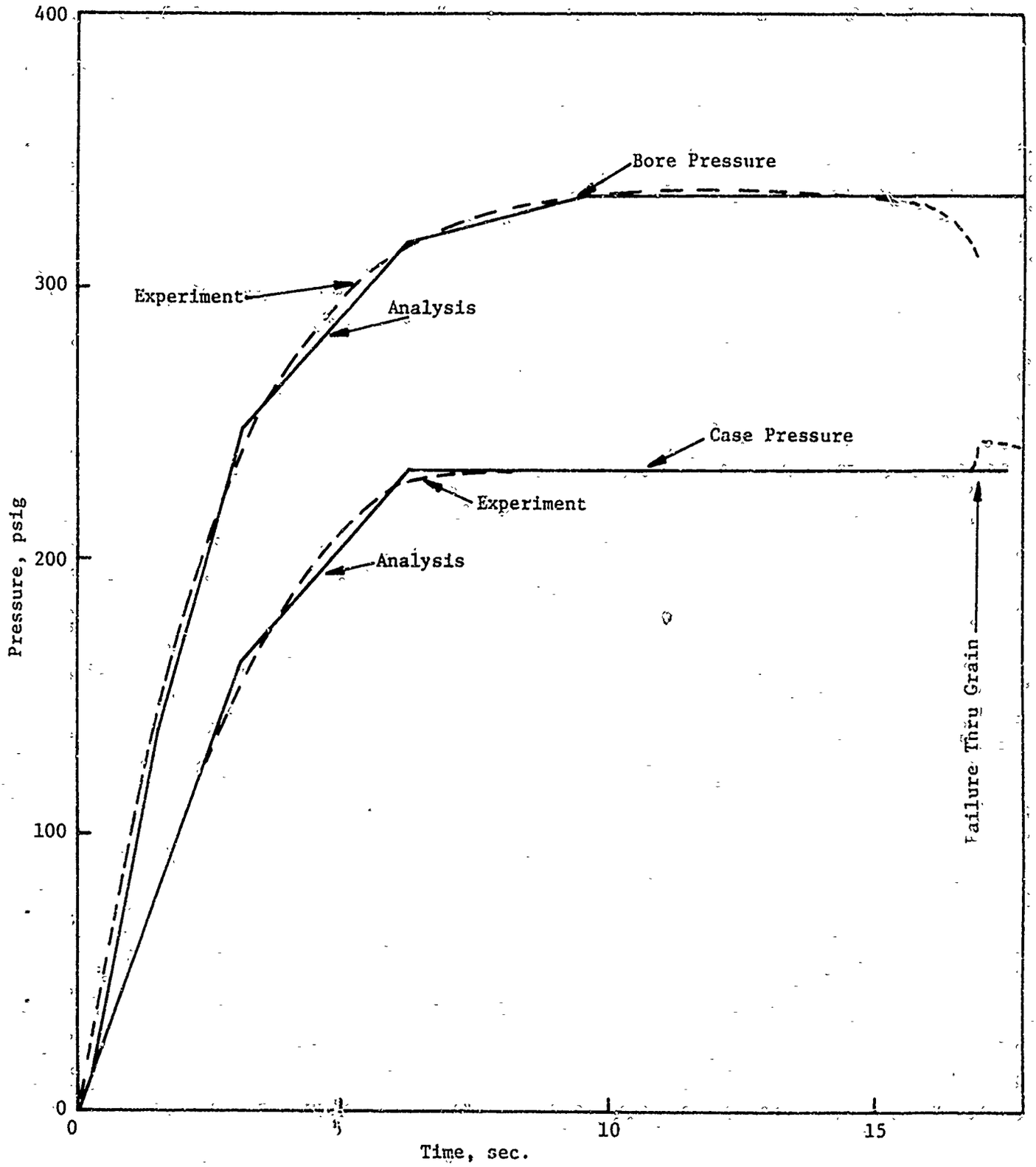

Figure 57

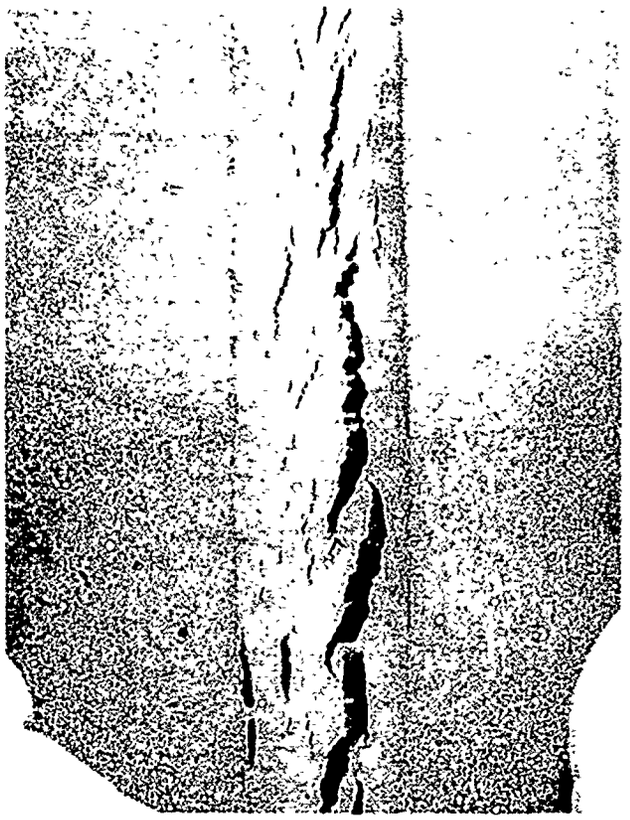

FIGURE 58. CLOSE-UP OF BORE FAILURES OF PRESSURIZATION ANALOG TEST D

FIGURE 59. CLOSE-UP OF BORE FAILURES OF PRESSURIZATION ANALOG TEST D

Figures 58 and 59

EXTENSION OF BORE CRACK THROUGH SIDEWALL OF PRESSURIZATION
ANALOG TEST D

Figure 60

Aerojet Solid Propulsion Company
Report 1341-26F

PRESSURE TIME TRACES FOR ANALOG

TEST E - Dimensions: b = 2.0 in., a = 0.9 in.

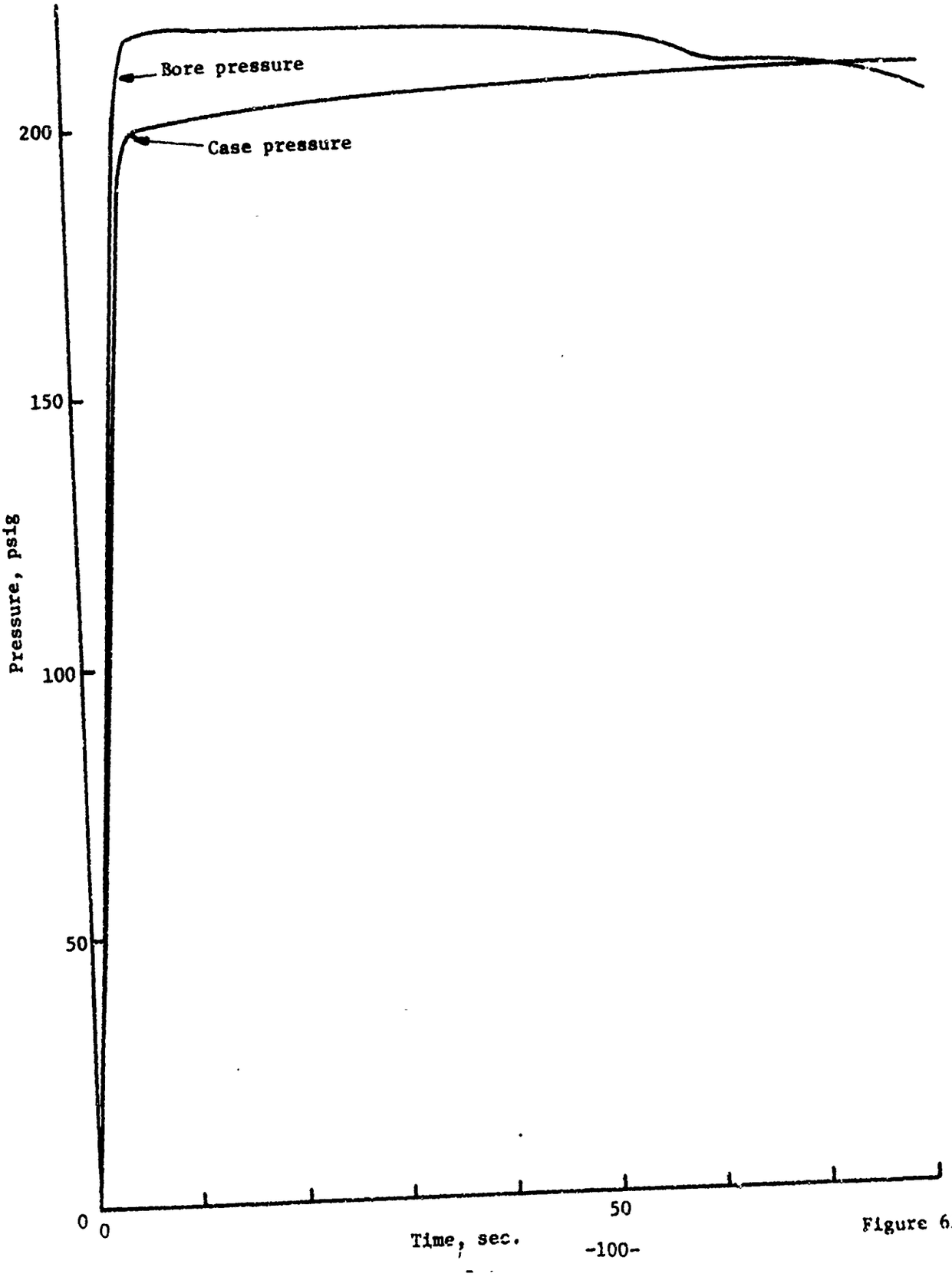

Figure 61

COMPARISON OF CALCULATED AND OBSERVED FAILURE DATA
- USING LCD ANALYSES -

Test	Time-to-Failure, sec.		Calculated Strains*, %	
	Observed	Calculated	Observed	Calculated
A	2.25	1.64	50	44
B	2.7	2.0	51	44
C	6.3	3.7	60	46
D	16.6	3.9	56	42

* At given times-to-failure

Table 7

calculated and observed times-to-failure. Also shown in Table 7 are the strains at failure derived from these times to failure.

Although the linear cumulative damage criterion did not accurately predict failures on pressurization, the LCD approach did give consistently conservative results for this particular case. The error observed is believed to stem from the stress analysis which does not account for finite deformations nor dilatation.

A strain failure criterion was applied to these data and found to be still more conservative, even though we made no consideration for the statistical effects and we ignored the biaxial correction factor which is usually required when using uniaxial data to estimate grain failures. The strain criterion was based on the average data in Figure 46. The maximum value of $\dot{\varepsilon}a_p$ was estimated from the pressure history and the calculated strains. The failure strains thus obtained are given in Table 8 where they are compared to the failure strains of Table 7 derived from the times to failure observed* and from the LCD analyses. The results are about 50 to 60% of the observed values and about 75% of those predicted by linear cumulative damage.

* From the time-to-failure, by calculation.

COMPARISON OF ESTIMATED FAILURE STRAIN VALUES

Test	Failure Strains, % From Observed Time to Failure*	From LCD calc. Time to Failure	From Maximum Strain Rate, Fig. 46
A	50	44	33-34
B	51	44	31-33
C	60	46	30-34
D	56	42	28-33

* At given time-to-failure, by calculation

Table 8

V. TECHNOLOGICAL FORECAST

At the beginning of this program the linear cumulative damage concept had been well established for solid propellants while thermoviscoelastic stress analyses had been advanced to include finite length grains with continuously varying boundary temperatures. In this program we have completed a study to evaluate the effects of grain design parameters upon thermoviscoelastic stresses, strains and damage effects; prepared simplified parametric design curves suitable for early grain design and propellant selection; developed normalization methods for the relaxation modulus which can further simplify methods for selecting or formulating propellants for a given application; improved upon the existing two-dimensional, thermal viscoelastic, stress analysis capability, adding the capability to handle planar geometries; investigated non-linear analyses based upon propellant dilatational behavior, finding the analytical evaluation to be straightforward and useful; extended cumulative damage studies to include failures on motor pressurization, the experimental confirmation of these relations requiring the development of a novel pressurization analog test and the testing to failure of ten propellant grains. It is reasonable now to give our overall estimate of the work in this field leading to predictions of the future state-of-the-art.

A. PROBLEM

The problem approached here was to advance the state-of-the-art in viscoelastic stress analyses and to extend the range of application of the linear cumulative damage relation for solid propellants with emphasis placed upon the development of practical tools for engineering, propellant development and mechanical property characterizations. In particular we planned to: (1) provide practical engineering design curves for rocket grains, in terms of their stress, strain and damage behaviors; (2) make basic improvements in stress analysis methods; and (3) verify the linear cumulative damage predictions for grain failures on motor pressurization.

The successful completion of this program provides the following benefits to the Navy: (1) improved methods of grain design and propellant formulation; (2) a simplified procedure for the experimental characterization of propellant modulus; (3) an accurate, inexpensive method for estimating the grain stresses for new candidate propellant formulations; (4) a guide to improved propellant formulation for a given grain design shows the relative importance of binder crosslinking and internal flow processes (oxidizer-binder bond effects and others); (5) the most advanced thermoviscoelastic stress analysis capability has been expanded in scope and versatility; (6) a promising approach to propellant non-linear viscoelasticity was investigated and shown to be practical, offering an area of study which should be pursued; (7) a new analog test for evaluating the failures of grains on motor pressurization; (8) a technical basis for understanding the time-pressure shift factor, a_p, for propellants; and (9) confirmation that the linear cumulative damage approach can predict grain failures on pressurization, although a little conservatively.

B. STATE-OF-THE-ART, SOLUTION AND FORECAST

Let us next summarize the state-of-the-art at the beginning of this program, consider the advancements made as a result of the current efforts, and offer a prediction of the future state-of-the-art based on this understanding.

1. Parametric Design Curves

Only one parametric study for grain stresses and strains had been previously performed and that was based upon elastic analyses.[18] The current effort extends that study to include transient thermal histories evaluated by thermoviscoelastic analyses. The normalization of the relaxation modulus had been performed previously, but it did not offer the advantages of the approach presented here. Also, the use of the new normalization parameters permits normalizing grain stress analyses, which had not been previously done. Also, these new normalization procedures provide simple guides to the chemist for specific formulation improvements. This capability was not available previously.

The forecast for the generation and use of parametric design curves and the new normalization methods is given in Figure 62.

2. Improved Analytical Methods

The earlier analytical developments provided a thermo-viscoelastic stress analysis for finite length grains, where the boundary temperature may be continuously varying. The effects of the previous strain rate history was included as an essential feature required by the constantly changing boundary temperatures and, especially, for rapid heating. In addition, provision was made to calculate the stored and dissipated strain energies. This latter was included to support those engineers using energy approaches to propellant failure predictions.

Although the existing analytical methods gave us advanced capabilities, they were, nevertheless, limited. The two-dimensional analyses gave numerical difficulties after 500 calculation-time points and were limited to circular bore grains. In addition, the non-linear viscoelastic effects of strain-dilatation in propellants were ignored. The current program was designed to extend the present analytical methods in these areas. The numerical difficulties were associated with the short word length of the computer leading to turncation errors. Reformulating the method of solution partially alleviated this difficulty.

The previous analytical capability was designed to analyze case-bonded cylindrical grains. For arbitrary solids of revolution, a complete analysis would entail three-dimensional programs which are beyond current computer capabilities. Therefore, the existing thermo-viscoelastic analysis was extended to include evaluations of planar sections. This will permit us to evaluate actual grain cross-sections, but without considering the influence of the end conditions.

FORECAST OF PARAMETRIC DESICN CURVE STUDIES

Parametric design curves based upon non-linear viscoelastic stress and damage analyses

Use of normalization parameters to guide aging and surveillance studies

Use of normalized stress analyses by engineers for economical evaluations

Use of normalization parameters by chemists to guide propellant formualtion

Normalization of relaxation moduli and viscoelastic stress analyses

Parametric design curves for thermoviscoelastic response and failure

Preliminary design evaluation curves for cumulative damage predictions

Parametric design curves - elastic analysis

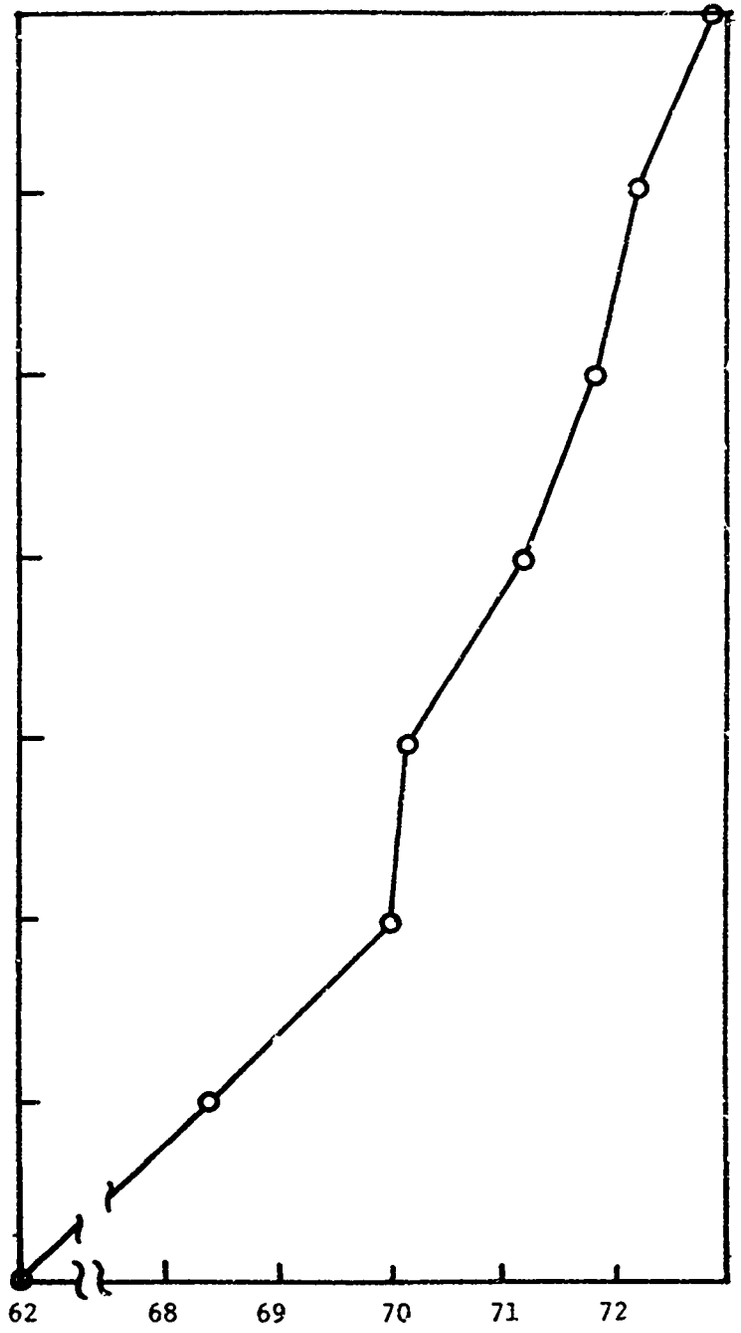

Aerojet Solid Propulsion Company
Report 1341-26F

Figure 62

The fact that the viscoelastic response of solid propellants is highly non-linear had been well established by numerous investigators. Although many non-linear analyses had been developed none had considered the effects of binder-filler bond failures and strain dilatation, a primary factor in propellant response and failure. We found that an analytical evaluation appeared to be very straightforward and useful. The non-linear behavior was approximated by an equation which could be incorporated into the existing analysis with a minimum of effort. The procedure was verified on a sample problem and found to be qualitatively in accord with observations on real grains.

Figure 63 provides a forecast for further studies of the viscoelastic analysis methods. The work centers around non-linear viscoelastic approaches both with and without linear viscoelasticity. Since the analytical developments can proceed no faster than the experimental confirmation of them we have included in the forecast the experimental verification of the analyses.

3. Grain Failures on Pressurization

Prior to this program tests (other than ballistic) on propellants under superimposed pressures had been limited to laboratory measurements on uniaxial, biaxial and triaxial (poker chip) specimens. The maximum principal stress failure criterion and the linear cumulative damage (LCD) approch were found to apply as good approximations. Tests of the LCD analyses for predicting grain failures on pressurization had not been attempted and the time-pressure shift factor, a_p, had not been defined for three-dimensional stress conditions.

A new evaluation of propellant failure mechanisms provided the technical basis for defining and using the time-pressure shift factor, a_p, in a three-dimensional grain problem; the value of a_p was found to be dependent upon the critical stress σ_{cr}, which is readily defined.

The effects on propellant failure properties of the damage accumulated from some past history was considered next. It was found that propellant ultimate properties are significantly affected only when the grain is nearing a failure. This led to the conclusion that a motor tends to ignore its previous damage history. (That is, if it would have fired successfully before the damage treatment it probably would fire successfully after that history, providing actual failures were not present at the time of firing.)

An especially successful effort was the development of a grain pressurization analog test. This test permits the direct evaluation of a propellant in determining its ability to function as a grain during motor pressurization, and offers a great potential for evaluating propellants in general.

FORECAST OF THERMOVISCOELASTIC STRESS ANALYSIS AND EXPERIMENTAL VERIFICATION OF THEM

Stress measurements and correlation with non-linear analyses

Non-linear viscoelastic analysis based upon strain dilatation, combined with non-fading memory approach

Application of improved stress transducer technology (either verification of an existing method or generation of a new one) to verify thermoviscoelastic predictions

Non-linear viscoelastic analysis based upon non-fading memory (Mullin's Effect), combined with stress measurements on models

Investigation of non-linear analyses based upon strain dilatation

Second two-dimensional thermoviscoelastic stress and damage analyses, with generalized planar options.

One- and two-dimensional viscoelastic stress and damage analyses for motor firing

First two-dimensional thermoviscoelastic stress and damage analyses (analyses for rapid heating conditions)

Experimental stress measurements on propellant grains and cylinders

Combined stress and damage analyses by computer

Second one-dimensional thermoviscoelastic stress analysis

First one-dimensional thermoviscoelastic stress analysis

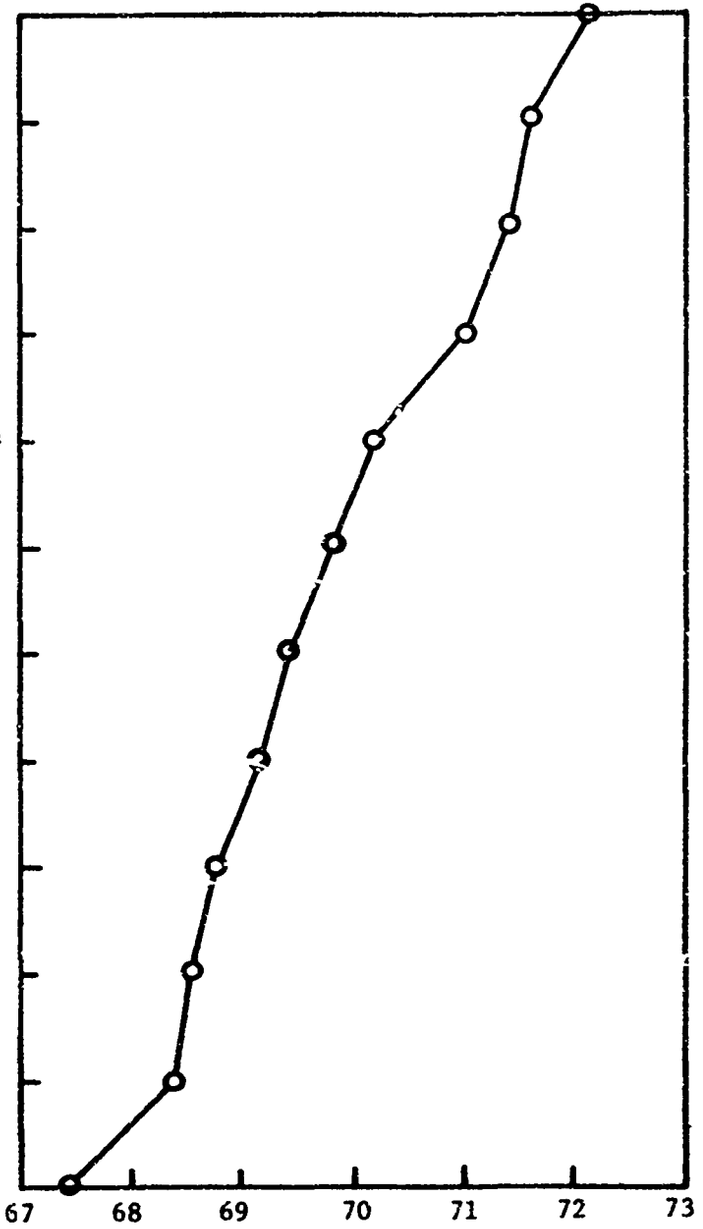

Figure 63

A total of ten grains were tested in developing the pressurization analog test, four of these were used in comparing predictions with observed motor failures. The predictions were consistently conservative.

No further studies are envisioned in this area in the near future. However, it is felt that further efforts should be made to utilize the pressurization analog test since it is both convenient and inexpensive to use.

C. SUGGESTIONS AND IMPLICATIONS

It is pertinent finally to present suggestions for further extending the state-of-the-art and the implications of this work on other technical areas. These are considered below.

1. Extending the State-of-the-Art

A number of very important study areas exist and we have listed some of them.

The currently employed methods of viscoelastic stress analysis and experimental stress measurements can show marked differences which the existing, non-linear methods of viscoelastic analysis cannot account for. As a matter of fact, the non-linear corrections usually lead to stress predictions which increase the error, not decrease it. Since the most useful current methods of failure analysis depend directly upon grain stresses, it is mandatory that this analytical difficulty be evaluated and the problems resolved.

A highly important part of the problem stated above is the experimental measurement of grain stresses. It appears that significant errors exist even in the simple uniaxial test of large specimens. Reliable and accurate methods of grain stress measurement need to be defined.

Realistic response behaviors of solid propellants must be defined for analytical purposes. For low strain applications the Mullin's effect leads to non-linear viscoelastic behaviors. This type of non-linear analysis is currently being studied for the Navy at Aerojet.

A still greater non-linearity of the propellant response occurs at high strains on strain-dilatation. Specifically, an improved analysis method should be developed based upon the dilatation relations reported in Appendix I. These relations could be used together with both the linear and non-linear viscoelastic analysis procedures.

A significant barrier limiting development of propellant failure criteria is the chemical instability of most composite solid propellants. By instability, we mean those chemical changes within the bulk of propellant which markedly affect times-to-failure, as in constant load testing, for example. This behavior does not affect the ballistic utility of the propellant, but it does greatly limit our ability to predict failures of propellant grains. One consequence of this behavior is the requirement for very large margins of safety which are usually hidden within the statistical arguments for defining stress and strain allowables for grain design.

Extension of cumulative damage prediction methods to account for aging effects would have substantial economic advantages to the services. The introduction of time shifts, analogous to the a_T and a_p methods, but accounting also for changes in equilibrium properties by vertical shift factors as well have already been demonstrated for natural and synthetic rubbers and could be developed for application to prediction of property changes on aging. This work coupled with the examination of the use of early changes and failures to predict inventory behavior, would allow improved accuracy in replacement and retrofit forecasting with significant cost savings.

2. Influence of Effort on Other Technical Areas

The primary technical areas receiving benefit from this work are propellant development and design analysis, where the results directly assist in performing the required tasks. However, the results are of great benefit to the Navy in providing better tools for evaluating the properties of a candidate propellant with respect to a given grain application. Furthermore, as the work develops fewer measurements and lower development costs will result.

In addition to these material benefits, an important byproduct of these efforts is the advance made in understanding of material response and failure. The effort reported here is practically oriented, but the basic concepts studied are providing also fundamental knowledge in areas related to basic failure research.

REFERENCES

1. Bills, K. W., Jr., Peterson, F. E., and Steele, R. D., "Study of Cumulative Damage Techniques for the Prediction of Motor Failure", Aerojet-General Corporation Report No. 4158-81F (Contract No. NOw 66-0545-c) (July 1967).

2. Bills, K. W., Jr., Peterson, F. E., Steele, R. D., and Sampson, R. C., "Development of Criteria for Solid Propellant Screening and Preliminary Engineering Design", Aerojet Report 1159-81F (Contract No. N00017-67-C-2415) (December 1968).

3. Bills, K. W., Jr., Campbell, D. M., Sampson, R. C., and Steele, R. D., "Failures in Grains Exposed to Rapid Changes of Environmental Temperatures", Aerojet Report 1236-81F (Contract No. N00017-68-C-4415) (April 1969).

4. Bills, K. W., Jr., et. al, "Solid Propellant Cumulative Damage Program", Final Report No. AFRPL-TR-68-131, Contract No. F04611-67-C-0102, (October 1968).

5. Anderson, J. M., "Rate Dependent Aspects of Failure in Cast Double Base Propellant", Bulletin of the 8th Meeting of the JANNAF Mechanical Behavior Working Group, Vol. I, p. 515 (March 1970).

6. Wiegand, J. H., "The Interrelation of Modulus and Nominal Maximum Stress", Bulletin of the Fourth Meeting of the ICRPG Working Group on Mechanical Behavior, 235 (November 1965).

7. Bersche, C. V., Graham, P. H., and Robinson, C. N., Technical Note: "Further Studies of the Interrelation of Propellant Modulus and Nominal Maximum Stress", Bulletin of the 8th Meeting of the JANNAF Mechanical Behavior Working Group, Vol. I, p. 207 (March 1970).

8. Freudenthal, A. M., "The Expected Time to First Failure", Air Force Materials Laboratory, Report AFML-TR-66-37 (February 1966).

9. Herrmann, L. R., and Peterson, F. E., "A Numerical Procedure for Viscoelastic Stress Analysis", Bulletin of the 7th Meeting of the ICRPG Mechanical Behavior Working Group, CPIA Pub. No. 177, p. 155 (October 1968).

10. Herrmann, L. R., "Elasticity Equations for Incompressible and Nearly Incompressible Materials by a Variational Theorem", AIAA, J., Vol. 3, No. 10, pp. 1896-1901, October 1965.

REFERENCES

11. Farris, R. J., "The Character of the Stress-Strain Function for Highly Filled Elastomers", Trans. of the Soc. of Rheology 12:2, 303-314 (1968).

12. Farris, R. J., "The Influence of Vacuole Formation on the Response and Failure of Filled Elastomers", Trans. of the Soc. of Rheology, 12:2, 315-334 (1968).

13. Farris, R. J., Thesis for Doctor of Science, Univ. of Utah, Dept. of Civil Engineering (June 1970).

14. Bills, K. W., Jr., "Applications of the Linear Cumulative Damage Criterion to Motor Failure Problems", Bulletin of the 7th Meeting of the ICRPG Working Group on Mechanical Behavior, p. 13 (October 1968).

15. Ferry, J. D., Viscoelastic Properties of Polymers, John Wiley & Sons, Inc., (1961).

16. Smith, T. L., "Stress-Strain-Time Temperature Relationship for Polymers", Reprint from Symposium on Stress-Strain-Time-Temperature Relationships in Materials, Special Technical Publication No. 325, ASME.

17. Bills, K. W., Jr., Svob, G. J., Planck, R. W., and Eriksson, T. L., "A Cumulative Damage Concept for Propellant-Liner Bonds in Solid Rocket Motors", J. Spacecraft. Vol. 3, No. 3, March 1966.

18. Wiegand, J. H., "Study of Mechanical Properties of Solid Propellants", Report No. 0411-10F, Aerojet-General Corporation, 1962.

UNCLASSIFIED

Security Classification

DOCUMENT CONTROL DATA - R & D

(Security classification of title, body of abstract and indexing annotation must be entered when the overall report is classified)

1. ORIGINATING ACTIVITY *(Corporate author)*
Aerojet Solid Propulsion Company
Sacramento, California

2a. REPORT SECURITY CLASSIFICATION
Unclassified

2b. GROUP
--

3. REPORT TITLE
Applications of Cumulative Damage in the Preparation of Parametric Design Curves and the Prediction of Grain Failures on Pressurization

4. DESCRIPTIVE NOTES *(Type of report and inclusive dates)*
Final Report, 1 April 1969 through 28 February 1970

5. AUTHOR(S) *(First name, middle initial, last name)*
Kenneth W. Bills, Jr., Douglas M. Campbell, Robert D. Steele, Joseph D. McConnell, Leonard R. Herrmann, and Richard J. Farris

6. REPORT DATE	7a. TOTAL NO. OF PAGES	7b. NO. OF REFS
August 1970	280	42

8a. CONTRACT OR GRANT NO	9a. ORIGINATOR'S REPORT NUMBER(S)
N00017-69-C-4423	1341-26F
b. PROJECT NO.	
c.	9b. OTHER REPORT NO(S) *(Any other numbers that may be assigned this report)*
d.	None

10. DISTRIBUTION STATEMENT
None

11. SUPPLEMENTARY NOTES	12. SPONSORING MILITARY ACTIVITY
None	Naval Ordnance Systems Command (ORD-0331) (Department of the Navy)

13. ABSTRACT

The problem approached here was to advance the state-of-the-art in viscoelastic stress analyses and to extend the range of application of the linear cumulative damage relation for solid propellants with emphasis placed upon the development of practical tools for engineering, propellant development and mechanical property characterizations. In particular, we planned to: (1) provide practical engineering design curves for rocket grains, in terms of their stress, strain and damage behaviors; (2) make basic improvements in stress analysis methods; and (3) verify the linear cumulative damage predictions for grain failures on motor pressurization. At the beginning of this program the linear cumulative damage concept had been well established for solid propellants while thermoviscoelastic stress analyses had been advanced to include finite length grains with continuously varying boundary temperatures. In this program we have completed a study to evaluate the effects of grain design parameters upon thermoviscoelastic stresses, strains and damage effects; prepared simplified parametric design curves suitable for early grain design and propellant selection; developed normalization methods for the relaxation modulus which can further simplify methods for selecting or formulating propellants for a given application; improved upon the existing two-dimensional, thermal viscoelastic, stress analysis capability, adding the capability to handle planar geometries; investigated non-linear analyses based upon propellant dilatational behavior, finding the analytical evaluation to be straightforward and useful; extended cumulative damage studies to include failures on motor pressurization, the experimental confirmation of these relations requiring the development of a novel pressurization analog test and the testing to failure of ten propellant grains.

DD FORM 1 NOV 65 1473

Unclassified

Security Classification

14 KEY WORDS	LINK A		LINK B		LINK C	
	ROLE	WT	ROLE	WT	ROLE	WT
Prediction of grain failure						
Linear cumulative damage						
Maximum principal stress failure criterion						
Mechanical properties						
Solid Propellants						
Viscoelastic stress analyses						
Parametric design curves						
Grain cracking on pressurization						
Time-pressure shift function						
Non-linear viscoelasticity						
Strain dilatation						
Pressurization analog test						